NUREG/CR-5010
EGG-2520
October 1987

RELAP5/MOD2 Assessment Using Semiscale Experiments S-NH-1 and S-LH-2

Ruey-ying Yuann
Kuo-shing Liang
Janice L. Jacobson

F O R M A L R E P O R T

EG&G Idaho

Work performed under DOE Contract No. DE-AC07-76ID01570 for the ***U.S. Nuclear Regulatory Commission***

Idaho National Engineering Laboratory

Managed by the U.S. Department of Energy

Available from

Superintendent of Documents
U.S. Government Printing Office
Post Office Box 37082
Washington, D.C. 20013-7982

and

National Technical Information Service
Springfield, VA 22161

NUREG/CR-5010
EGG-2520
Distribution Category: R4

RELAP5/MOD2 ASSESSMENT USING SEMISCALE EXPERIMENTS S-NH-1 AND S-LH-2

NUREG/CR--5010

TI88 002541

Ruey-ying Yuann[a]
Kuo-shing Liang[b]
Janice L. Jacobson

Published October 1987

EG&G Idaho, Inc.
Idaho Falls, Idaho 83415

Prepared for the
Division of Reactor Accident Analysis
Office of Nuclear Regulatory Research
U. S. Nuclear Regulatory Commission
Washington, D.C. 20555
under DOE Contract No. DE-AC07-75ID01570
FIN Number A6827

NRC Program Manager: David E. Bessette

a. Taiwan Power Company, 242 Roosevelt Rd, Sec. 3, Taipei, Taiwan.

b. Institute of Nuclear Energy Research, Atomic Energy Council, P.O. Box 3-3, Lung-tan, Taiwan.

ABSTRACT

This report presents the results of the RELAP5/MOD2 posttest assessment utilizing two small break loss-of-coolant accident (LOCA) tests (S-NH-1 and S-LH-2) which were performed in the Semiscale Mod-2C facility. Test S-NH-1 was a 0.5% small break LOCA where the high-pressure injection system (HPIS) was inoperable throughout the transient. Test S-LH-2 was a 5% small break LOCA involving a relatively high upper-head-to-downcomer initial bypass flow and nominal emergency core cooling. Through comparisons between data and best-estimate RELAP5 calculations, the capabilities of RELAP5 to calculate the transient phenomena are assessed. For S-NH-1, emphasis was placed on the capability of the code to calculate various operator actions to initiate core heatup in the absence of HPIS. For S-LH-2, the capability of the code to calculate basic small break system response, such as vessel level during loop seal formation and clearing, break uncovery, and primary pressure response following accumulator injection, was assessed.

FIN No. A6827—International Code Assessment and Applications Program (ICAP)

Available from

Superintendent of Documents
U.S. Government Printing Office
Post Office Box 37082
Washington, D.C. 20013-7982

and

National Technical Information Service
Springfield, VA 22161

SUMMARY

This report includes the results and conclusions of assessment studies involving comparisons between data from Semiscale Tests S-NH-1 and S-LH-2 and RELAP5/MOD2 code calculations. Both tests simulated small break LOCA events with break sizes of 0.5% for S-NH-1 and 5% for S-LH-2. RELAP5/MOD2 is an advanced, one-dimensional, thermal-hydraulic computer code used to calculate reactor transient response.

Test S-NH-1 was designed to investigate a small break LOCA with the compounding failure of high-pressure injection and specified recoveries to mitigate core temperature excursions. Test S-LH-2 was designed to examine the thermal-hydraulic phenomena associated with a 5% small break LOCA with nominal emergency core cooling. Results of Test S-LH-2 provide insight into upper head drain characteristics, break size, and a possible safety issue involving pressure hold-up following accumulator injection.

Data from Test S-NH-1 were used to assess the effectiveness of the code in calculating system response to various operator actions taken to mitigate a core heatup. The test assumed total loss of the high-pressure injection system (HPIS) simultaneously with the break. Without HPIS, operator action would be required to reduce the primary pressure to accumulator set points prior to a heater rod temperature excursion.

The RELAP5 calculation correctly modeled several of the important thermal-hydraulic responses for Test S-NH-1. Primary and secondary pressures were calculated to be slightly higher than the test data. Also, the calculated pressure rise in the steam generators and the calculated depressurization rate in the steam generators during recovery were higher than measured in the test. The break flow was undercalculated, and thus the primary mass was greater in the calculation than in the test data. Pressurizer interfacial liquid level early in the test and vessel upper plenum liquid level were correctly calculated. Primary system loop flow, including two-phase peaking in the downcomer, showed good agreement between the calculation and the test data. Overall, the system power response and temperature response were calculated to be in good agreement with the test data; however temperature discrepancies in the calculation and test data were noted between hot metal and fluid, primarily in the voided areas. A calculation involving the accumulator model that used the primary pressure data from Test S-NH-1 concluded that the accumulator model in RELAP5 worked well.

The assessment of RELAP5/MOD2 using Test S-LH-2 specifically focused in the area of liquid holdup in the steam generator, manometrically induced core liquid depressions (pump suction seal formation and clearing), and the effect of downcomer-to-upper-head bypass flow rate on the core liquid level depressions. Also examined were the sensitivity of depressurization rate and its effect on accumulator flow rates and the possible introduction of an extensive core heatup before LPIS setpoints were reached.

RELAP5 correctly calculated several of the important small break LOCA thermal-hydraulic responses for Test S-LH-2. The early primary system pressure response was correctly calculated because of a good calculation of break flow. However, RELAP5 calculated a larger depressurization rate when the pump suction seals cleared and the break uncovered. The system fluid mass distribution showed good agreement between the calculation and the test. Reflux seen in the test was also calculated by RELAP5. The magnitude of the core liquid level depression was correctly calculated, and no core heatup at the time of this level depression was calculated, as in the test. The vessel was filled more rapidly in the test than in the calculation because there was more accumulator injection mass in the test.

ACKNOWLEDGMENTS

The authors wish to gratefully acknowledge the following people for their contributions that were made during the course of this project and in producing the report. Those people are: R. G. Hanson, D. M. Kiser, N. S. Larson, G. G. Loomis, and G. E. Wilson. Specific gratitude goes to G. G. Loomis for providing technical assistance in writing this report.

CONTENTS

FIGURES

TABLES

RELAP5/MOD2 ASSESSMENT USING SEMISCALE EXPERIMENTS S-NH-1 AND S-LH-2

INTRODUCTION

The assessment study documented in this report contributes to the overall code assessment effort, which is coordinated within the International Code Assessment and Applications Program (ICAP) sponsored by the U.S. Nuclear Regulatory Commission (NRC). The objective of the ICAP is to provide qualitative assessment of the major thermal-hydraulic computer codes relative to code development, code improvement, and the enhancement of user guidelines. In addition, the ICAP has the objective of providing the necessary data base for the qualitative characterization of computer codes when applied in a best-estimate fashion to hypothetical accident scenarios.

This report includes the results and conclusions of assessment studies involving comparisons between data from Semiscale Tests S-NH-1 and S-LH-2 and RELAP5/MOD2[1] code calculations. Both tests simulated small break loss-of-coolant accident (LOCA) events with break sizes of 0.5% for S-NH-1 and 5% for S-LH-2. RELAP5/MOD2 is an advanced, one-dimensional, thermal-hydraulic computer code used to calculate reactor transient response.

Test S-NH-1 was designed to investigate a small break LOCA with the compounding failure of high-pressure injection and specified recoveries to mitigate core temperature excursions.

Test S-LH-2 was designed to examine the thermal-hydraulic phenomena associated with a 5% small break LOCA with nominal emergency core cooling. Results of this test provide insight into upper head drain characteristics, break size, and a possible safety issue involving pressure holdup following accumulator injection.

Data from Test S-NH-1 were used to assess the effectiveness of the code in calculating system response to various operator actions taken to mitigate a core heatup. The test assumed total loss of the high-pressure injection system (HPIS) simultaneously with the break. Without HPIS, operator action would be required to reduce the primary pressure to accumulator set points prior to a heater rod temperature excursion.

The assessment of RELAP5/MOD2 using Test S-LH-2 specifically focused in the area of liquid holdup in the steam generator, manometrically induced core liquid depressions (pump suction seal formation and clearing), and the effect of downcomer-to-upper-head bypass flow rate on the core liquid level depressions. Also examined were the sensitivity of depressurization rate and its effect on accumulator flow rates and the possible introduction of an extensive core heatup before LPIS set points were reached.

The first two sections of this report contain a description of the tests and the RELAP5/MOD2 modeling techniques employed in the calculation. Results of the assessment and pertinent features of the RELAP5/MOD2 code necessary for understanding the assessment are then presented, followed by conclusions and recommendations.

TEST FACILITY AND TRANSIENT DESCRIPTION

The Semiscale Mod-2C system is a scaled, two-loop representation of a pressurized water reactor (PWR), with a fluid volume and core power of about 1/1705 of a full-sized PWR. Geometric similarities of component layout have been maintained between the Semiscale system and a PWR, as shown in Figure 1. The Semiscale Mod-2C system consists of a pressure vessel with simulated reactor internals and an external downcomer. The intact loop simulates three unaffected loops of a four-loop PWR, and the broken loop simulates an affected loop in which the small break is assumed to occur. The unique feature of the Mod-2C system is the installation of a Type III steam generator which has an external downcomer to allow gamma densitometers to measure the riser density. The unaffected loop steam generator consists of six inverted U-tubes, and the affected loop steam generator consists of two inverted U-tubes. The outside diameter of the U-tubes is 0.022 m (0.86 in.), which is similar to the outside diameter of typical PWR steam generator U-tubes [about 0.018 m (0.70 in.)]. The reactor internals consist of a 5 x 5 array of internally heated electric rods of which 23 are powered, as shown on Figure 2. The rods are geometrically similar to nuclear fuel rods, with a heated length of 3.66 m (144 in.) and outside diameter of 0.011 m (0.42 in.).

The upper head (Figure 3) contains a simulated control rod guide tube and two simulated support columns, with an upper core support plate as the boundary between the upper head and upper plenum. The two support columns were plugged to allow drainage only through the guide tube. The bypass line which extends from the external downcomer to the upper head was used to simulate the major leakage path between the upper downcomer and the upper head for a typical PWR. The bypass flow rate was adjusted by installing a flat plate orifice in the tubing bypass line.

External heaters were installed in a relatively uniform manner on the vessel, downcomer, pressurizer, and primary loop piping to offset environmental heat losses.

Conditions in the system were monitored by an extensive network of metal and fluid thermocouples and differential pressure transducers. Average fluid density was measured in the loops and vessel with gamma densitometers. The volumetric flow was measured with turbine meters. Condensing systems and catch tanks were installed to measure the effluent from the break flow and steam generator atmospheric dump valves (ADV).

Both Tests S-NH-1 and S-LH-2 were conducted in the Semiscale Mod-2C system. The S-NH-1 test represents a 0.5% centerline pipe break between the broken loop pump and the vessel. The break was simulated by an orifice that has a scaled area equivalent to a 0.051-m (2-in.) break diameter in a PWR. The break was initiated at 0 s, and complete loss of HPIS was assumed to occur. The core scram, primary coolant pump trip, auxiliary feedwater flow initiation, and main steam isolation valve (MSIV) isolation all automatically occurred after the low pressurizer pressure signal was reached. The core power decreased to ANS decay heat 3 s after the scram signal was initiated to simulate the control rod drop time. An operator-induced recovery was initiated at a peak cladding temperature of 811 K (1000°F), at which time the steam generator ADVs in both loops were latched open. Auxiliary feedwater flow was continued to maintain the secondary level between 9 and 10 m (354 and 394 in.). The steam generator ADVs were cyclically closed and opened when the steam generator level was at 2 and 4 m (78.7 and 157.4 in.), respectively. Accumulator injection flow was terminated when the primary system pressure exceeded 4.2 MPa (600 psia), or when the accumulator emptied. The test was terminated when the pressurizer pressure dropped to 1.38 MPa (200 psia), which is the nominal low pressure injection (LPIS) set point. No LPIS was used for S-NH-1.

Test S-LH-2 represented a 5% cold leg centerline pipe break between the broken loop pump and the vessel. The break was simulated by an orifice that has a scaled area equivalent to a 0.156-m (6.14-in.) break diameter in a PWR. The transient was started at 0 s by opening a block valve which allowed primary fluid to flow through the break orifice to the break condensing system. The core scram, feedwater trip, coolant pump trip, MSIV closure, and HPIS initiator were all automatically occurring events when the low pressurizer pressure trip set point of 12.59 MPa (1827 psia) was reached. Because the offsite power was assumed to be completely lost during the test, there was a time delay in the HPIS initiation (25.9 s). The core was assumed to scram, and the ANS decay heat curve was utilized 3.4 s after the scram signal was reached in order to simulate the control rod drop time. Auxiliary feedwater was assumed to be unavailable during the transient, and accumulator injection

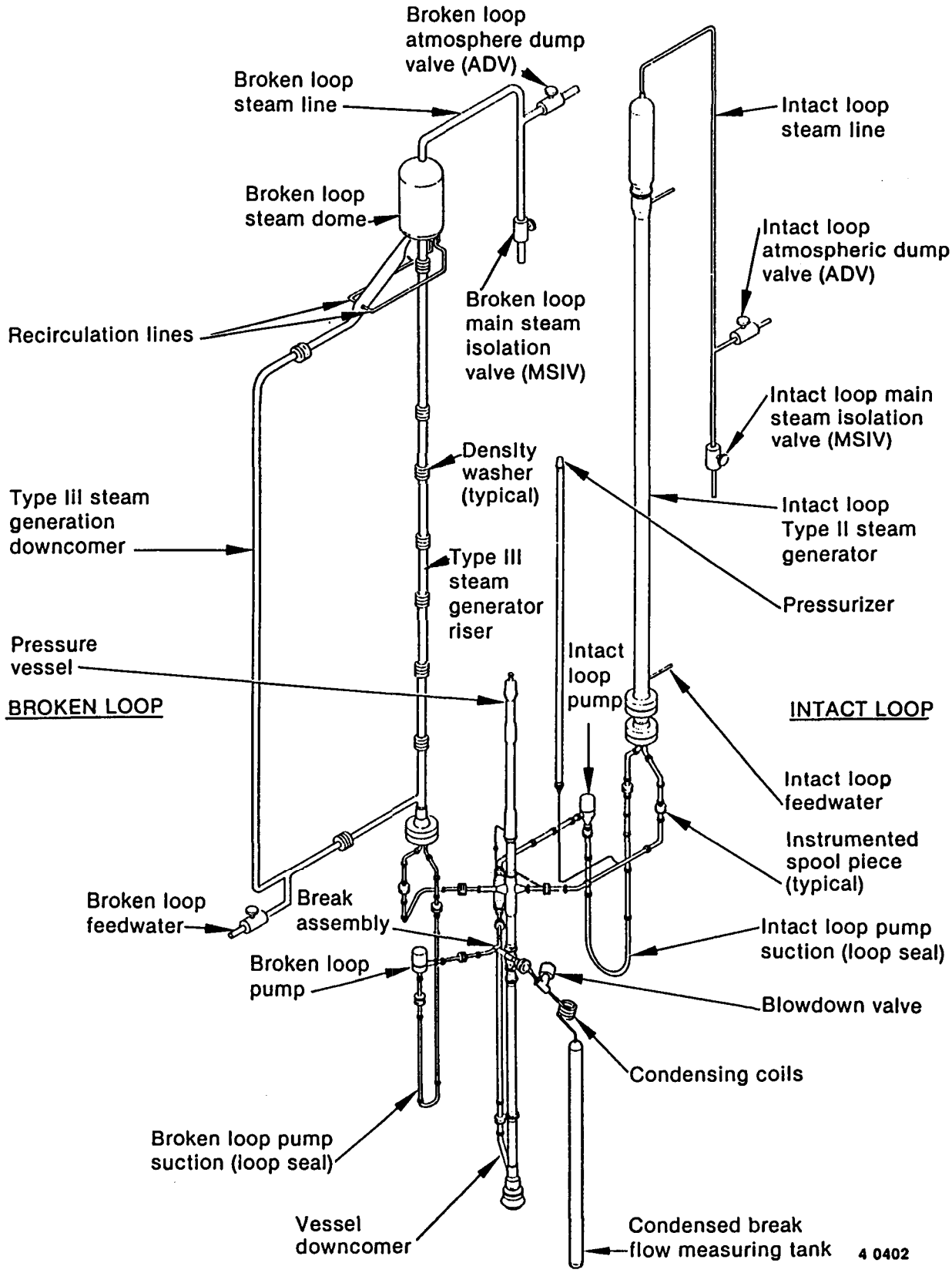

Figure 1. Semiscale Mod-2C system as configured for Tests S-LH-2 and S-NH-1.

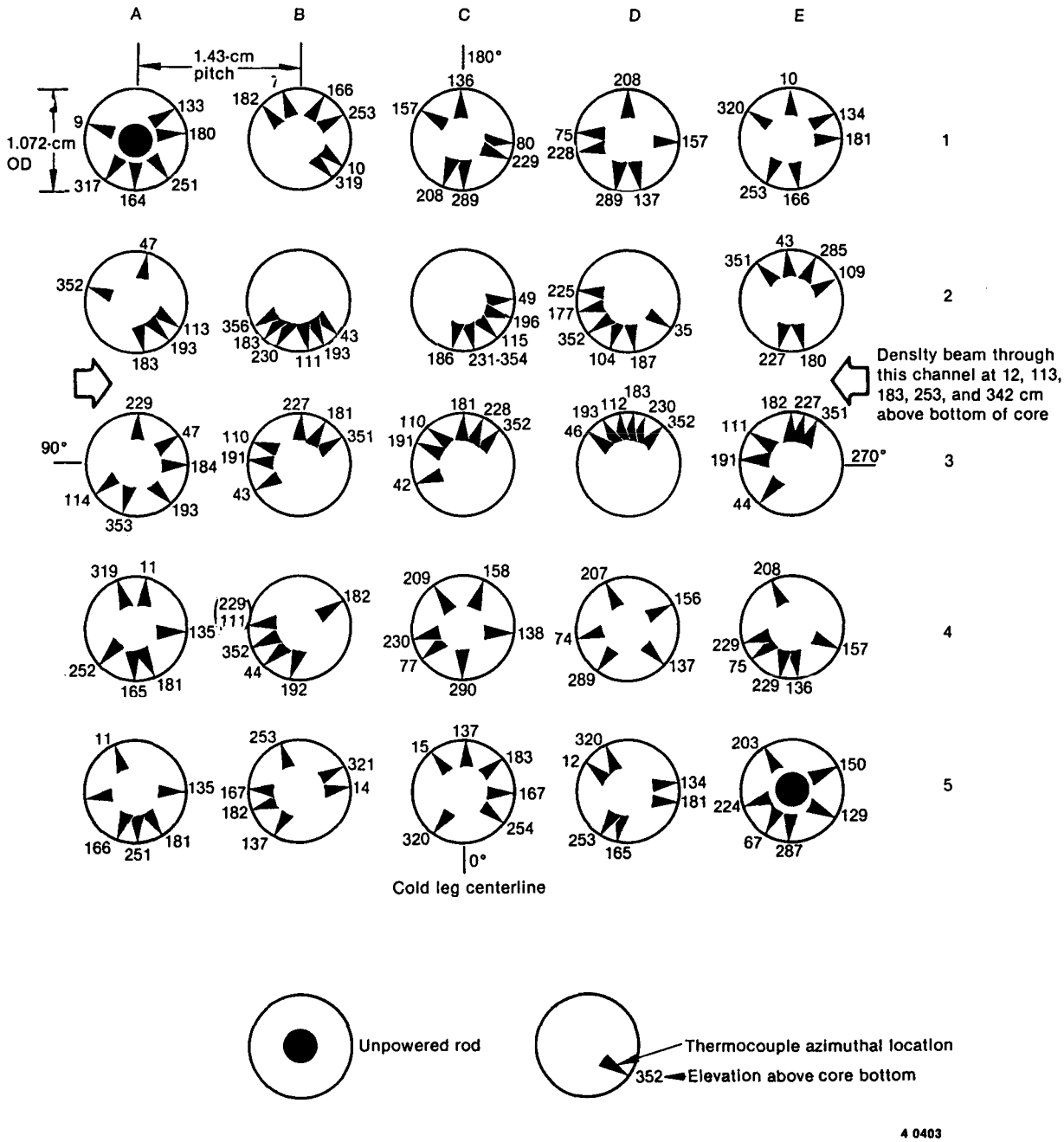

Figure 2. Semiscale Mod-2C core heater rod thermocouple orientation.

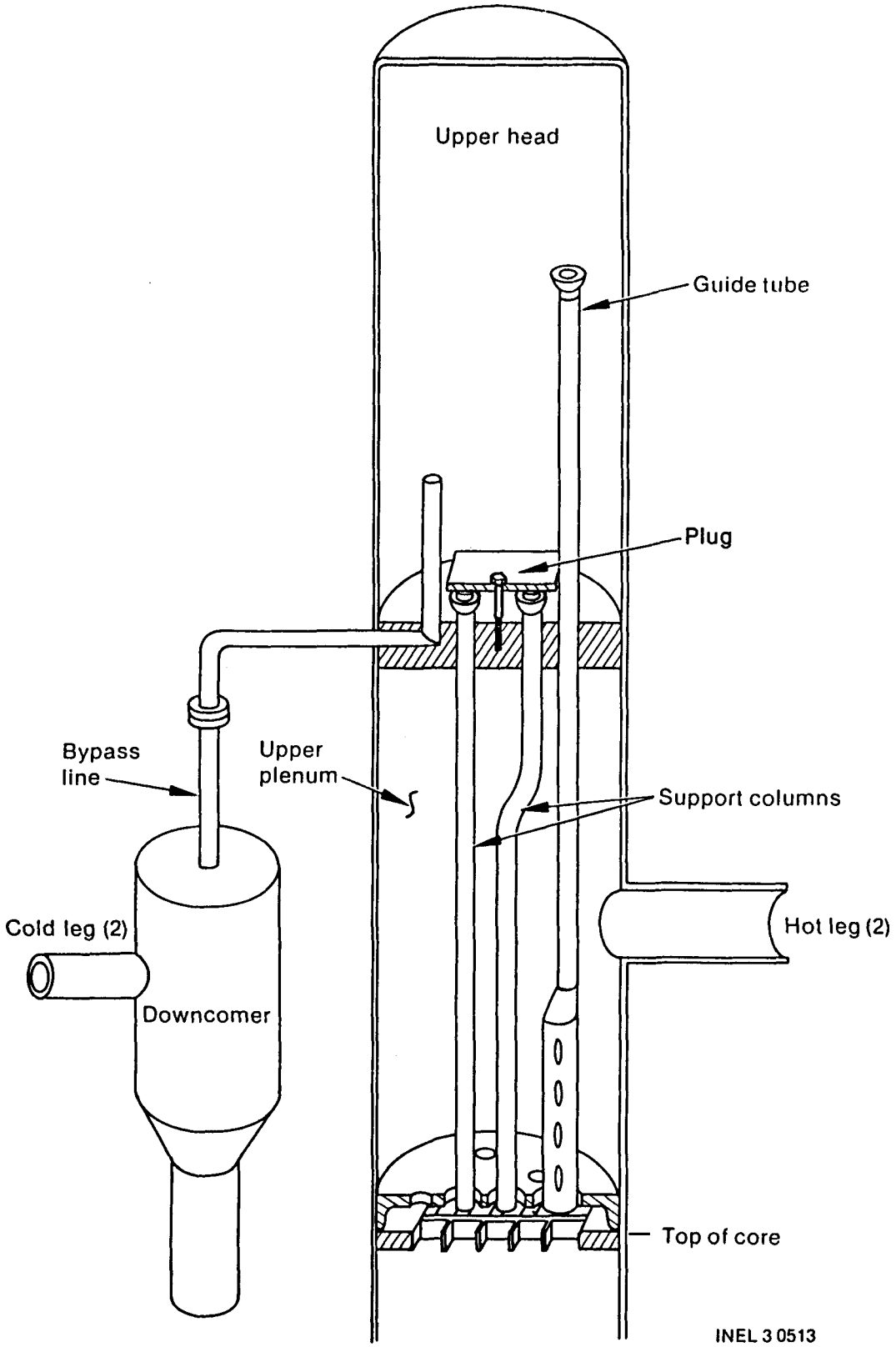

Figure 3. Vessel upper head configuration for Tests S-LH-2 and S-NH-1.

was initiated at the primary system pressure of 4.2 MPa (600 psia) in the intact loop only. The test was terminated at about 1000 s, at which time the core was quenched and the core liquid level was stable; however, the primary pressure was above the LPIS set point.

RELAP5/MOD2 MODELING DESCRIPTION

The RELAP5/MOD2 code is an advanced, one-dimensional, system analysis computer code developed at the INEL for the U.S. Nuclear Regulatory Commission, Office of Reactor Safety Research. Cycle 36.04 of the RELAP5/MOD2 code was used for the assessment studies. The Semiscale Mod-2C input model is represented by the nodalization diagram shown on Figure 4. It consists of 181 hydrodynamic volumes and 256 heat structures. Steam generator secondary sides, emergency core cooling system (ECCS) injection systems, vessel and piping external heaters, and system environmental heat loss were all modeled in detail. Also, a chopped cosine curve (Figure 5) for the core axial power profile was modeled by 12 consecutive heat structures.

For both tests, the non-equilibrium option was applied to all hydrodynamic volumes and junctions except the pump discharge, where the one-velocity momentum equation was used. However, because of the inability to precisely predict the two-phase break flow in the S-NH-1 test with the general two-velocity option, the one-velocity option was applied to the break junction in the S-NH-1 model. Moreover, as revealed from the S-NH-1 pretest calculation,[2] liquid entrainment would be underpredicted when the physical central-oriented horizontal stabilization model is applied to the break. Also, when the non-crossflow option was applied to the break, single-phase break flow would be overestimated. To compensate for the underprediction of liquid entrainment and to avoid the overprediction of single-phase break flow, a downward-oriented and crossflow break junction was used in the Test S-NH-1 calculation.

The upper plenum and upper head regions were nodalized to allow junctions at the top of the core bypass line, control rod guide tube, and support columns. Also modeled was the junction at the elevation of the holes in the control rod guide tube below the upper support plate. Although the support columns were plugged, a small leak path existed in the lower part of the upper head. This leak path was simulated by using a large junction loss coefficient.

Discharge coefficients for single-phase (CD1) and two-phase (CD2) flow were applied to the RELAP5 critical flow model at the break. In Test S-LH-2 modeling, based on the comparison of calculation to data for the break flow rate, the best values of both CD1 and CD2 were determined to be 0.9. In Test S-NH-1 modeling, as an attempt to justify the RELAP5 critical flow model, all bias of break flow calculation was removed; i.e., both CD1 and CD2 were set to be 1.0.

The vessel and piping external heaters were modeled mechanically in RELAP5, and the measured power was input as a boundary condition. The measured core power and normalized pump coastdown speed were also input as boundary conditions. The HPIS flow rates were input as a function of primary system pressure, which was calculated from the test data for the S-LH-2 test. The HPIS was disabled for the S-NH-1 test.

Steady-state initialization was achieved by adjusting the steam generator secondary pressure using control systems to achieve the desired primary cold leg temperature. The results are shown in Table 1 for Test S-NH-1 and Table 2 for Test S-LH-2. The calculated and measured initial conditions[a] compare well with a few exceptions. These exceptions are due to the adjustment of the steam generator pressure.

---

a. The measurement uncertainties for Test S-NH-1 are discussed in Reference 3.

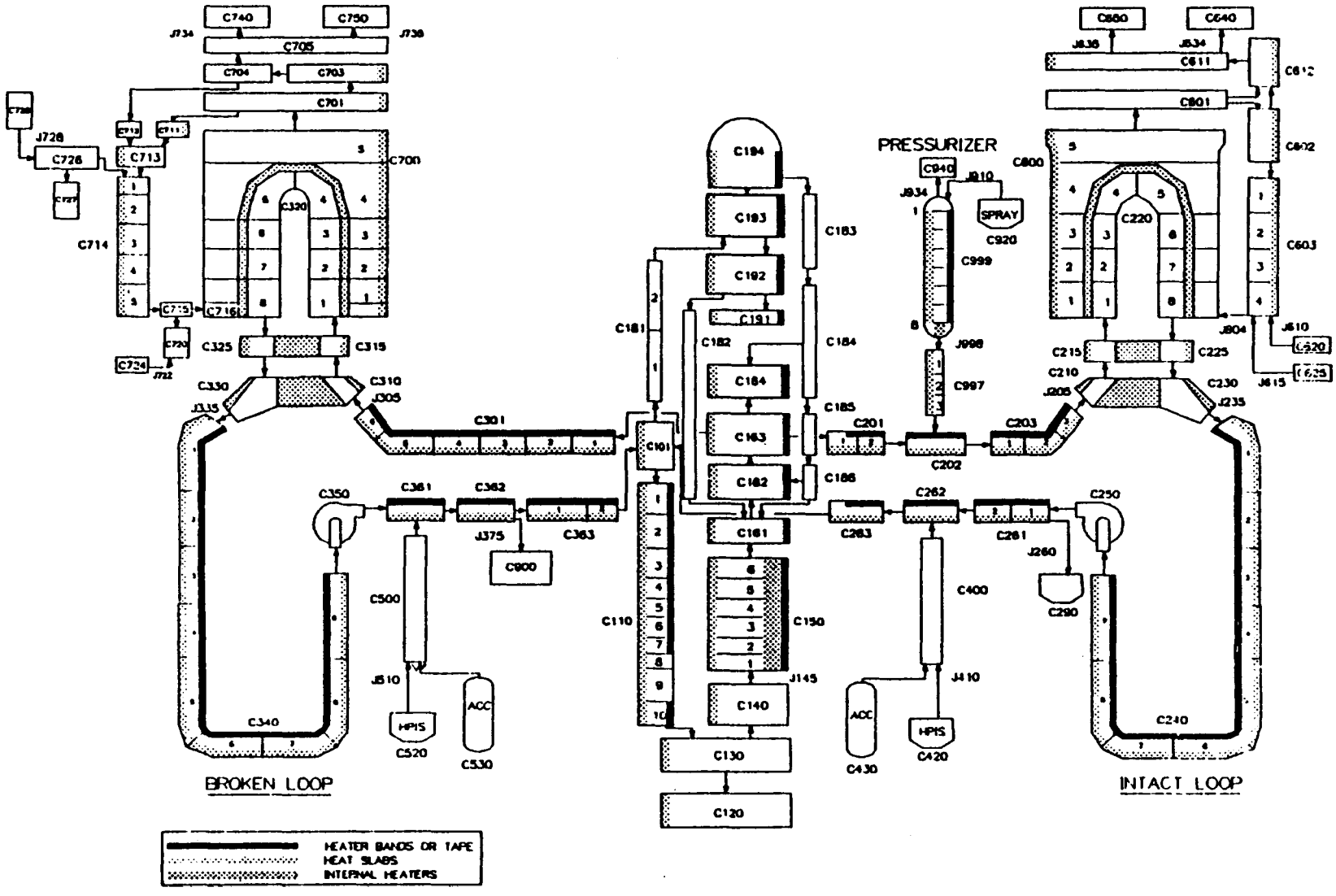

Figure 4. Nodalization diagram for RELAP5 calculations.

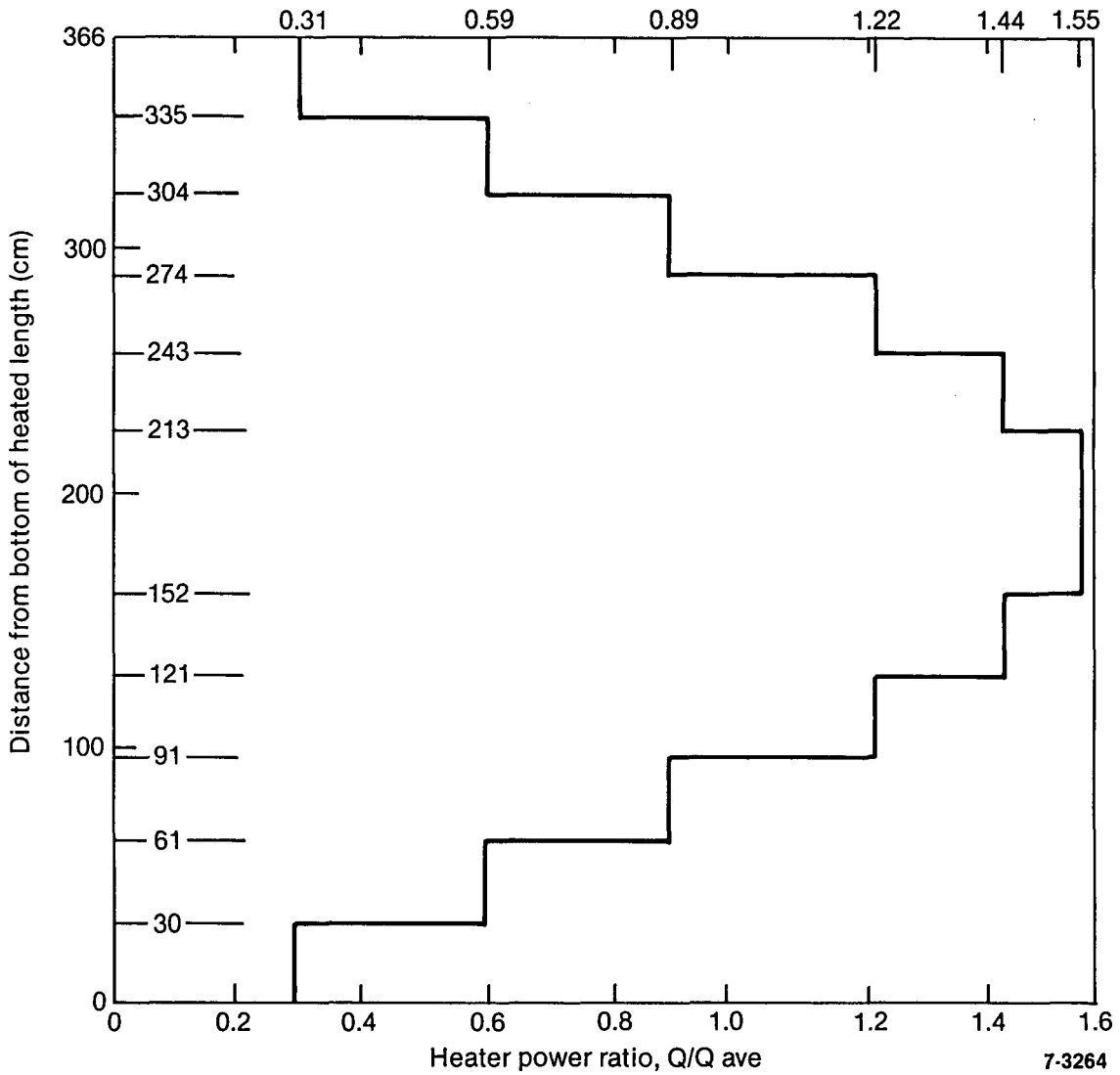

Figure 5. Axial core power profile.

Table 1. Comparison of calculated and measured initial conditions for Test S-NH-1

Parameter	Measured[a]	RELAP5
Pressurizer pressure, MPa (psia)	15.64 (2268)	15.64 (2268)
Core power, MW	2.00	2.00
Core ΔT, K (°F)	39.0 (72.0)	37.5 (67.5)
Pressurizer collapsed liquid level, cm (in.)	257 (101)	259 (102)
Cold leg fluid temperatures loop-to-loop difference, K (°F)	4.2 (7.5)	2.7 (4.9)
Cold leg fluid temperature, K (°F)	550 (530)	550 (530)
Primary flow rates, L/s (gpm)		
Intact loop cold leg	9.1 (144)	9.1 (144)
Broken loop cold leg	3.2 (51)	3.2 (51)
Loop flow split	2.84:1	2.84:1
Maximum primary leakage, kg/s (lbm/s)	0.002 (0.004)	0.002 (0.004)
S. G. secondary pressures, MPa (psia)		
Intact loop	4.55 (665)	4.76 (690)
Broken loop	4.48 (651)	4.50 (653)
S. G. secondary masses, kg (lbm)		
Intact loop	73 (161)	73 (161)
Broken loop	23 (51)	23 (51)
S. G. feedwater flow rates, kg/s (lbm/s)		
Intact loop	0.82 (1.78)	0.83 (1.80)
Broken loop	0.25 (0.55)	0.23 (0.51)
S. G. feedwater temperatures, K (°F)	494 (429)	494 (429)

a. Uncertainties of each measurement are discussed in Reference 3.

Table 2. Comparison of calculated and measured initial conditions for Test S-LH-2

Parameter	Measured	RELAP5
Pressurizer pressure, MPa (psia)	15.42 (2236.5)	15.42 (2236.5)
Core power, kW	2007.09	2007.09
Core ΔT, K (°F)	37.17 (66.9)	37.66 (67.8)
Pressurizer liquid level, cm (in.)	393 (154.7)	393.13 (154.8)
Cold leg fluid temperature, K (°F)		
Intact loop	561.94 (551.8)	561.60 (551.5)
Broken loop	564.35 (556.2)	563.76 (555.6)
Primary flow rate, kg/s (lbm/s)		
Intact loop	7.37 (16.2)	7.35 (16.2)
Broken loop	1.99 (4.4)	2.18 (4.8)
Initial bypass flow (% of total core flow)	3.0	3.15
Steam generator secondary pressure, (MPa, psia)		
Intact loop	5.7 (826.7)	5.89 (854.3)
Broken loop	5.95 (863.8)	5.99 (869.6)
Steam generator secondary mass, kg (lbm)		
Intact loop	191 (421.0)[a]	169.94 (374.6)[a]
Broken loop	48.2 (106.3)	35.00 (77.2)

a. In order to approach stable operation of the steam generators by the RELAP5 self-initialization package, the initial steam generator secondary mass is lower than measured. The effect will be very small, since the energy balance effect on primary system pressure from break flow (5% break) is much higher than primary-to-secondary heat transfer.

COMPARISON OF RELAP5 CALCULATIONS TO TEST DATA

Test S-NH-1

Included in this subsection is a comparison of the calculated results and measured data. Comparisons were made for three different phases: the blowdown phase, the primary boiloff and core heatup phase, and the recovery phase. In the first two phases, only automatic plant responses were assumed and no operator actions were taken. The last phase, the recovery phase, was distinguished by recovery actions taken by the operators. The operators opened the ADV valve of each steam generator to bring the primary system pressure down when the fuel temperature was higher than 811 K (1000°F). This was done so that the other two operable ECCS subsystems, the accumulators and the LPIS, could inject emergency cooling water into the vessel, although no LPIS was used for S-NH-1. The general plant response to a small break LOCA has been extensively described in a number of works.[2,4,5] The following discussion will briefly present the system responses and compare the calculated results with the test data.

Blowdown Phase (0 to 150 s). The calculated and measured initial conditions are listed in Table 1. The calculated steady-state parameters are in good agreement with the corresponding measured values from S-NH-1.

The initiating event in the S-NH-1 test was the opening of the blowdown valve in the broken loop between the pump and vessel. After the break was opened, break flow was first characterized as subcooled critical flow, followed by saturated liquid blowdown and finally two-phase mixture blowdown. The break flow measurement system in Semiscale[6] is subject to a considerable lag time due to the distance between the break plane and the catch tank. Therefore, a direct comparison between the measured and calculated break flow is not meaningful during the early blowdown phase. However, the pressurizer interfacial liquid level is a good indication of the early water inventory loss, and it suggests good agreement between the calculation and test data, as shown on Figure 6. As the pressurizer drained, a rapid depressurization of the primary system resulted, as shown on Figure 7. An inflection point was observed at about 60.0 s in both the calculated and measured pressure responses. This abrupt increase in depressurization rate was caused by the pressurizer emptying and the system power trip. The pressurizer emptying influenced the depressurization because flashing occurred in the saturated pressurizer with a large surface area. When the level dropped to the surge line, the surface area was reduced; thus, flashing was also reduced (Figure 7).

The power trip signal in the calculation was generated at 57.5 s, which was 3.5 s earlier than measured. System power responses from both the measurement and calculation are shown on Figure 8. Except for the timing, excellent agreement can be observed. After the scram signal, the reactor coolant pumps (RCPs) coasted down and the main steam valves of both steam generators began to close. The trend of volumetric flow rate throughout the system was correctly calculated, as shown on Figures 9 through 13 which show flow rates in the downcomer, loop hot legs, and main steam flow rates in the steam generator. The decreases in loop flow rate and main steam flow rate follow the main coolant pump trip, pump coastdown, and MSIV closure, respectively.

Due to the closure of the main steam valve on each steam generator, the steam generator shell-side pressures rose sharply and then stabilized, as shown on Figures 14 and 15. Because of the pressurization of the secondary, core scram, and loss of pumped flow, the overall energy balance across the steam generators was disrupted, which caused a change in the differential temperature across the steam generators as shown on Figures 16 and 17. RELAP5/MOD2 correctly calculated the trend and magnitude in differential temperature in the intact loop (Figure 16); however, by 150 s the differential temperature was calculated to be about 5 K (9°F) lower in the broken loop. The calculated pressure rise in each steam generator was about 0.3 MPa (43 psia) higher than in the test. The magnitude at which the pressure stabilizes is a function of energy addition to the secondary fluid after the closure of the main steam valves. This energy addition includes energy transfer from the primary fluid and from/to the metal in the steam generators. In the primary system, the predictions of loop flow (Figures 9, 10, 11) and temperature difference in each loop (Figures 16 and 17) are in good agreement with the test data. The energy transfers from the primary system in both calculation and test are not expected to be different by significant amounts of magnitude. However, the initial stored energy in the metal mass in the steam generators is an area of possible difference between the test and the calculation. Another important contributor to the much lower broken loop steam generator pressure was

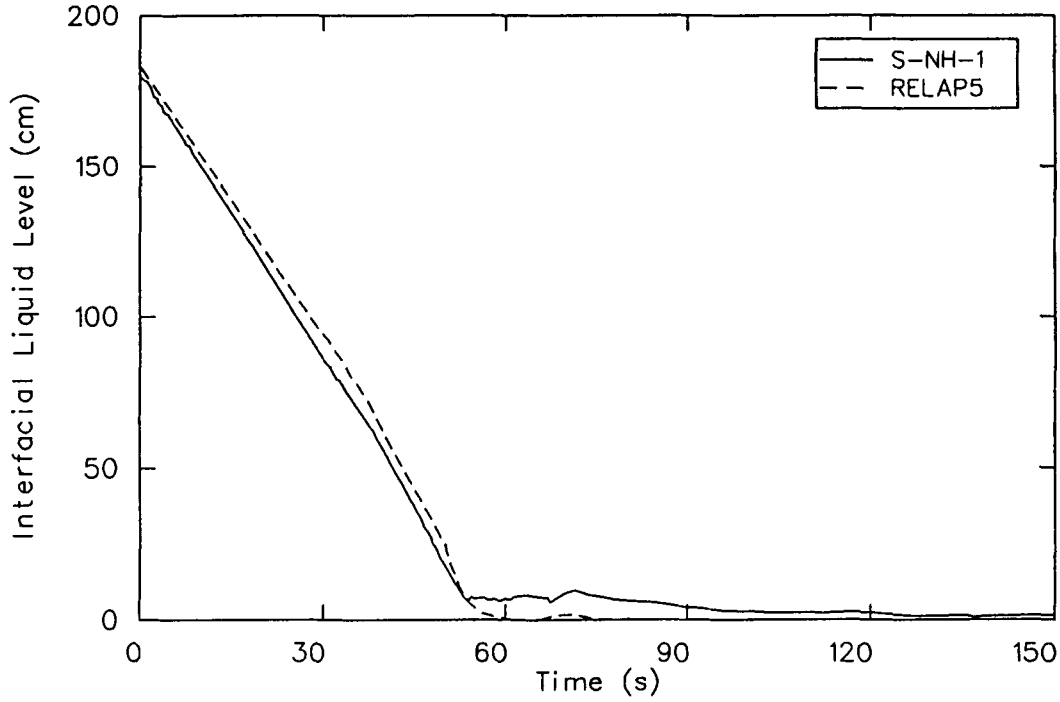

Figure 6. Comparison of calculated and measured pressurizer interfacial liquid levels during the blowdown phase of Test S-NH-1.

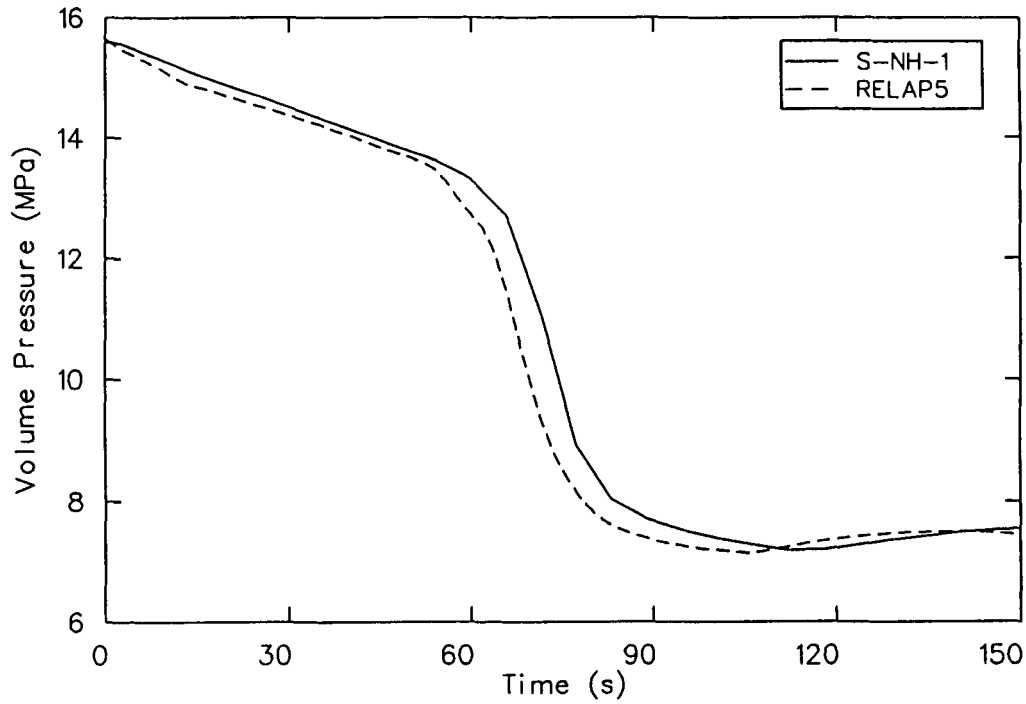

Figure 7. Comparison of calculated and measured pressurizer pressures during the blowdown phase of Test S-NH-1.

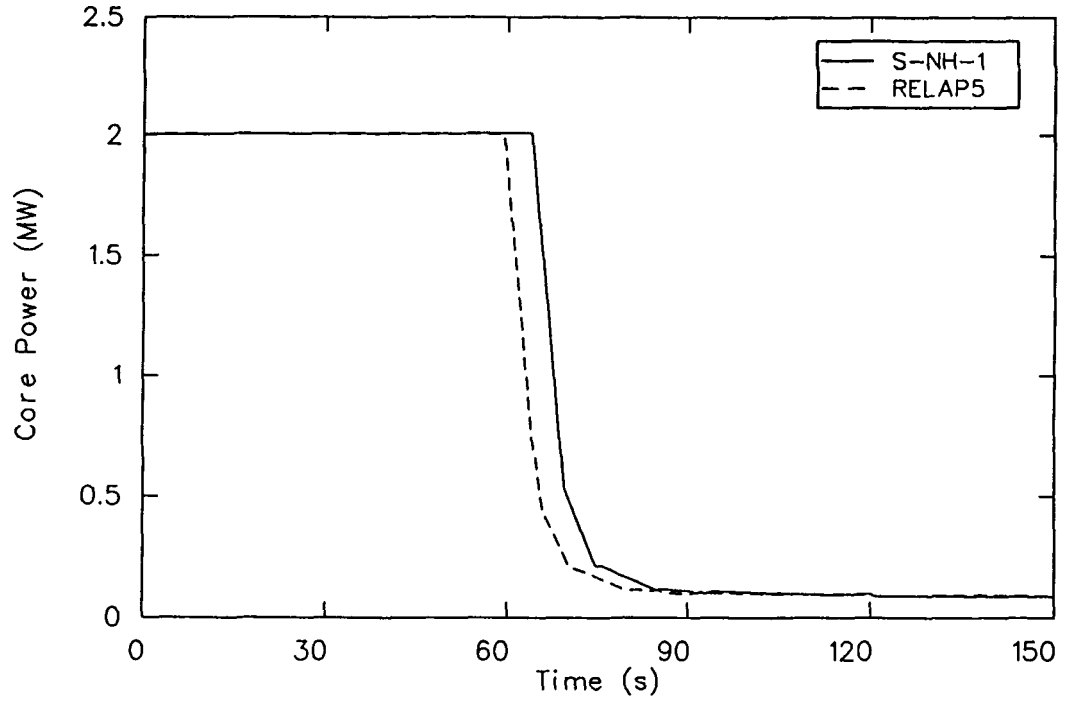

Figure 8. Comparison of calculated and measured core powers during the blowdown phase of Test S-NH-1.

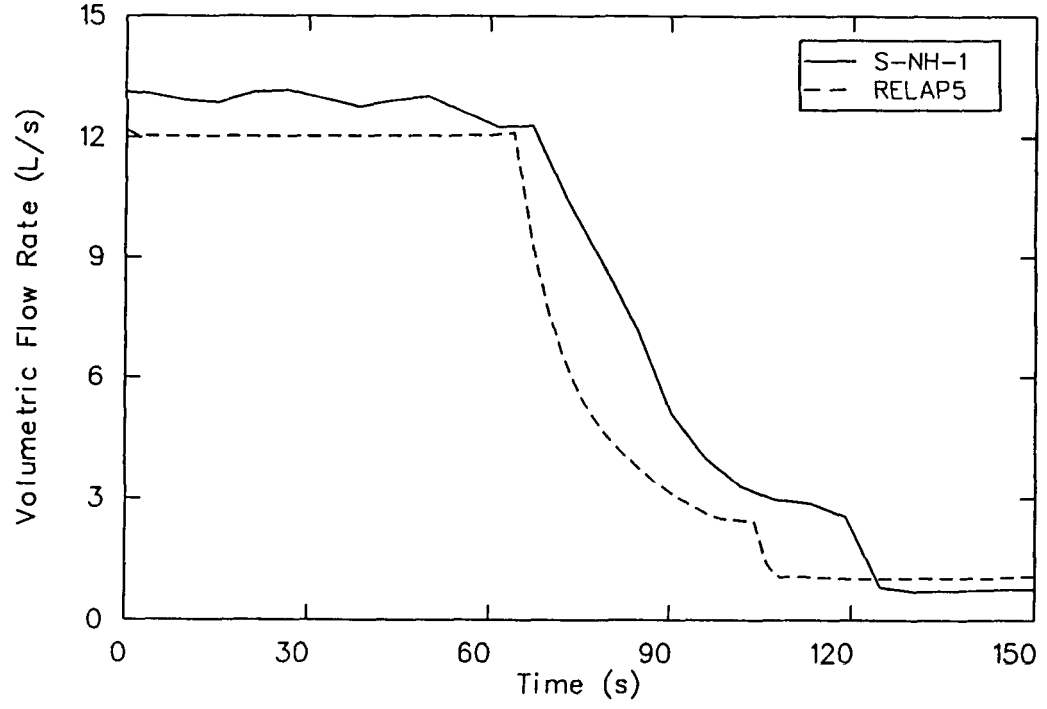

Figure 9. Comparison of calculated and measured downcomer flow rates during the blowdown phase of Test S-NH-1.

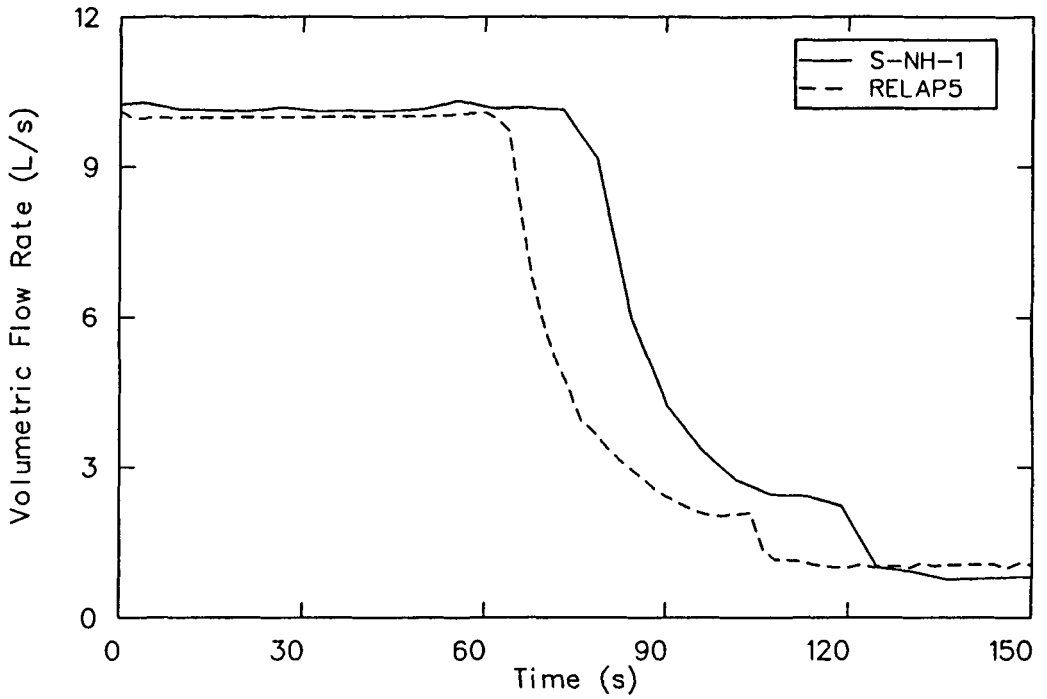

Figure 10. Comparison of calculated and measured intact loop hot leg flow rates during the blowdown phase of Test S-NH-1.

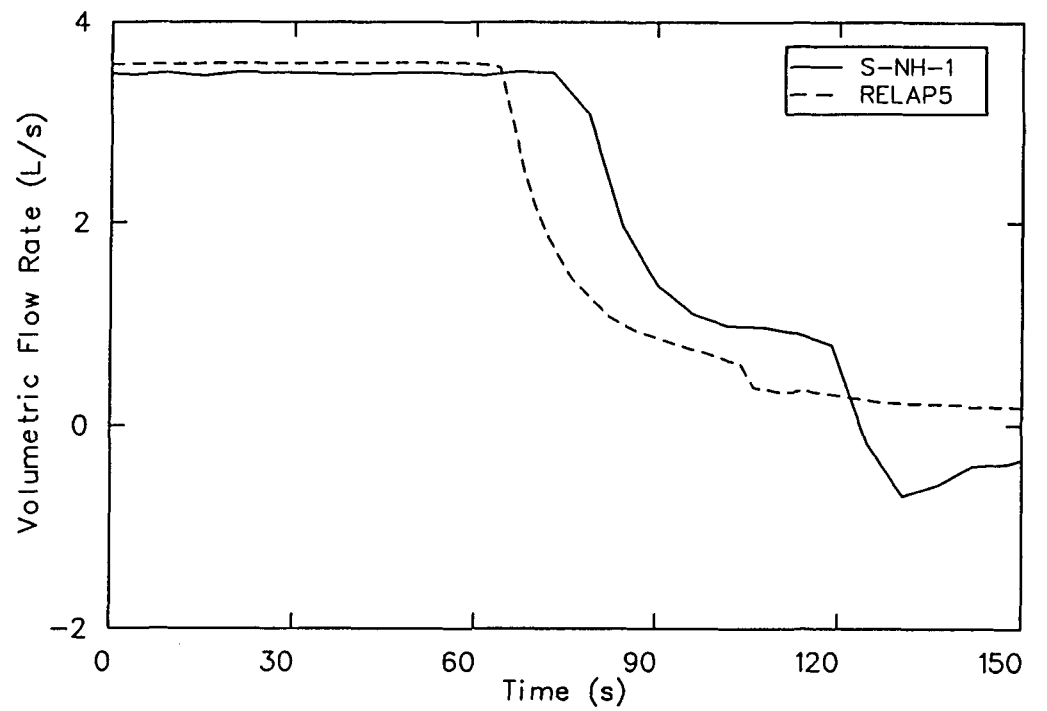

Figure 11. Comparison of calculated and measured broken loop hot leg flow rates during the blowdown phase of Test S-NH-1.

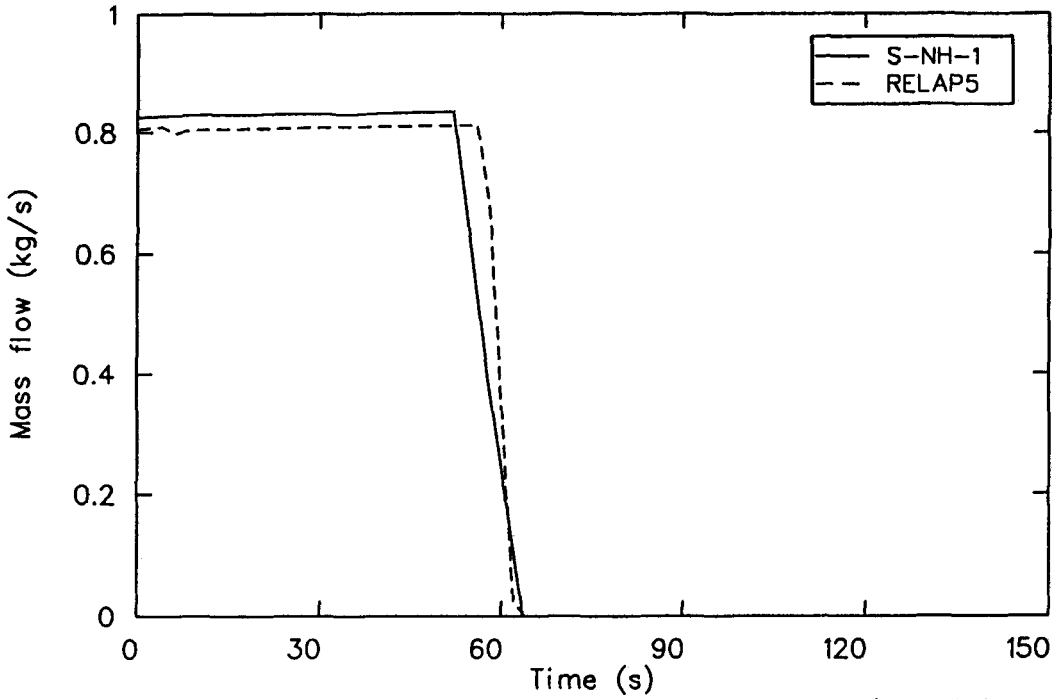

Figure 12. Comparison of calculated and measured intact loop steam flow rates during the blowdown phase of Test S-NH-1.

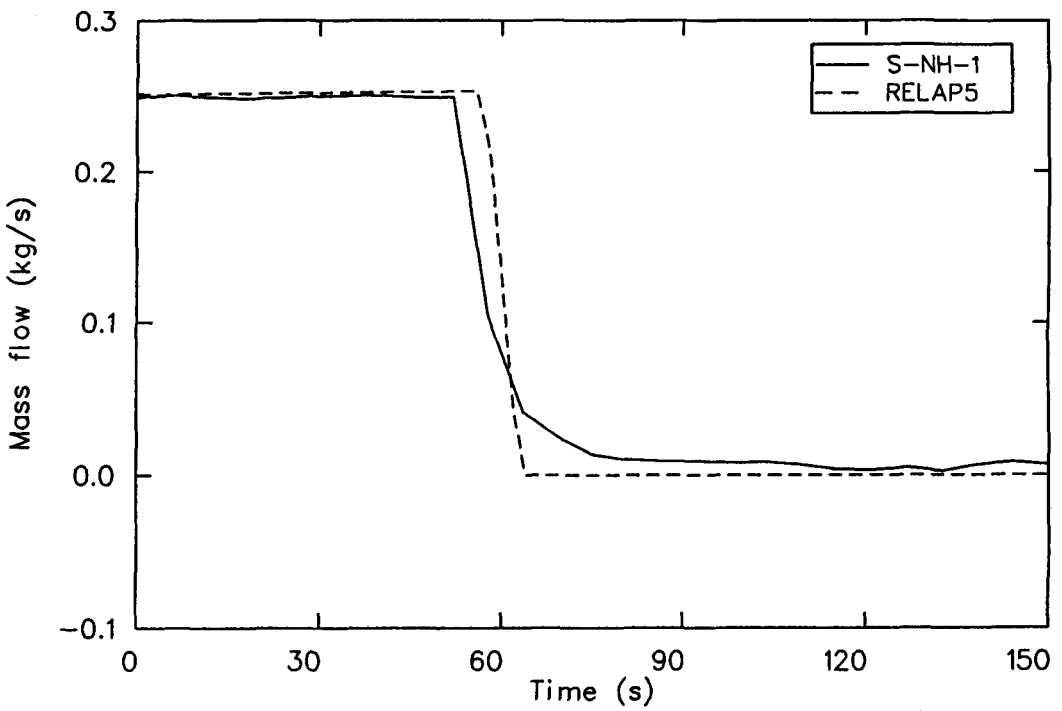

Figure 13. Comparison of calculated and measured broken loop steam flow rates during the blowdown phase of Test S-NH-1.

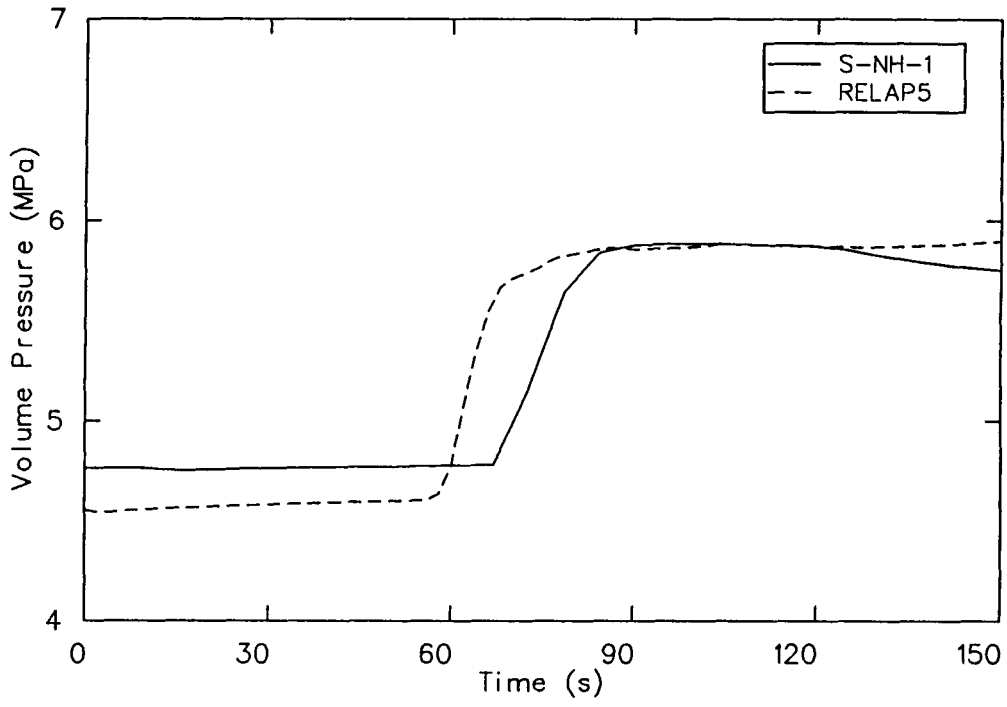

Figure 14. Comparison of calculated and measured intact loop steam generator pressures during the blowdown phase of Test S-NH-1.

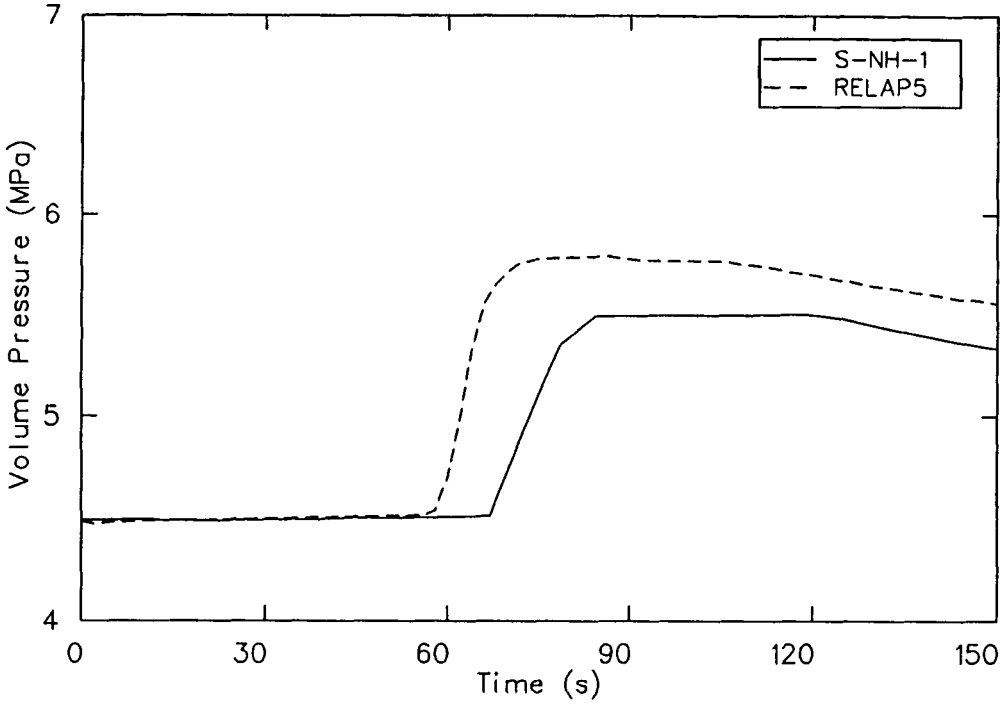

Figure 15. Comparison of calculated and measured broken loop steam generator pressures during the blowdown phase of Test S-NH-1.

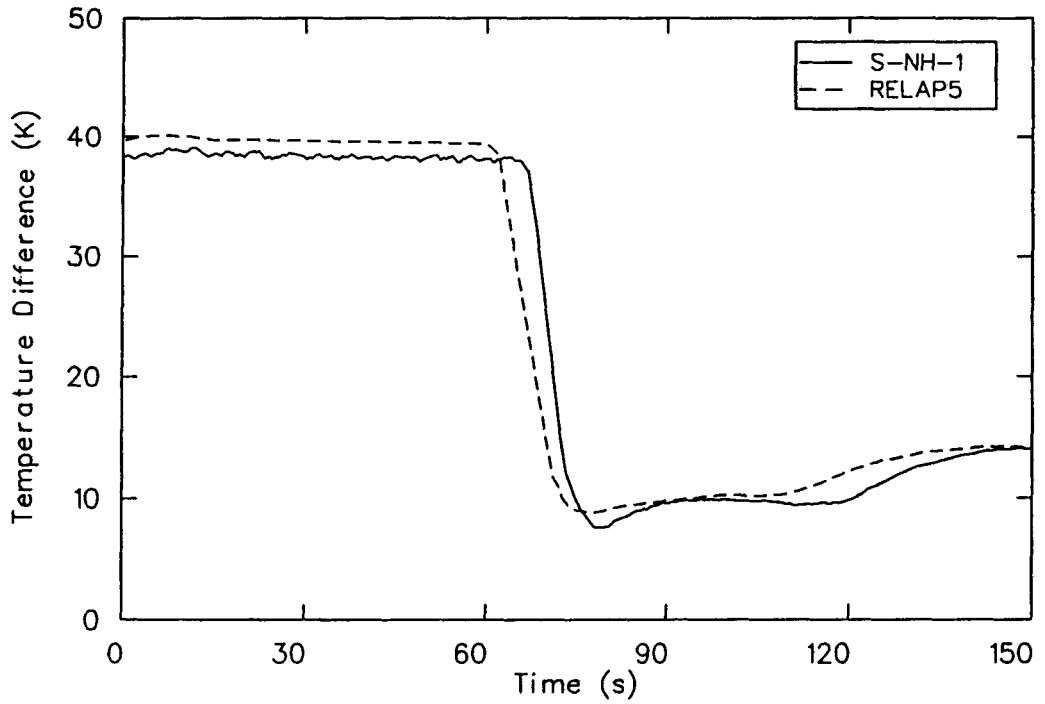

Figure 16. Comparison of calculated and measured intact loop temperature differences during the blowdown phase of Test S-NH-1.

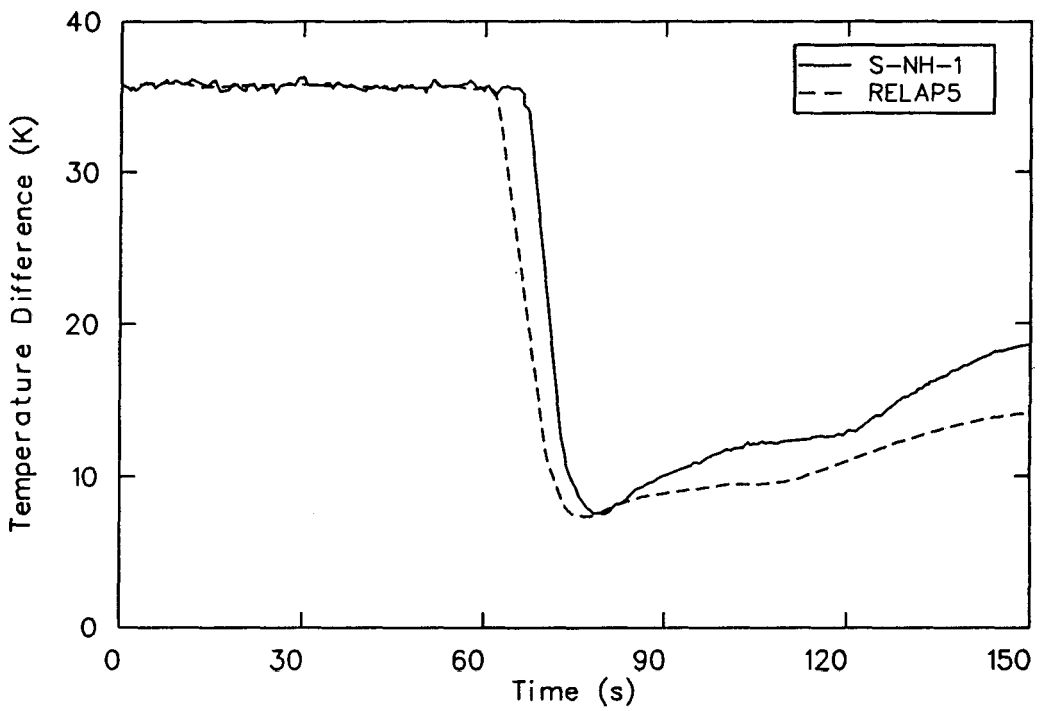

Figure 17. Comparison of calculated and measured broken loop temperature differences during the blowdown phase of Test S-NH-1.

the failure of the broken loop main steam valve to close completely, as shown in Figure 13.

As system pressure continuously decreased after the scram, the safety injection system signal was generated at 2.5 s in the calculation, which was 4 s ahead of the test. Also, when the pumps were tripped off, core steam generation established a flow path from the upper plenum to the upper head and back through the bypass line to the downcomer. This additional vessel drainage path through the bypass line was established at 105 s in the calculation and at 127 s in the experiment.

Primary Boiloff and Core Heatup Phase (150 to 3000 s). The period between the completion of automatic responses in the first 150 s and the initiation of the recovery phase is discussed in this section. This phase is characterized as a period of low depressurization rate and a boiloff of primary inventory leading to core uncovery and core heat up. During this period, auxiliary feedwater flows were terminated on high level signals in the steam generators, but no other automatic or operator-controlled responses occurred. Discussion in this subsection will include the break flow response, system pressure response, system flow response, primary mass distribution, and core heatup phenomena. The break flow discussion includes the results of a sensitivity study.

On an overall basis, RELAP5 undercalculates break flow, resulting in consistently more mass in the primary system throughout this period. A comparison of calculated and measured break flow rates is shown on Figure 18. It can be seen that the calculated break flow was initially higher during the subcooled blowdown period. However, during the phase of saturated liquid blowdown, the calculated break flow was lower, as shown on Figure 18. (In the calculation no bias was set; i.e., $C_D = 1.0$.) The calculated transition from single- to two-phase blowdown occurred at 982 s, which was 179 s earlier than in the test. This is evidenced by the responses of the broken loop cold leg density, which are shown on Figure 19. The fluid density and temperature were different, possibly because of vapor pullthrough and liquid entrainment. The trend of the calculated break flow followed the measured break flow during the two-phase period; however, again the calculated values were lower than the data. The total loss of primary water inventory in the calculation was almost consistently 7 kg (15.4 lbm) less than that measured, as shown on Figure 20, which yields the tendency to calculate a later core uncovery and heatup.

In general, both primary and secondary pressures were calculated to be slighted higher than measured, as shown on Figures 21, 22, and 23. As stated before, the magnitude at which pressure stabilizes is a function of the gross energy balance. For the whole system, such a balance involves core power, external heater power and efficiency, break energy, environmental heat loss, stored energy, and primary-to-secondary heat transfer. The core power was almost identical in both the calculation and test. The external heater power and efficiency and the environmental heat loss are best-estimated from the system characterization test.[a] The Semiscale break flow measurement provides the mass flow rate; however, the fluid quality is unknown. Therefore, there is no basis for comparison between calculated and actual break energy release rates. However, because the predicted break flow rate was quite close to the actual break flow rate and the break area was rather small (0.5%), the difference in the break energy release rate did not play a role of importance in the gross energy balance. The stored energy is a possible area of difference between the test and the calculation. The primary system was heat-soaked at 550 K (530°F) for 2 h in the test; however, full-power initial conditions were maintained for as short of a time as possible due to operational constraints. Thus, it is probable that the stored energy of the system was not at the same initial condition as in the calculation. Another factor that could have affected the overall energy balance, and thus the primary pressure, is the RELAP5 modeling of global heat loss.

After the coolant pumps were tripped, a two-phase natural circulation flow was established during the second phase, as shown on Figures 24 and 25. It can be seen that there was a certain amount of flow sustained in the downcomer, which terminated before the complete drainage of the intact loop steam generator. RELAP5 correctly calculated the two-phase peaking in flow with a slight shift in time. This peaking in flow is related to system mass inventory and is discussed in detail in Reference 7.

The calculated primary mass distribution generally agreed with the test measurement[b] during this phase. Exceptions were the broken loop steam generator liquid hold-up and the timing of events

---

a. W. A. Owca, Letter to Distribution, "System Heat Loss Test Summary," WAO-12-84, December 1984.

b. Until the primary coolant pumps were tripped off, it was not possible to accurately distinguish the primary system mass inventory distribution in the experiment, because liquid level measurements are determined from differential pressure measurements in the test which are sensitive to two-phase flow effects.

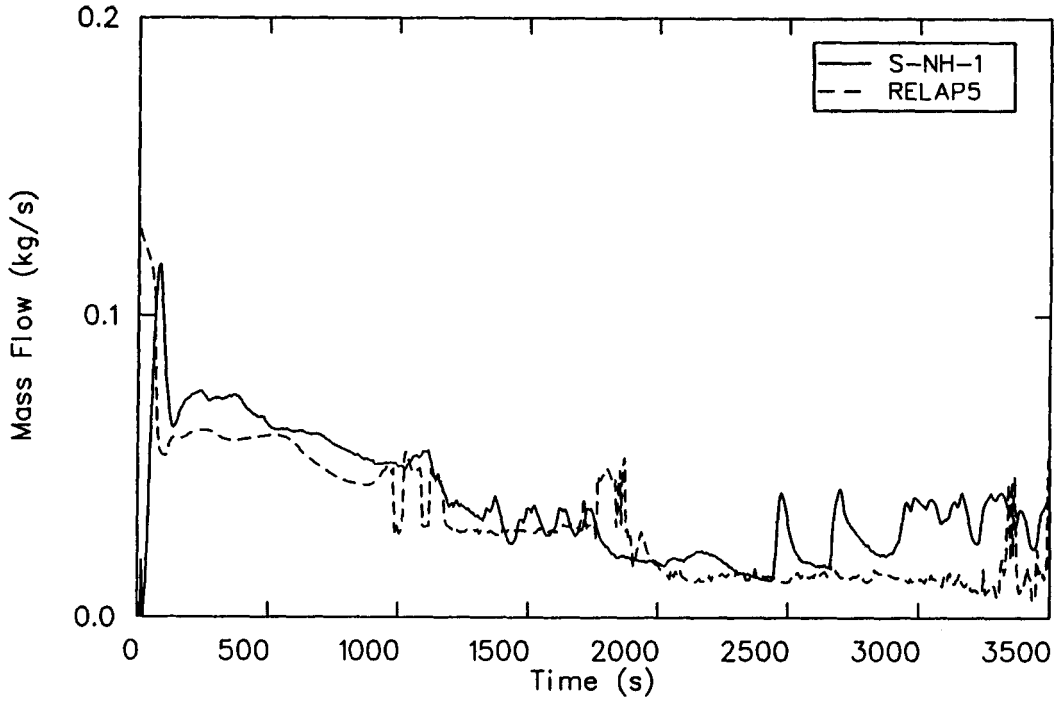

Figure 18. Comparison of calculated and measured break flow rates during the primary boiloff and core heatup phase of Test S-NH-1.

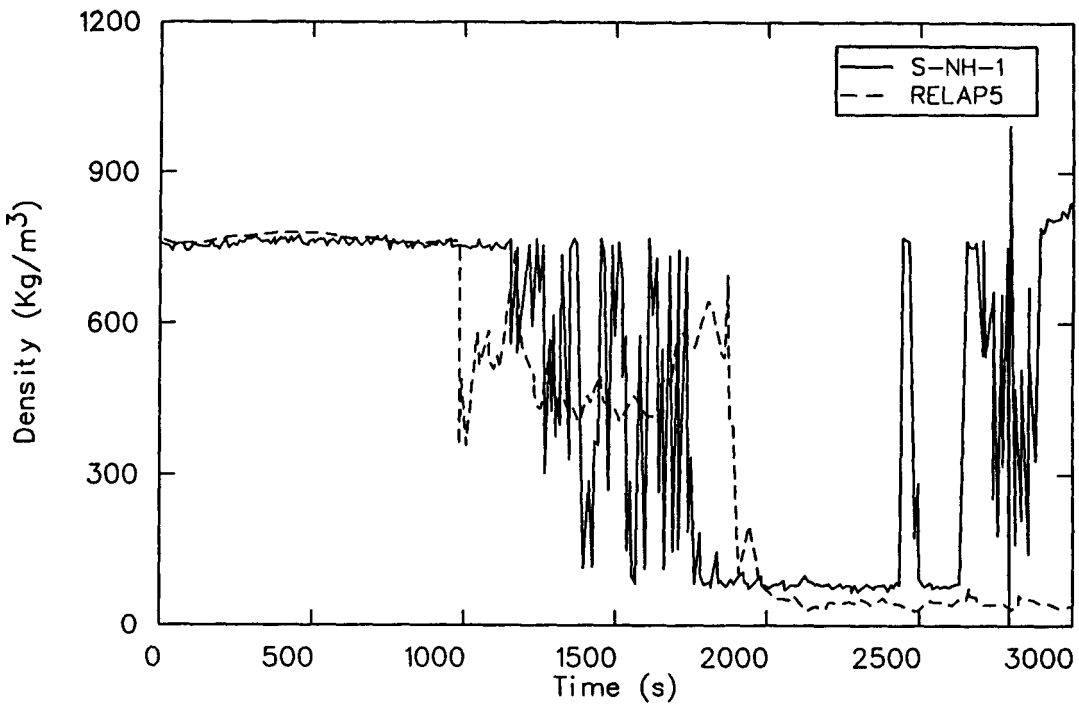

Figure 19. Comparison of calculated and measured broken loop cold leg densities during the primary boiloff and core heatup phase of Test S-NH-1.

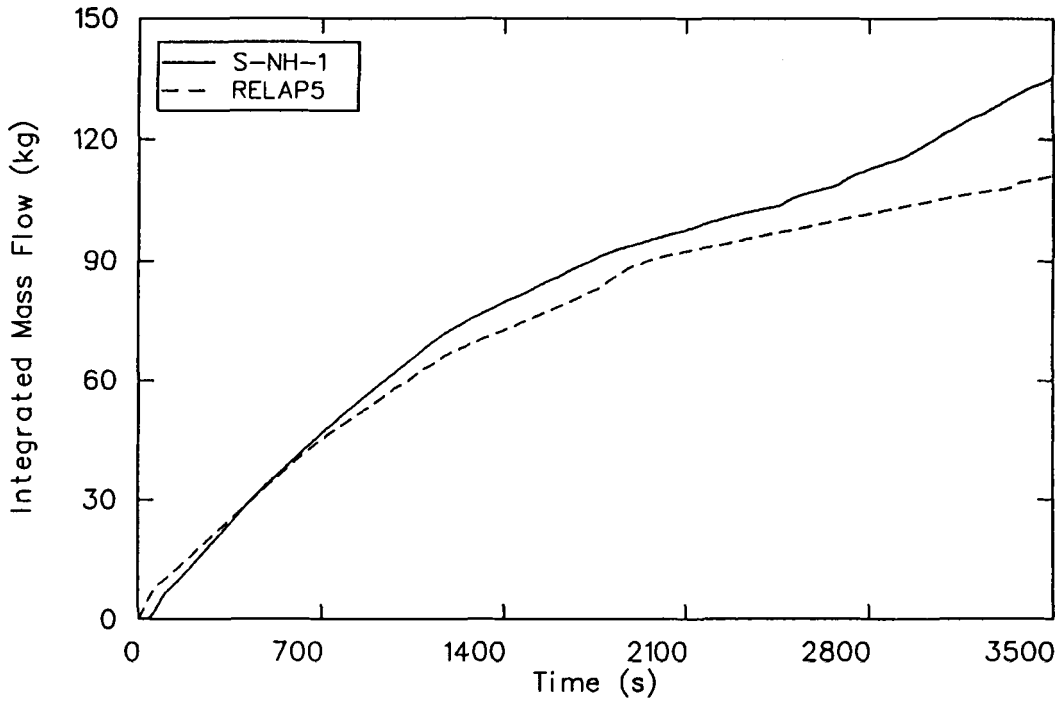

Figure 20. Comparison of calculated and measured integrated break flows during the primary boiloff and core heatup phase of Test S-NH-1.

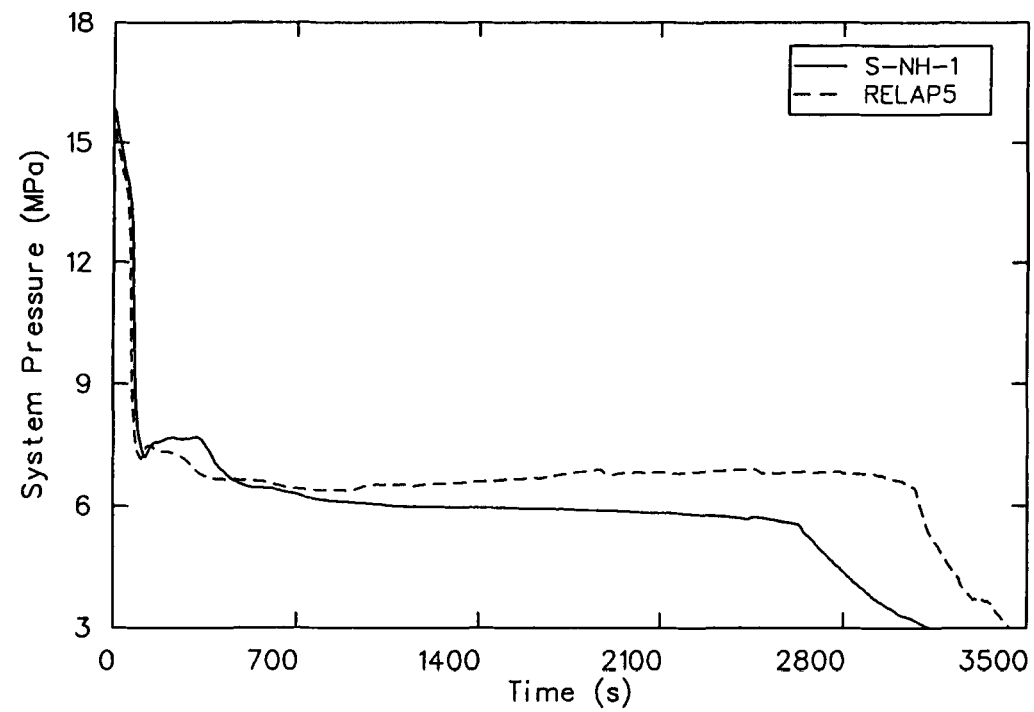

Figure 21. Comparison of calculated and measured primary system pressures during the primary boiloff and core heatup phase of Test S-NH-1.

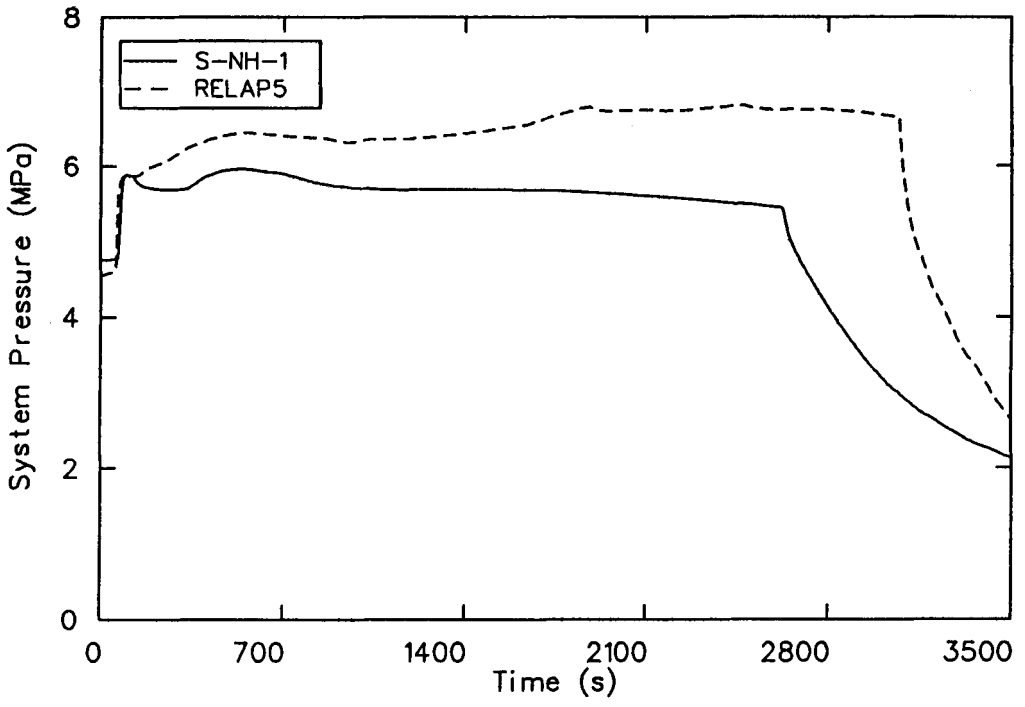

Figure 22. Comparison of calculated and measured intact loop steam generator pressures during the primary boiloff and core heatup phase of Test S-NH-1.

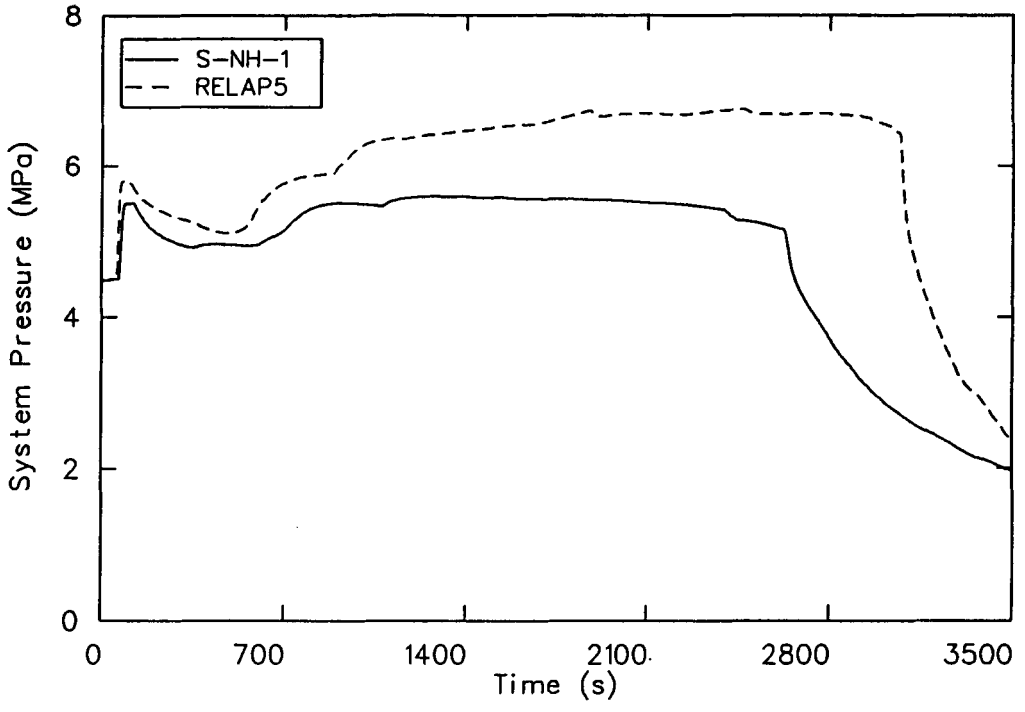

Figure 23. Comparison of calculated and measured broken loop steam generator pressures during the primary boiloff and core heatup phase of Test S-NH-1.

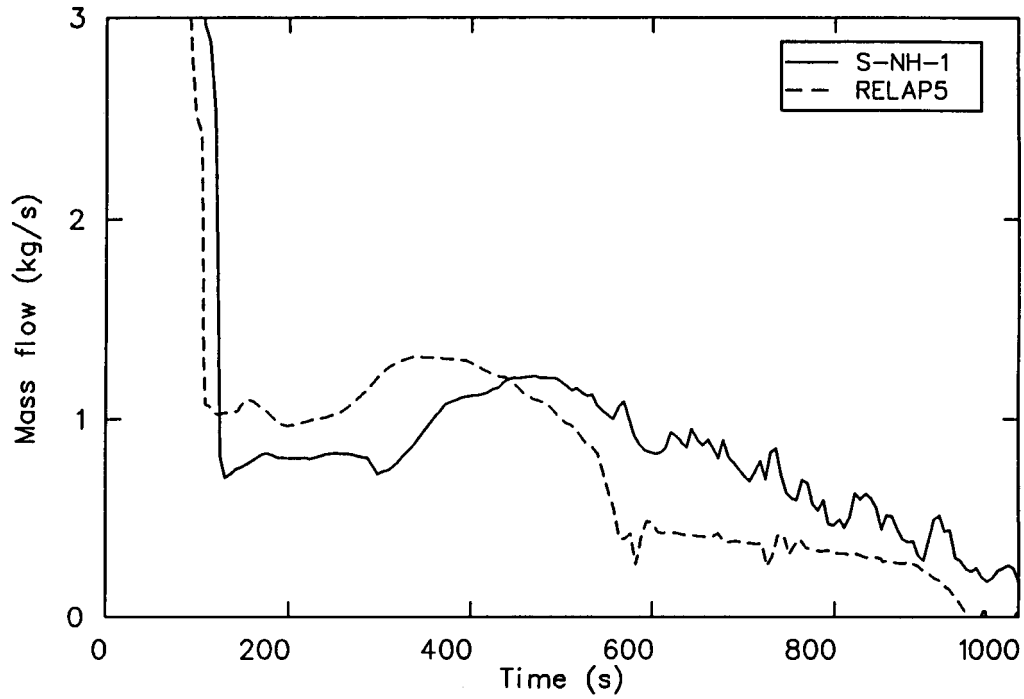

Figure 24. Comparison of calculated and measured downcomer flow rates of Test S-NH-1.

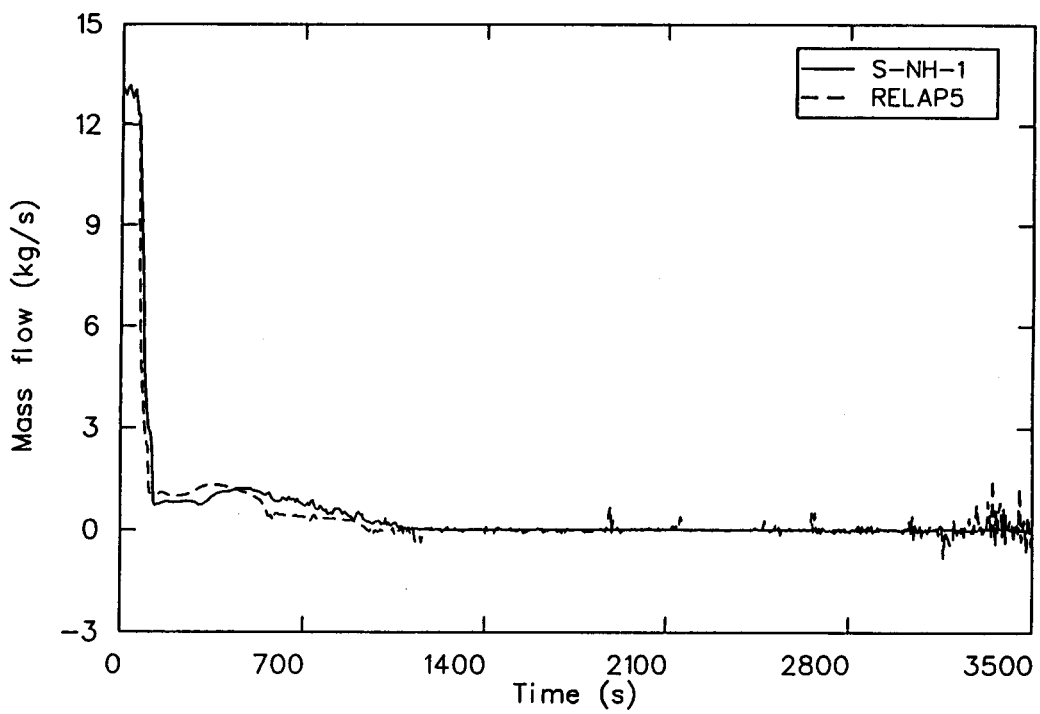

Figure 25. Comparison of calculated and measured downcomer coolant flow rates during the primary boiloff and core heatup phase of Test S-NH-1.

mainly caused by the difference in break flow. The primary system void formation generally progressed from the top down. The sequence of system drainage was as follows: pressurizer, upper vessel, hot and cold legs, primary U-tubes, pump suctions, and finally the downcomer and core.

Following the pressurizer drain, the code correctly calculated the drain of the upper head. The upper head fluid was calculated to drain earlier but with a slightly slower rate than in the test (Figure 26). This was probably caused by a higher calculated subcooled break flow followed by a lower saturated liquid break flow. Comparison of the calculated and measured vessel upper plenum liquid levels is shown on Figure 27. It also can be seen that before the level in the test dropped below the hot leg elevation, the calculation and the test levels were in good agreement. However, as a result of a higher single-phase break flow, the level in the test dropped across the elevation of the hot legs earlier than in the calculation by 540 s. A sudden drop of the level in the calculation at 1600 s was caused by a peak of break flow at the same time which resulted from the water expulsion of the broken loop pump suction. This will be described later.

The steam generator U-tubes started to drain at approximately the same time as the vessel. For both intact and broken loops, the drainage started about 160 s earlier in the calculation, as shown on Figures 28 and 29. The reason for early drainage of the steam generator in the calculation is also related to differences in break flow. Significant liquid hold-up was measured in the broken loop steam generator but not calculated by the code. In the calculation, the broken loop steam generator was empty by 1070 s. However, the data showed 5 m (197 in.) of head. It is not clear what effect the small leak in the secondary steam line (shown on Figure 13) had on the overall heat sink and liquid holdup. The disagreement between RELAP5 and the data could have also been caused by primary-to-secondary heat transfer differences. Even though in the data the broken loop steam generator was at a lower pressure than calculated (possibly because of the leak), the steam generator remained a heat sink for both the test and the code. Therefore, the code should have calculated condensation occurring in the primary tubes, indicated by a head of fluid rather than the 0 m (0 in.) level shown on Figure 29.

Following the drain of the steam generators, the pump suctions also started to drain, as shown on Figures 30 through 33. In the calculation, the drain was clear after the upflow side and the steam generator were empty. When drainage started, a sudden expulsion of water from the broken loop pump suction to the cold leg was observed in the calculation. As a result, a sudden drop of liquid level in the pump suction and a corresponding increase of cold leg density were observed, as shown on Figures 32, 33, and 19. In turn, a peak of the break flow was induced (Figure 18).

After the draining of the steam generators and partial draining of the pump suctions, the vessel and downcomer liquid levels decreased at a similar rate in both the calculation and the test, as fluid in the vessel simply boiled off (shown on Figures 34 and 35). Because of differences in the draining of loop components (most notably), the boiloff of vessel fluid started about 700 s later for the code than the data. With similar boiloff rates, the code showed a core heat-up about 560 s after the data, as shown on Figure 36. The temporary turnaround in core rod temperature in the data was due to the partial broken loop suction clearing. Relief of the liquid plug in the broken loop suction allowed a brief refill of the vessel; however, continued boiloff reinstated the ongoing core rod temperature excursion seen on Figure 36.

Finally, the recovery setpoint [peak cladding temperature (PCT) = 811 K (1000°F)] was reached at 2630 s in the test, which was about 442 s earlier than in the calculation. Except for differences in event timing, caused by differences in system drain and break flow, the core temperature responses to the vessel level and the core heatup rate show good agreement between the calculation and the test.

Because the primary forcing phenomenon in this transient was the break flow, a sensitivity study was performed. For the base-case study, the break flow was significantly underpredicted using a downward orientation with horizontal stratification and a one-velocity momentum equation. (The logical choice of break modeling would be to use a normal central orientation junction. However, this method had been used for a pretest calculation, and a general trend of underestimation of liquid entrainment was observed.) The sensitivity study consisted of using the base-case break configuration with a two-velocity momentum equation. The break flow for the sensitivity calculation is shown in Figure 37. The mass flow out the break was significantly underpredicted; and, as a result, sufficient primary system inventory was maintained to prevent a core heat-up until 1300 s after the observed core heat-up (Figure 38). In the base case, shown in Figure 36, the core heat-up was calculated to occur about

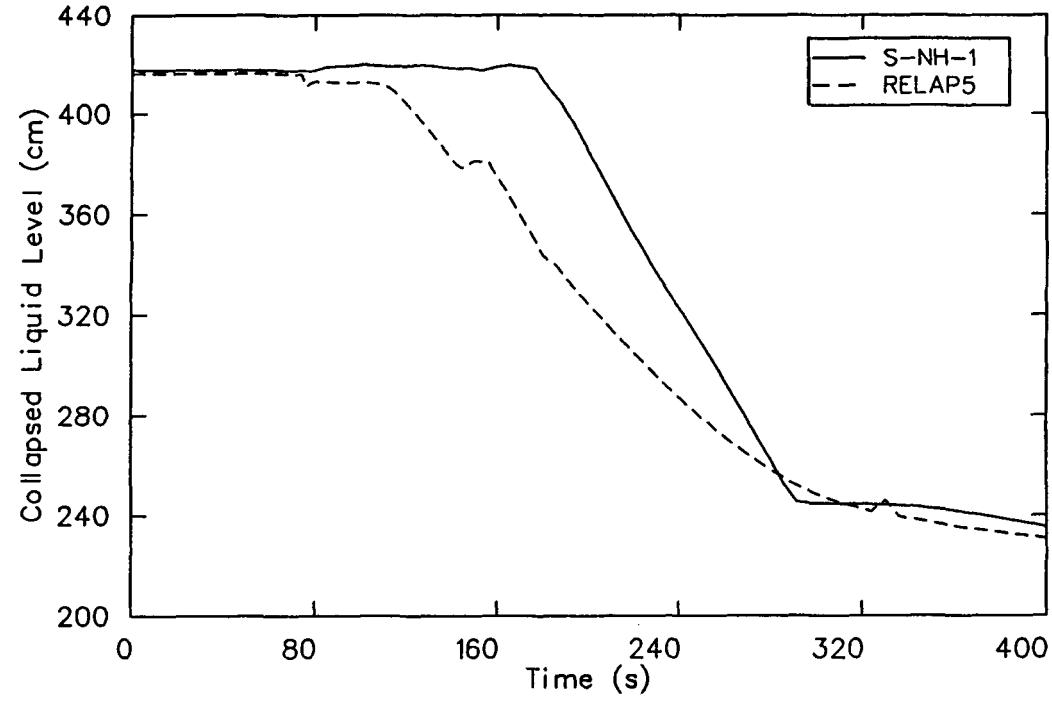

Figure 26. Comparison of calculated and measured liquid levels in the vessel head during the primary boiloff and core heatup phase of Test S-NH-1.

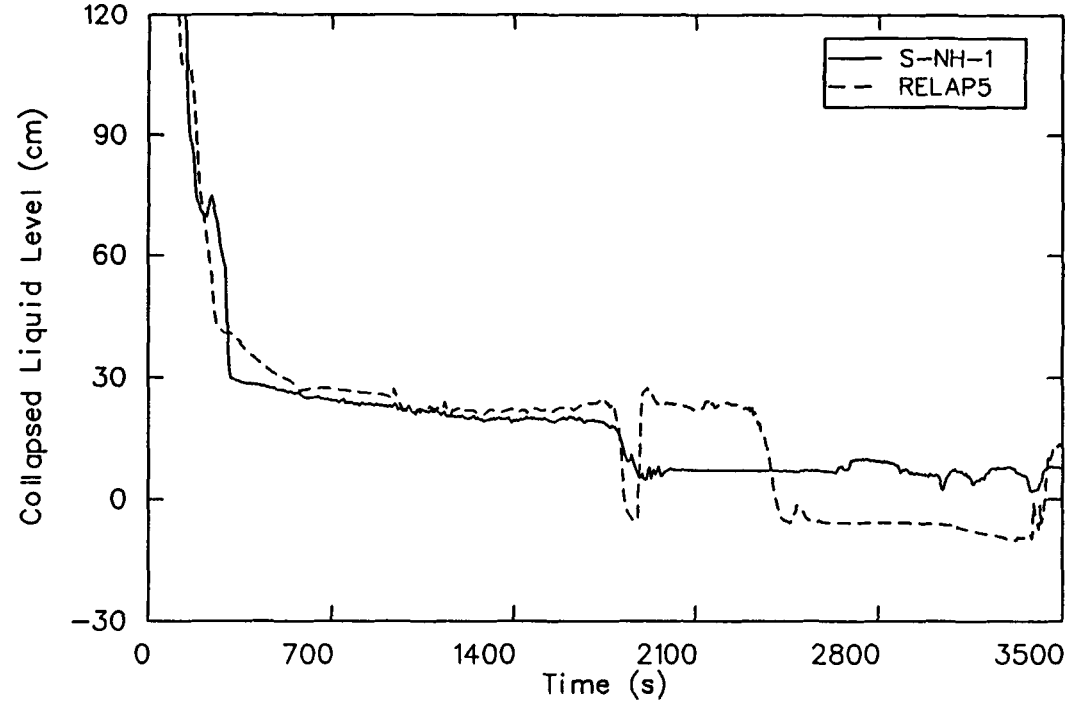

Figure 27. Comparison of calculated and measured liquid levels in the vessel upper plenum during the primary boiloff and core heatup phase of Test S-NH-1.

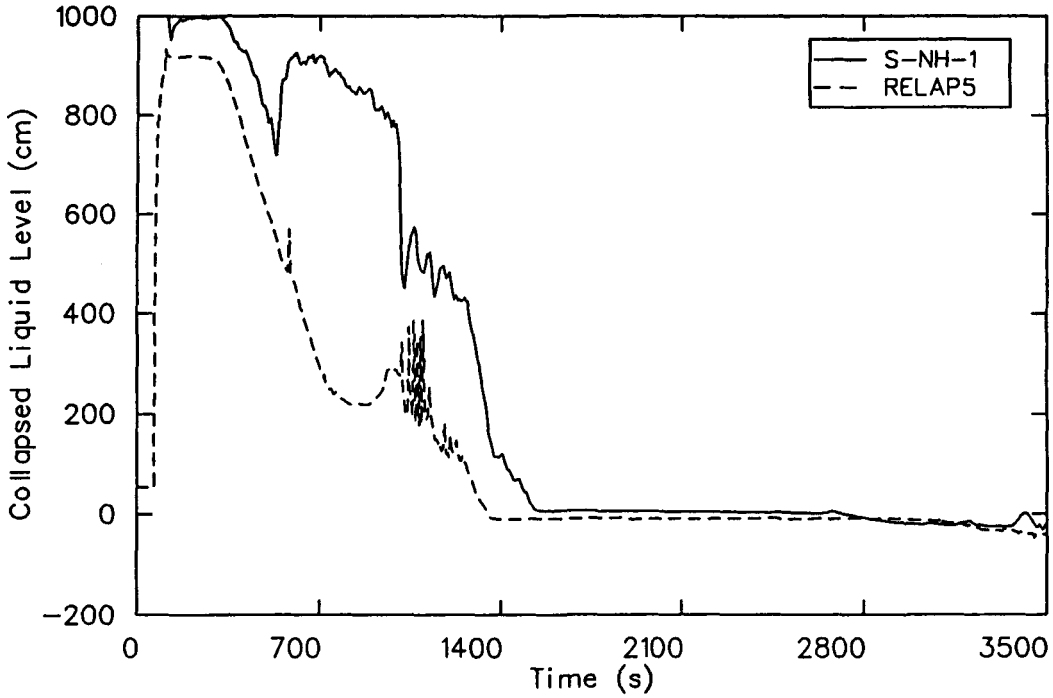

Figure 28. Comparison of calculated and measured liquid levels in intact loop steam generator during the primary boiloff and core heatup phase of Test S-NH-1.

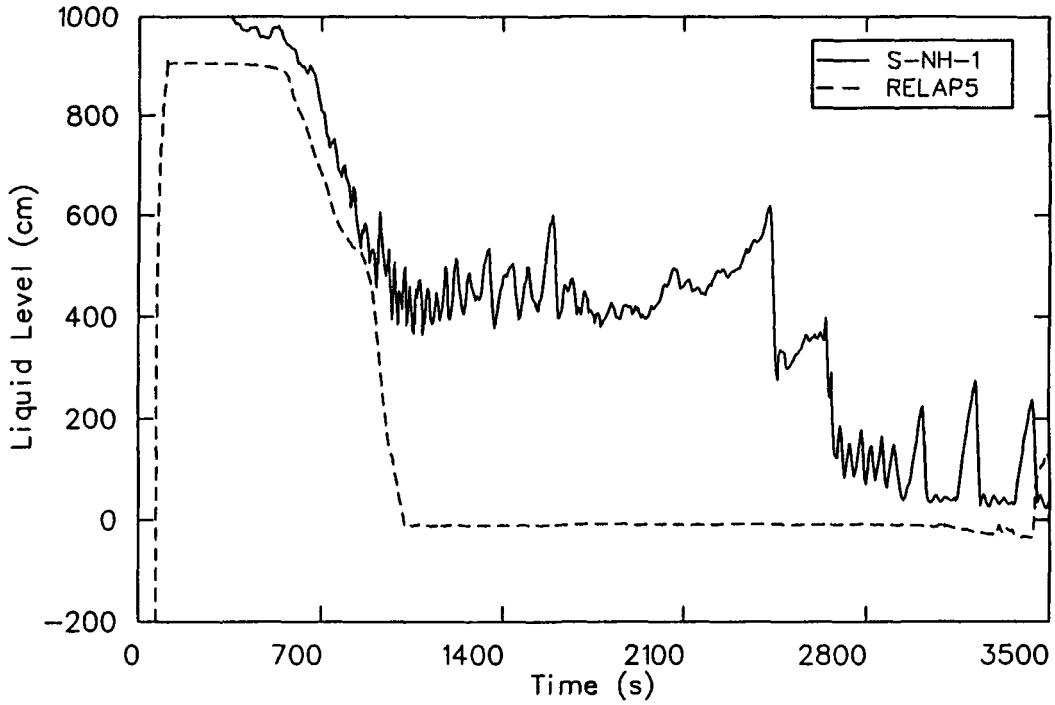

Figure 29. Comparison of calculated and measured liquid levels in broken loop steam generator during the primary boiloff and core heatup phase of Test S-NH-1.

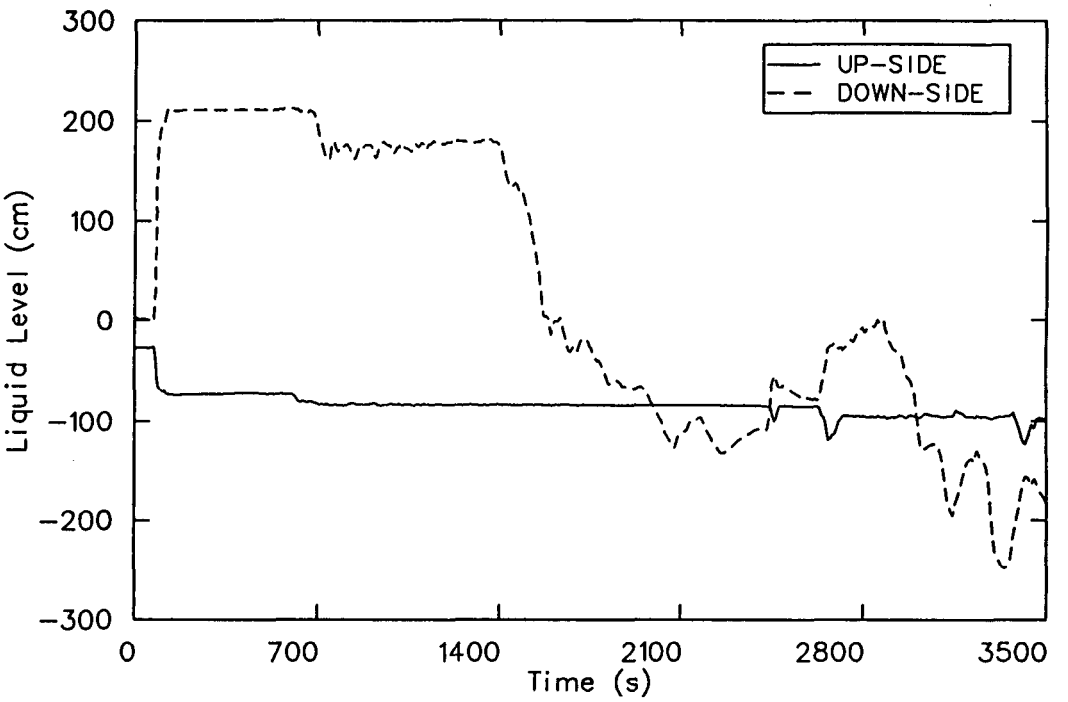

Figure 30. Comparison of measured liquid levels in intact loop pump suction during the primary boiloff and core heatup phase of Test S-NH-1.

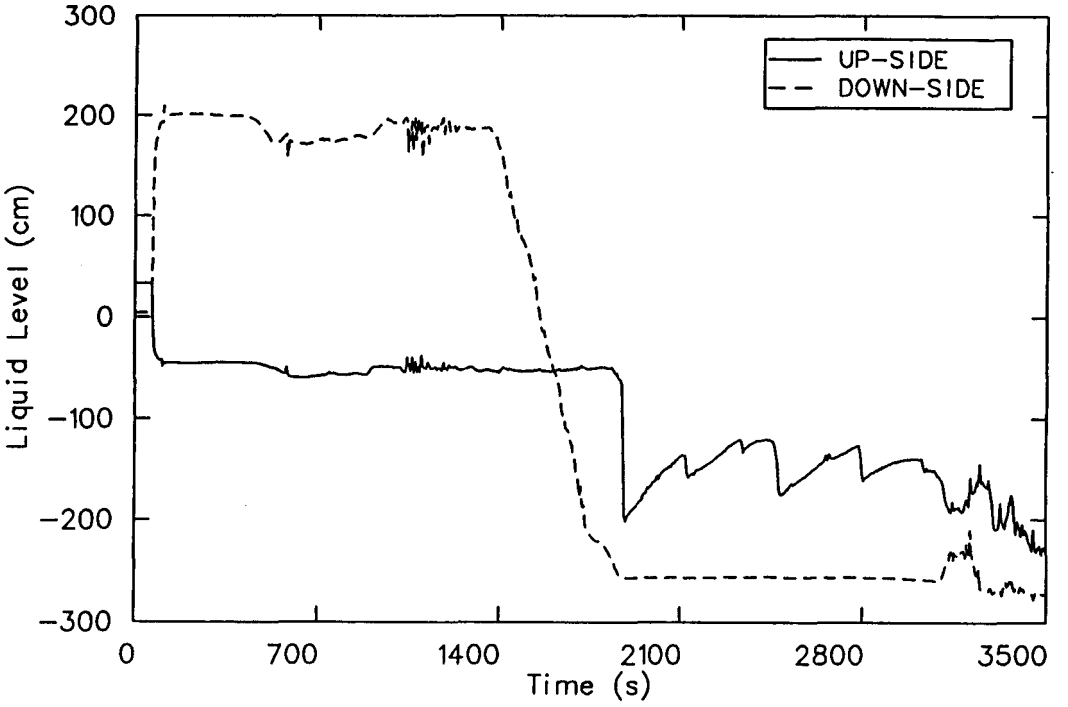

Figure 31. Comparison of calculated liquid levels in intact loop pump suction during the primary boiloff and core heatup phase of Test S-NH-1.

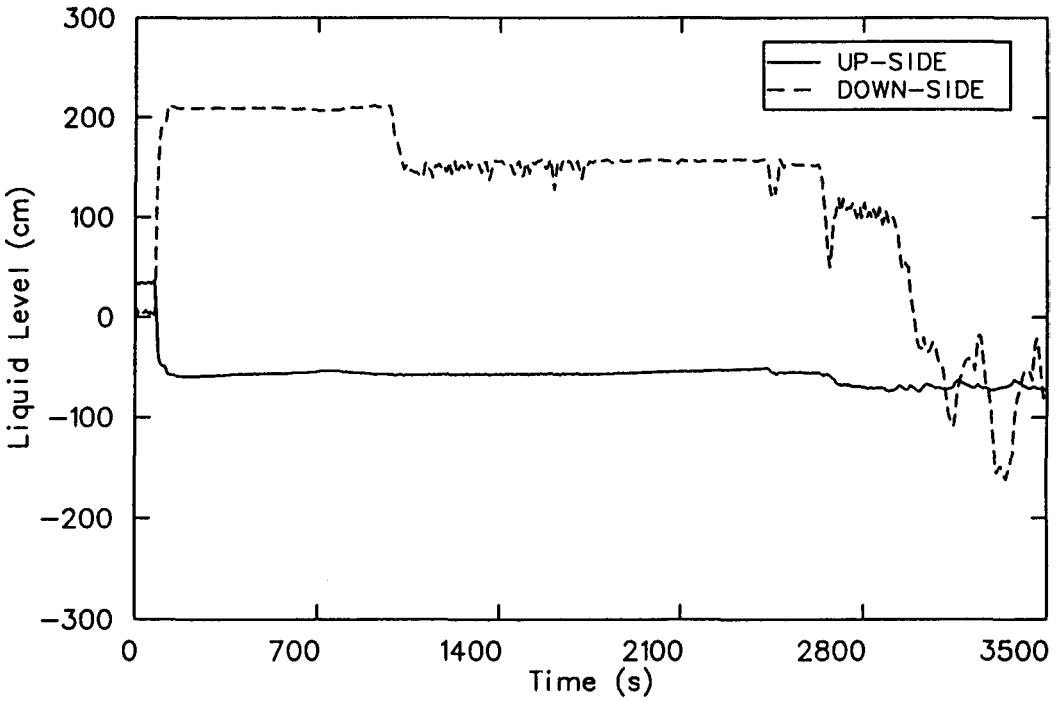

Figure 32. Comparison of measured liquid levels in broken loop pump suction during the primary boiloff and core heatup phase of Test S-NH-1.

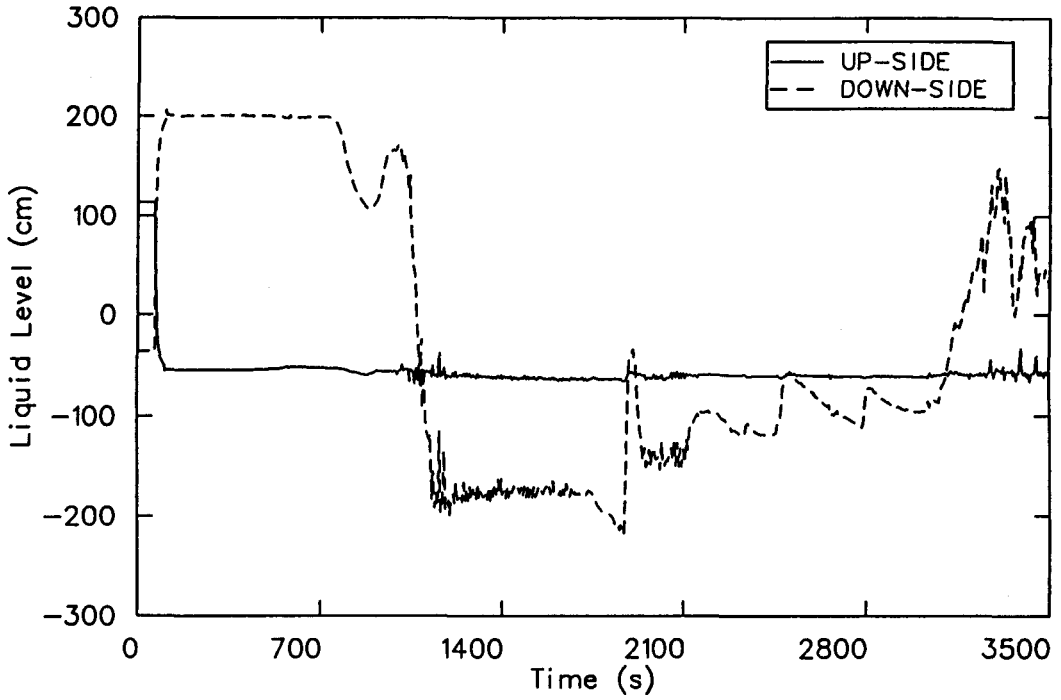

Figure 33. Comparison of calculated liquid levels in broken loop pump suction during the primary boiloff and core heatup phase of Test S-NH-1.

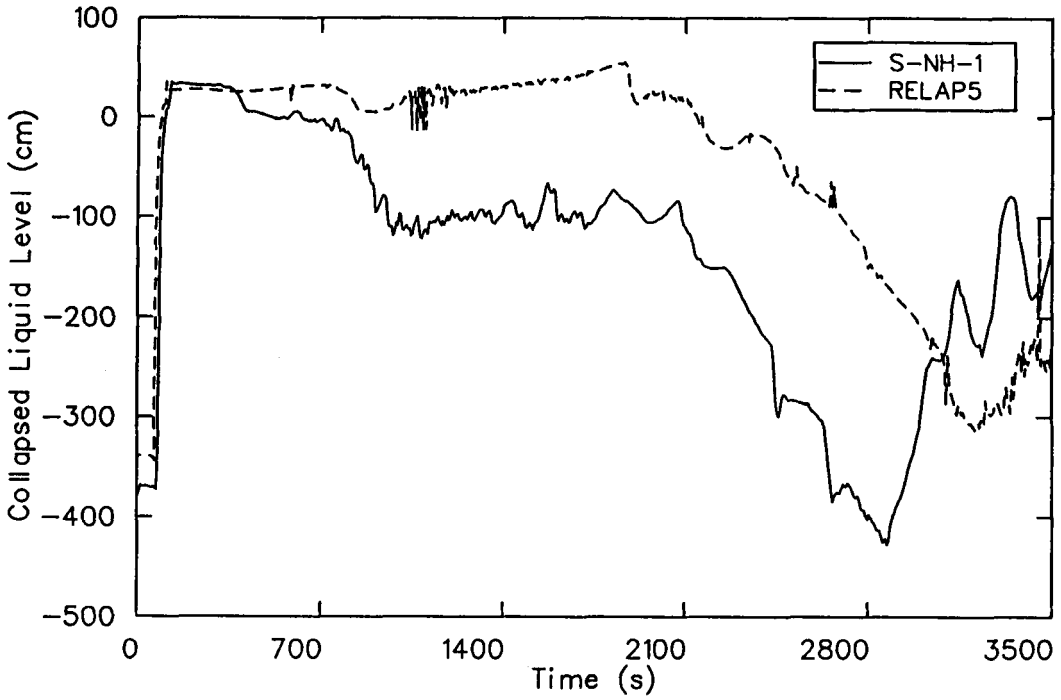

Figure 34. Comparison of calculated and measured downcomer liquid levels during the primary boiloff and core heatup phase of Test S-NH-1.

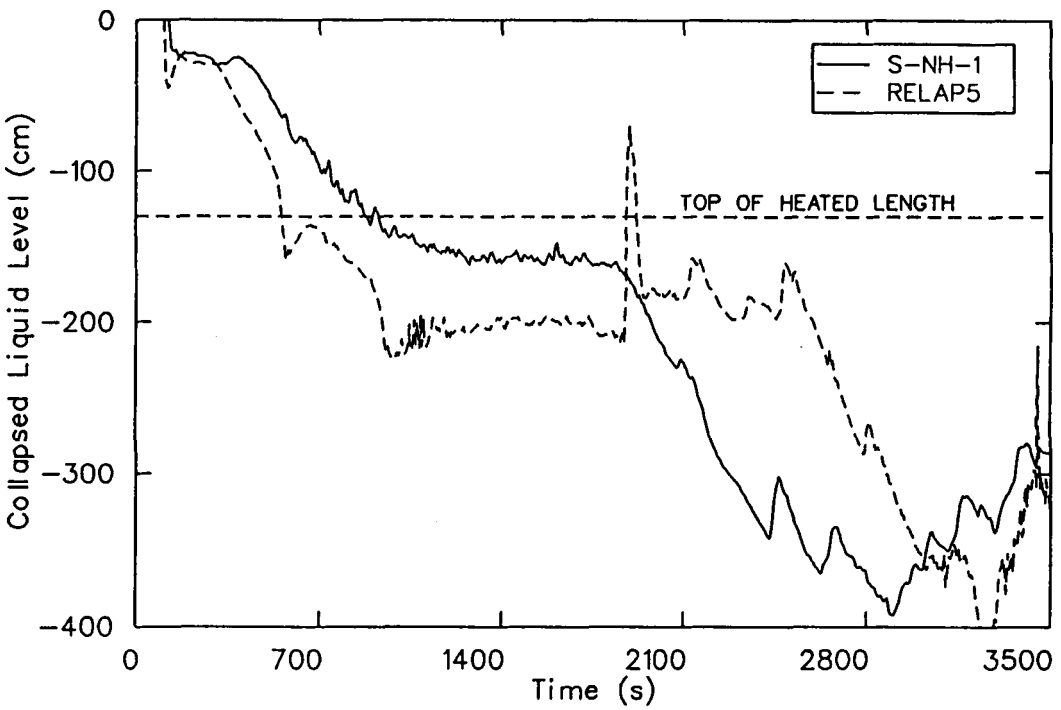

Figure 35. Comparison of calculated and measured vessel liquid levels during the primary boiloff and core heatup phase of Test S-NH-1.

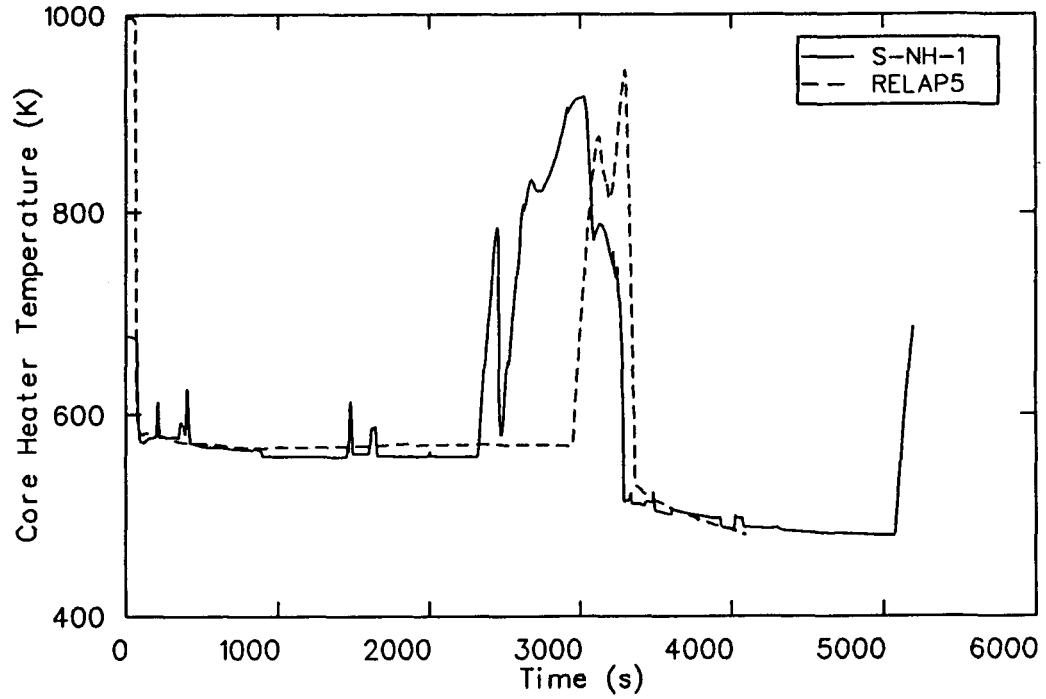

Figure 36. Comparison of calculated and measured peak cladding temperatures during the primary boiloff and core heatup phase of Test S-NH-1.

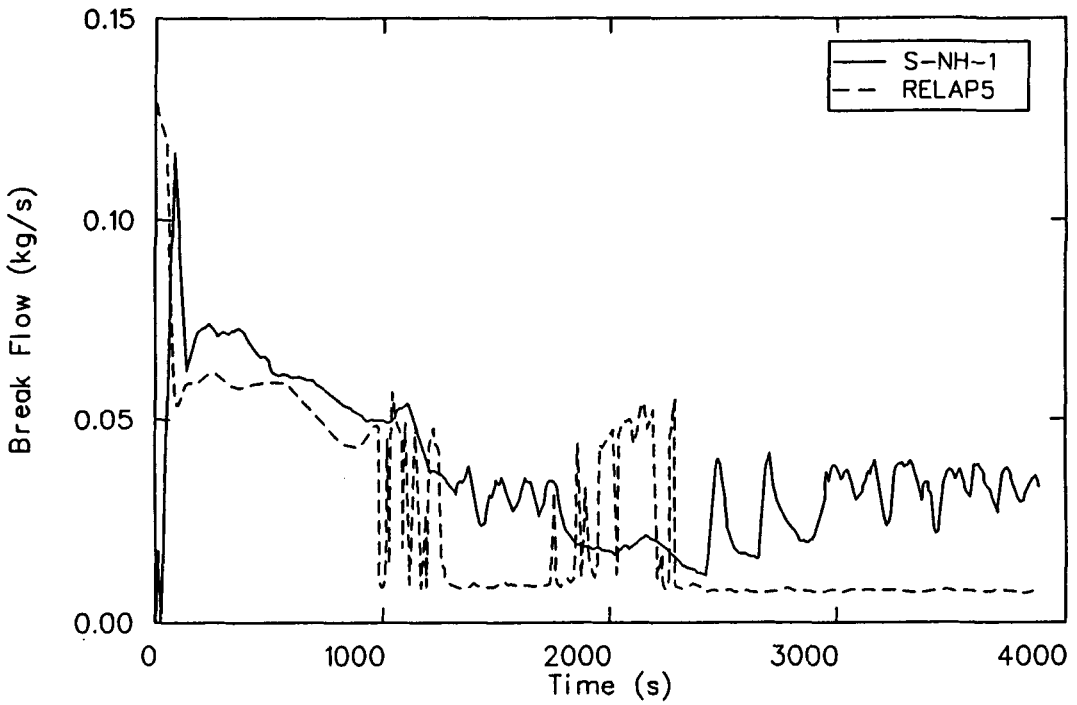

Figure 37. Comparison of the calculated and measured break flow (sensitivity study) of Test S-NH-1.

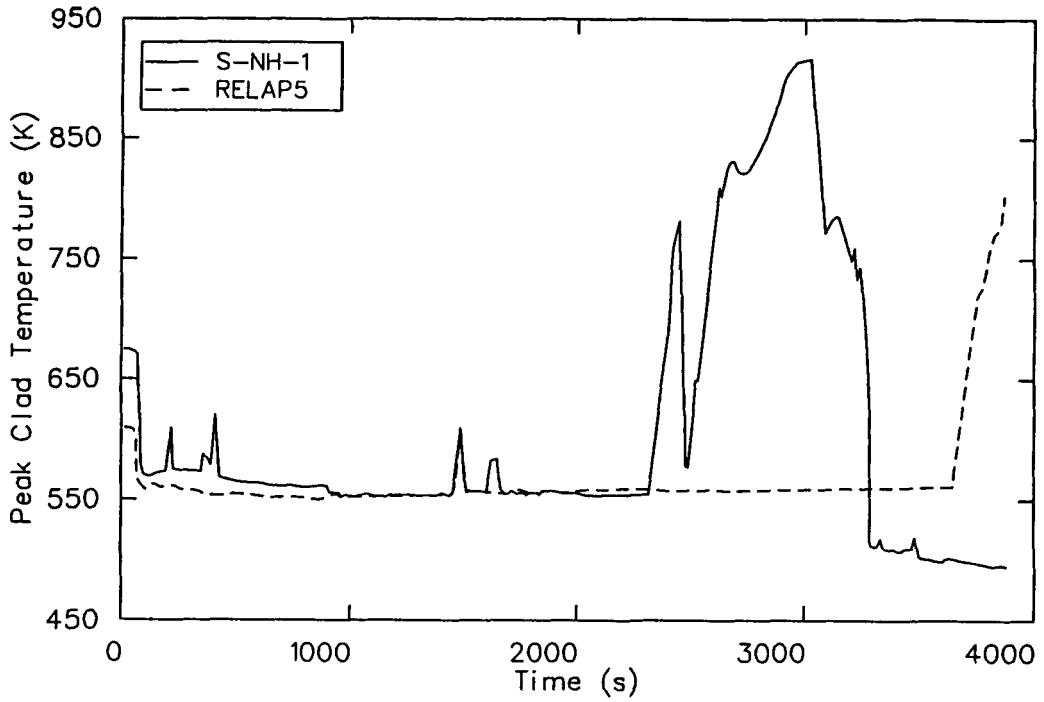

Figure 38. Comparison of the calculated and measured peak cladding temperatures (sensitivity study) of Test S-NH-1.

560 s after the observed occurrence. Clearly, of the two methods, the one-velocity momentum equation provided the better prediction of the mass flow at the break (see Figure 18).

Recovery Phase (3000 to 5000 s). The period between initiation of recovery actions and the test termination is discussed in this section. Recovery actions consisted of latching open both steam generator ADV valves while feeding with auxiliary feedwater and normal accumulator injection. The recovery action was taken to promote system depressurization to the accumulator and LPIS set points. Recovery was initiated when the PCT reached 811 K (1000°F), which occurred at 2630 s in the test and 3072 s in the calculation, as shown on Figure 36.

When the PCT reached 811 K (1000°F), the ADV valve on each steam generator was manually lifted and steam flow drastically increased, as shown on Figures 39 and 40 for each steam generator. Except for the timing, the calculated and measured ADV relief flows are in good agreement. As a result of ADV relief, the shell side of the steam generators depressurized significantly, as shown on Figures 41 and 42. The calculated depressurization rate in each steam generator was faster than measured. In turn, a faster primary system depressurization in the calculation resulted, as shown on Figure 43. There are two likely causes for the difference between the calculated and actual depressurization rates in the steam generators. The first possibility is that the energy relief rates through the ADV valves were different, and the second possibility is that the stored energy in the system metal and the corresponding rate of energy release were different. Since experimental information relating to the energy relief rates through the ADV valves was not provided, an alternate way to represent the steam flow was used so that an indirect judgment of difference in energy relief could be made. Energy relief rate is strongly related to the quality of relieved steam at a given pressure, and dependent upon the quality of steam. Under such circumstances, if the relief flow rates at a given pressure were the same, the energy relief rates via the relief flow at such a given pressure should not be different. The calculated and measured ADV relief flows versus pressure of both the intact loop and the broken loop steam generators are shown on Figures 44 and 45. It can be seen that both calculated and measured ADV relief flow rates were quite close at the same pressure. Based on the above, it can be concluded that at the same pressure, the difference in energy relief rates should not

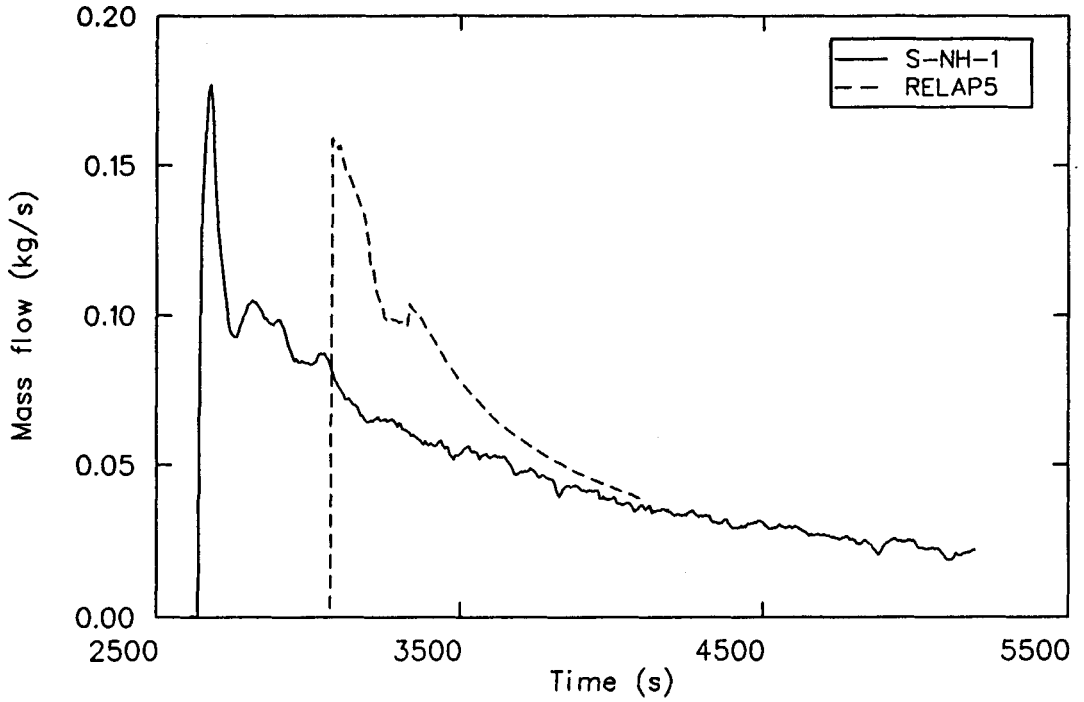

Figure 39. Comparison of calculated and measured intact loop steam generator ADV relief flow during the recovery phase of Test S-NH-1.

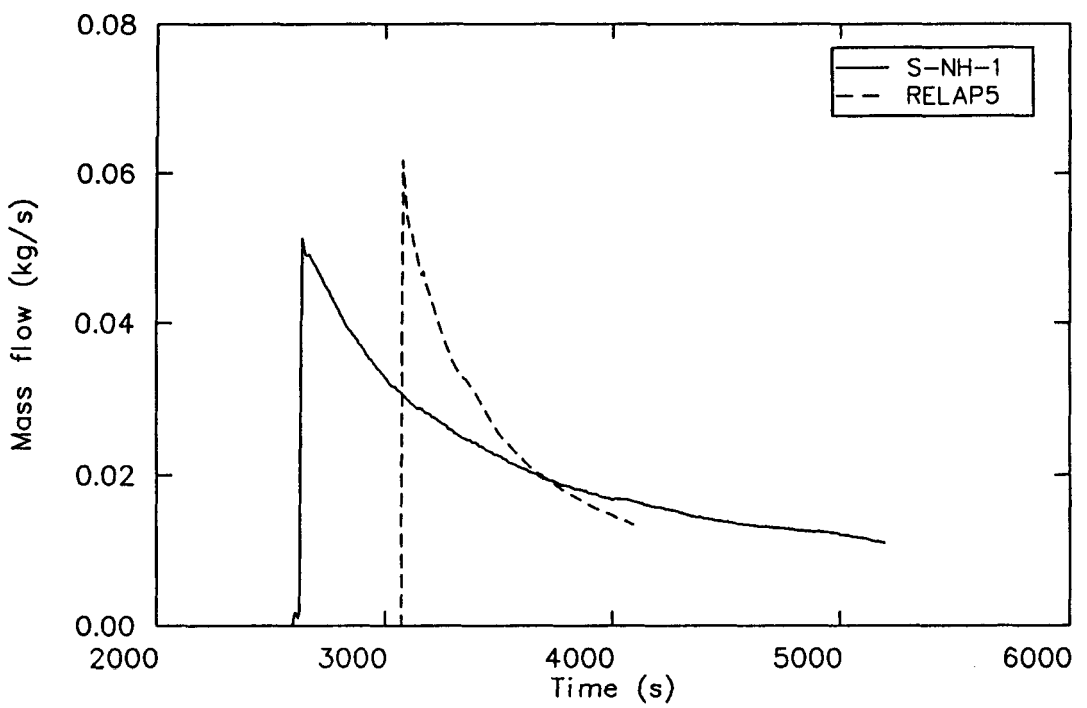

Figure 40. Comparison of calculated and measured broken loop steam generator ADV relief flow during the recovery phase of Test S-NH-1.

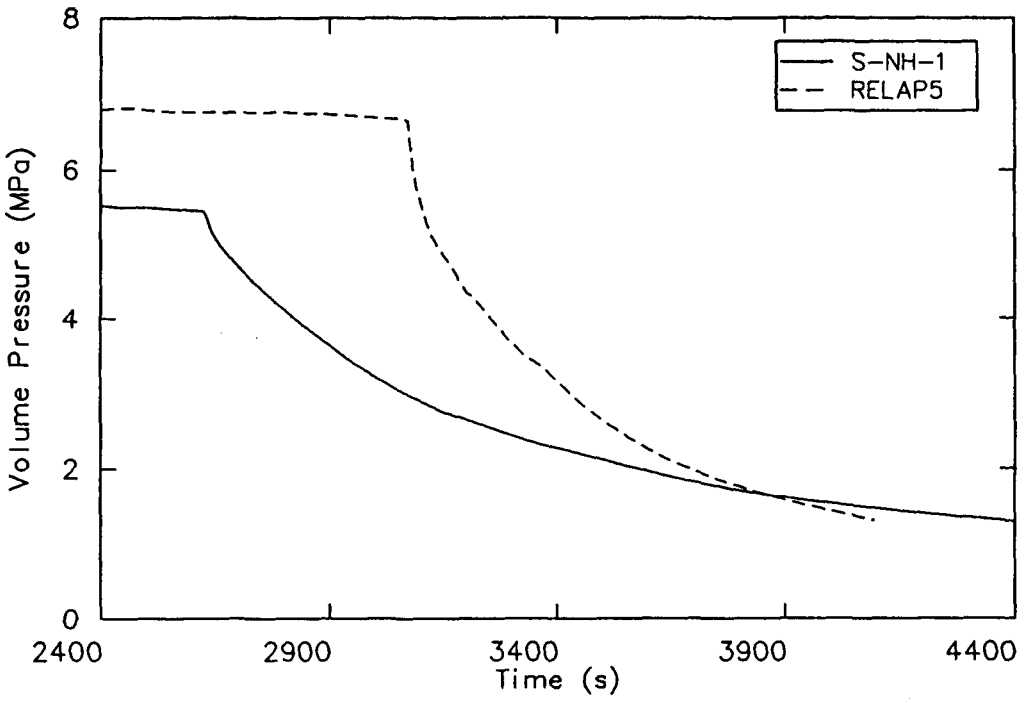

Figure 41. Comparison of calculated and measured intact loop steam generator pressures during the recovery phase of Test S-NH-1.

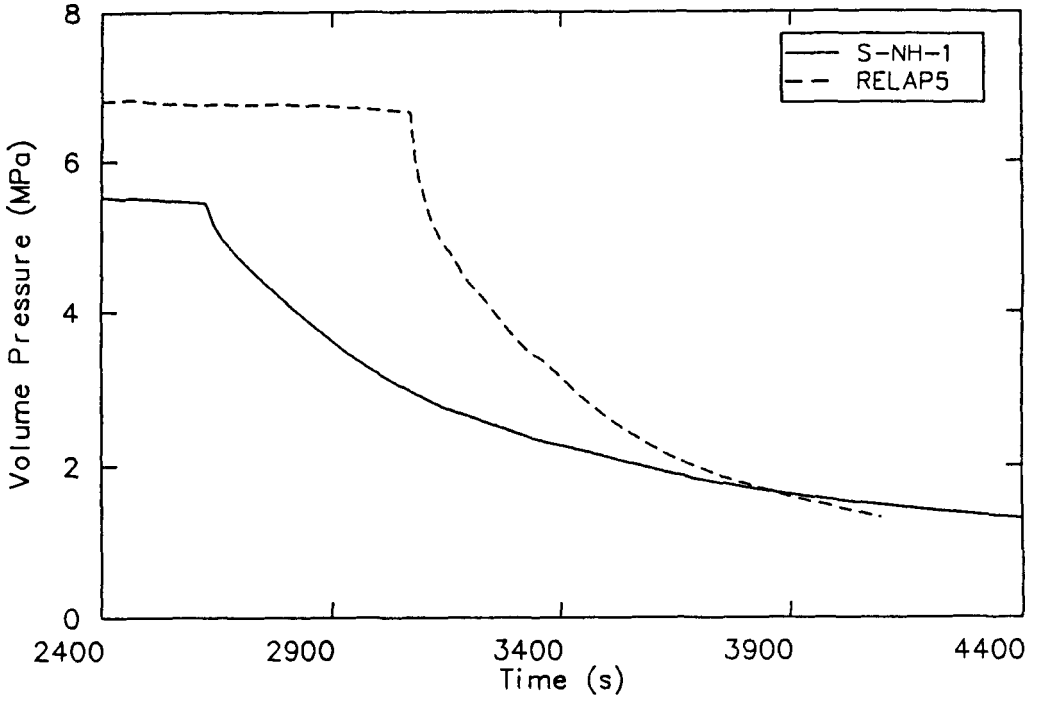

Figure 42. Comparison of calculated and measured broken loop steam generator pressures during the recovery phase of Test S-NH-1.

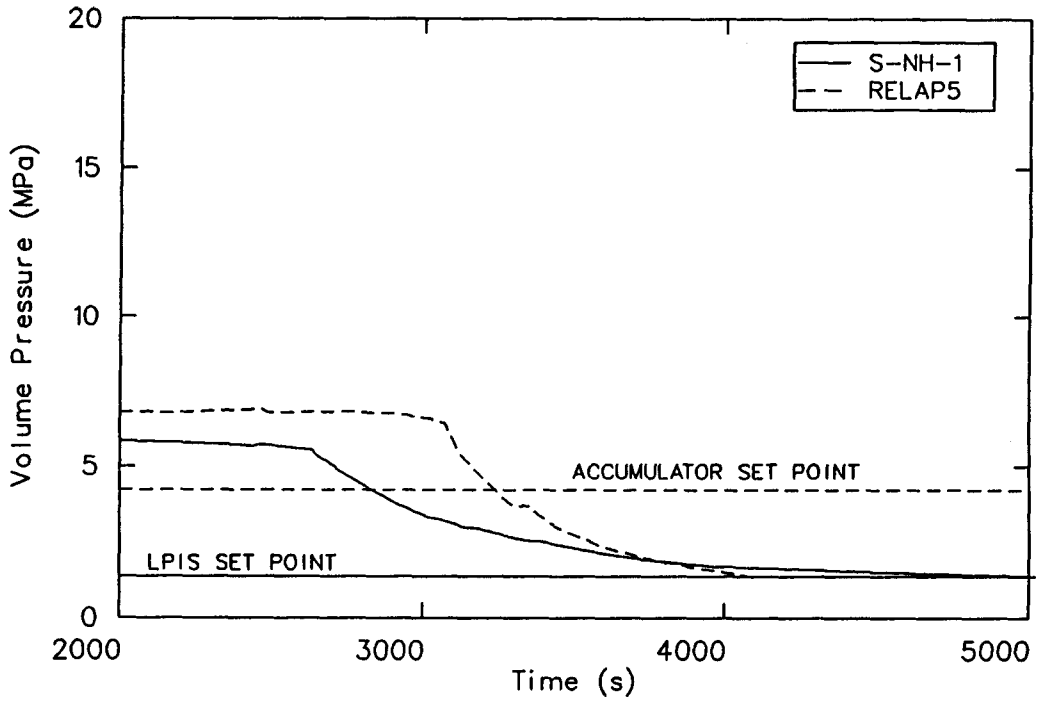

Figure 43. Comparison of calculated and measured primary system pressures during the recovery phase of Test S-NH-1.

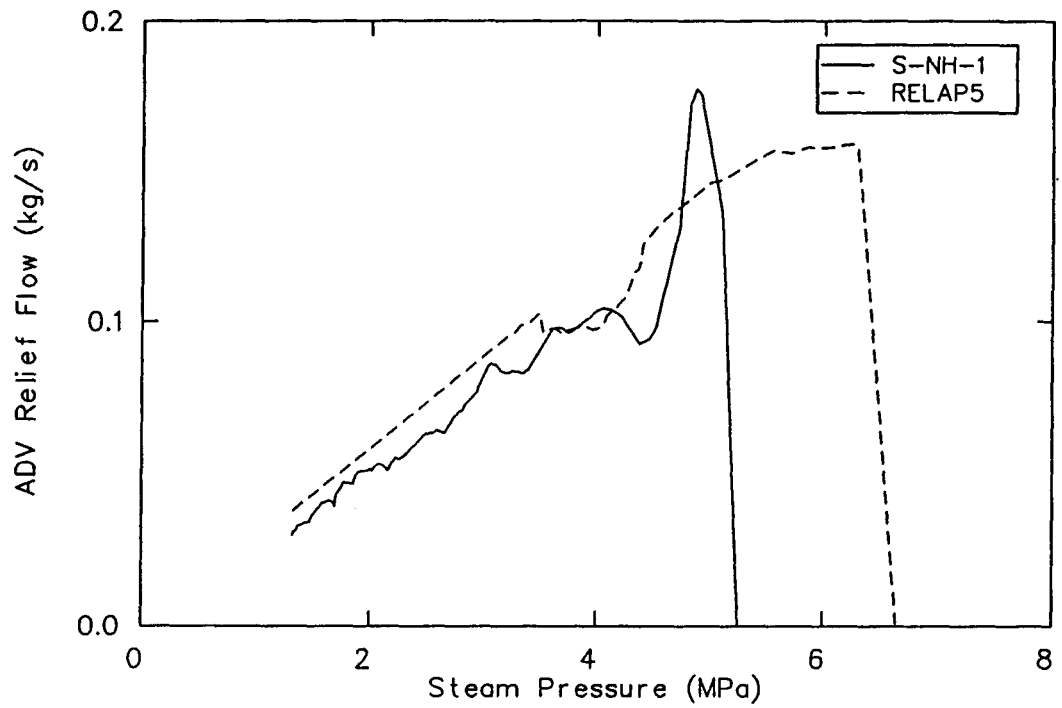

Figure 44. Comparison of calculated and measured intact loop steam generator ADV relief flow versus pressure during the recovery phase of Test S-NH-1.

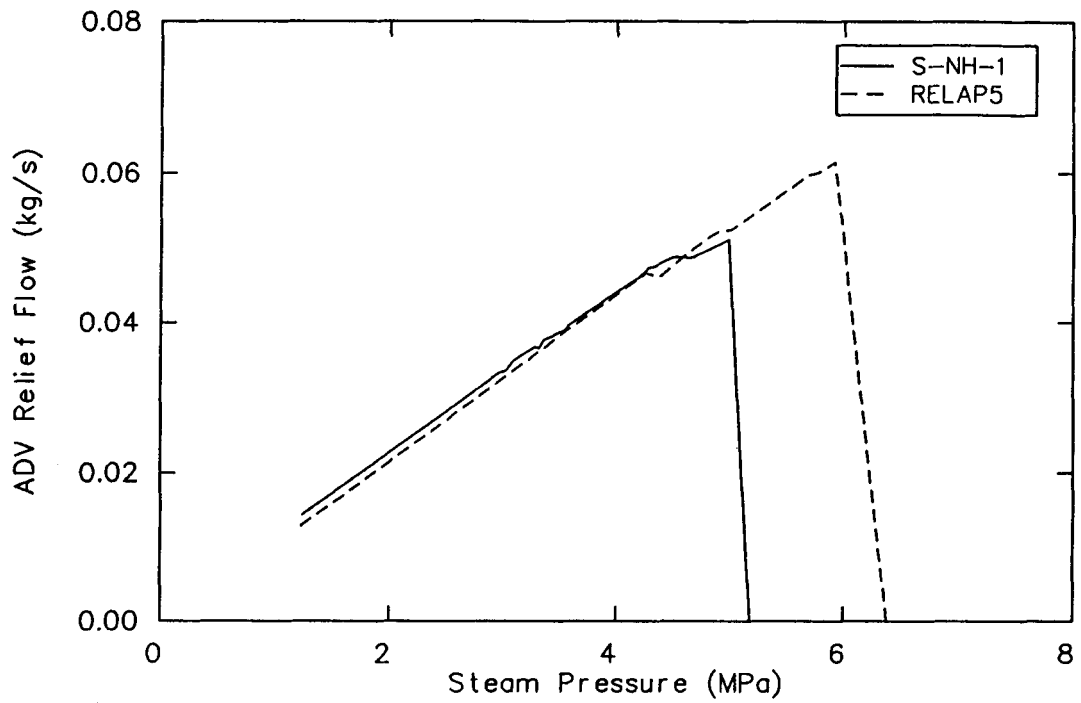

Figure 45. Comparison of calculated and measured broken loop steam generator ADV relief flow versus pressure during the recovery phase of Test S-NH-1.

play a role of importance in the different system depressurization rates.

During a rapid depressurization, heat transferred from hot metal to the fluid will generate steam, thereby slowing the depressurization. If more energy were released to the fluid in the test, it would appear as a slower depressurization than in the calculation. As evidence of this, the measured temperature difference between the hot metal and fluid was much higher than in the calculation at the same pressure, as shown on Figure 46. This appeared to be true for voided areas more than for liquid-filled volumes in the steam generators. The metal temperatures generally followed saturation temperature in liquid-filled volumes in both the test and calculation. Possible reasons for the discrepancy in temperature differences are either an incorrect heat-transfer-area-to-volume ratio for the calculation or an underpredicted heat transfer coefficient for energy transfer from the metal in the calculation. Also, the inability to simulate axial heat transfer in the steam generator walls with the RELAP5 code would contribute to the discrepancy. As shown on Figure 44, more moisture likely existed in the test, which may have produced a slightly higher actual heat transfer coefficient than was calculated.

As a result of the faster primary depressurization rate in the calculation, the accumulator injection set point [4.2 MPa (600 psia)] was reached earlier in the test than in the calculation (2828 s in the test versus 3232 s in the code). The faster depressurization rate contributed to the faster core quench shown on Figure 36. The accumulators injected emergency water into the vessel earlier in the test than in the calculation by about 400 s, as shown on Figures 47 and 48. The timing difference was caused by different primary depressurization in both the test and the calculation. Correctly calculating accumulator injection requires correct calculation of the primary depressurization during the injection period.

The posttest RELAP5 calculation for Test S-NH-1 used a higher intact loop accumulator line resistance (R′) than that used in the experiment (R′ experiment = .6 R′ code). Therefore, for the same differential pressure between the accumulator and the primary, the mass flow rate should have been higher for the experiment. The opposite trend is shown on Figure 47. The difference in trend between code and data was caused by the influence of a different primary depressurization rate and/or accumulator injection. The primary depressurization rate for the code calculation of

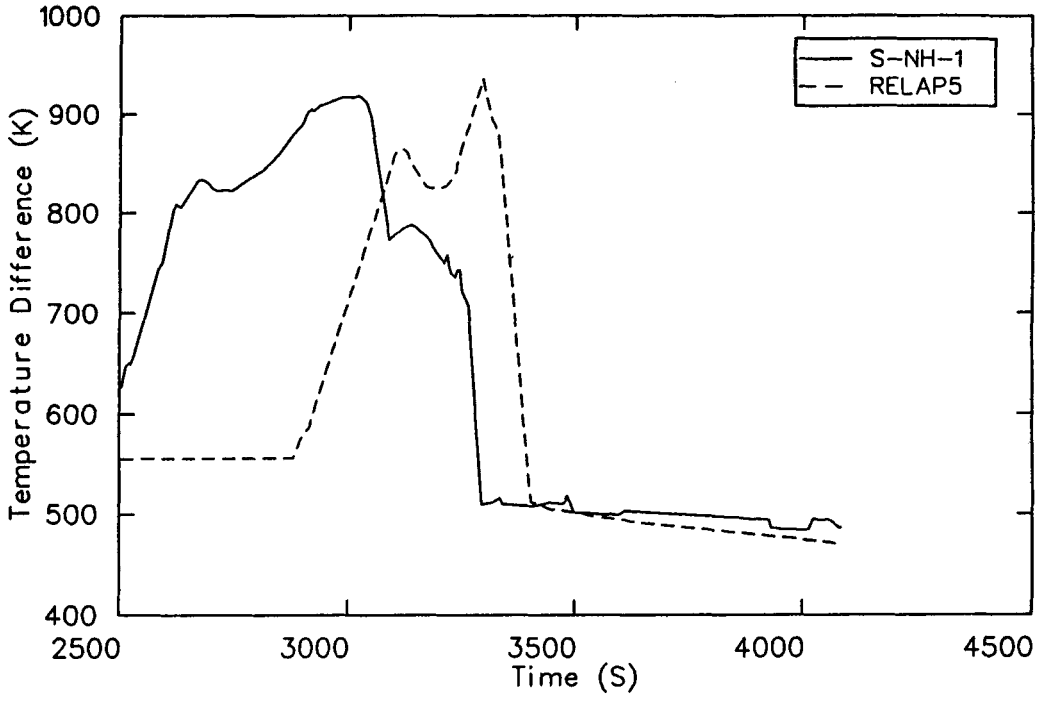

Figure 46. Comparison of calculated and measured intact loop steam dome fluid and metal temperature differences during the recovery phase of Test S-NH-1.

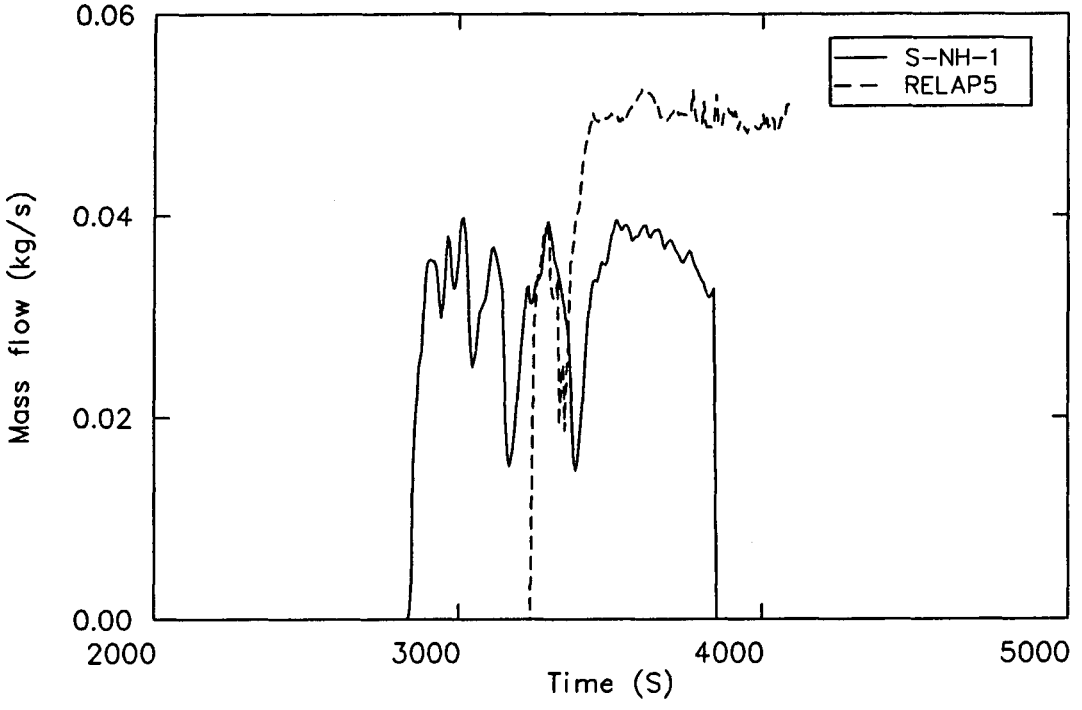

Figure 47. Comparison of calculated and measured intact loop accumulator injection flow during the recovery phase of Test S-NH-1.

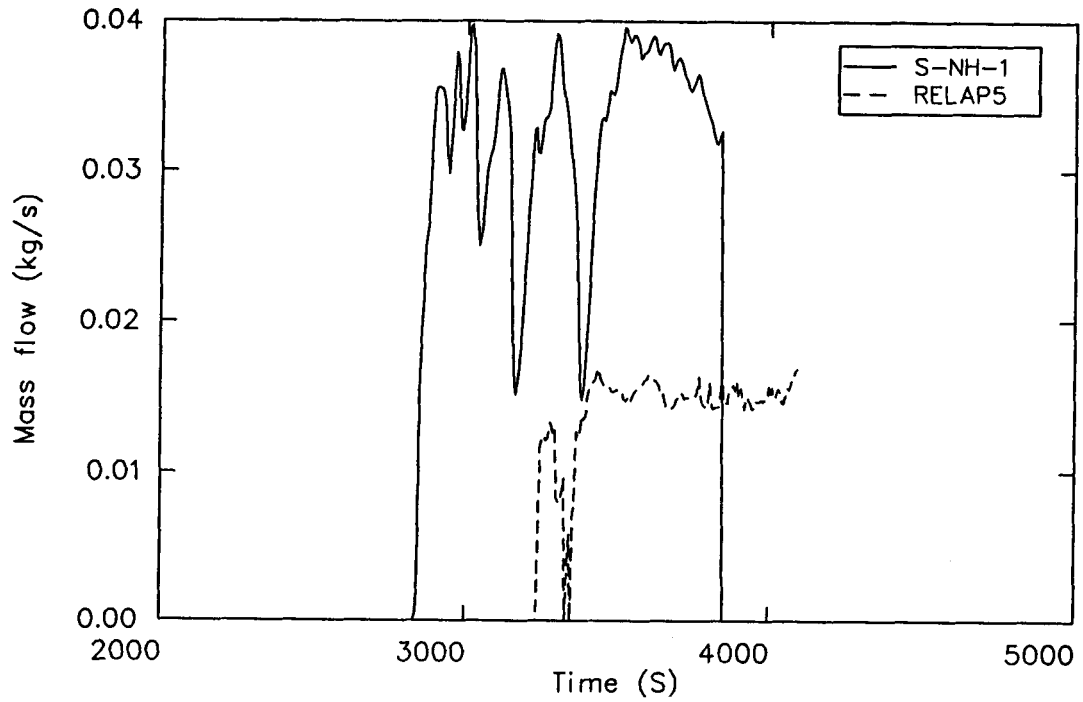

Figure 48. Comparison of calculated and measured broken loop accumulator injection flow during the recovery phase of Test S-NH-1.

S-NH-1 was approximately twice the depressurization rate in the S-NH-1 data. The higher calculated primary depressurization rate caused the calculated accumulator injection to be higher. The implication of this observation is that a correct calculation of the primary depressurization rate during accumulator injection is important if the correct accumulator flow is to be realized.

A RELAP5 calculation using only the accumulator model and a time-dependent volume driven by the primary pressure response from Semiscale Test S-LH-1 (Reference 4) was performed. Figure 49 shows that the accumulator mass flow agrees with the data, which indicates that the accumulator model in the code worked well. As an "add on," the primary depressurization rate in the time-dependent volume was arbitrarily increased by a factor of two, as shown on Figure 50. The increase in depressurization rate dramatically increased the injection rate as shown on Figure 49. Because of the higher injection flow rate, it was expected that the core would be quenched faster in the calculation. Shortly after accumulator injection began, both the downcomer and the vessel liquid levels began to increase, as shown on Figures 51 and 52. Because of the later injection of the accumulators in the calculation, a corresponding later level rise was observed.

The PCTs are shown on Figure 36. Because of the higher accumulator injection flow rate and the more rapid system depressurization in the calculation, the core quench was slower than measured by about 180 s, while the difference in PCTs was quite small, less than 16 K (29°F). The calculation was terminated at 4092 s when the LPIS set point of 1.38 MPa (200 psia) was reached. As can be seen on Figure 36, the temperature was increasing in the test at this time. For comparison, the sequence of events are recorded for both the test and the calculation (Table 3).

Summary. The RELAP5 calculation correctly modeled several of the important thermal-hydraulic responses for Test S-NH-1. Primary and secondary pressures were calculated to be slightly higher than the test data. Also, the calculated pressure rise in the steam generators and the calculated depressurization rate in the steam generators during recovery were higher than measured in the test. The break flow was undercalculated, and thus the primary mass was greater in the calculation than in the test data. Pressurizer interfacial liquid level

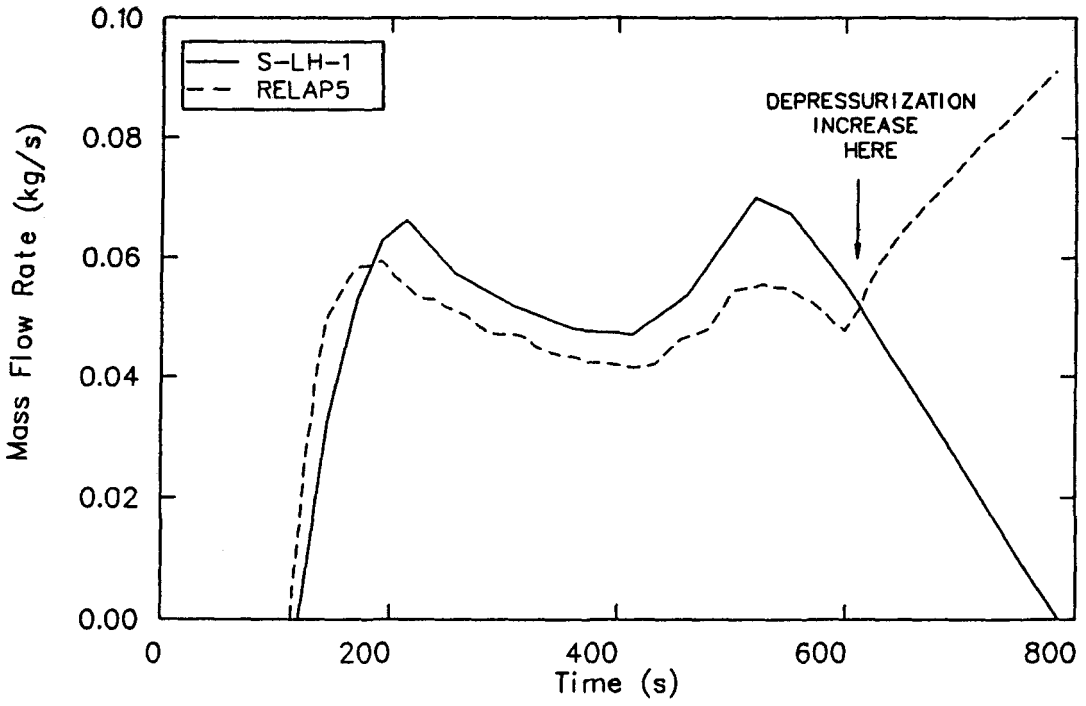

Figure 49. Comparison of calculated and measured intact loop accumulator flow of Test S-NH-1.

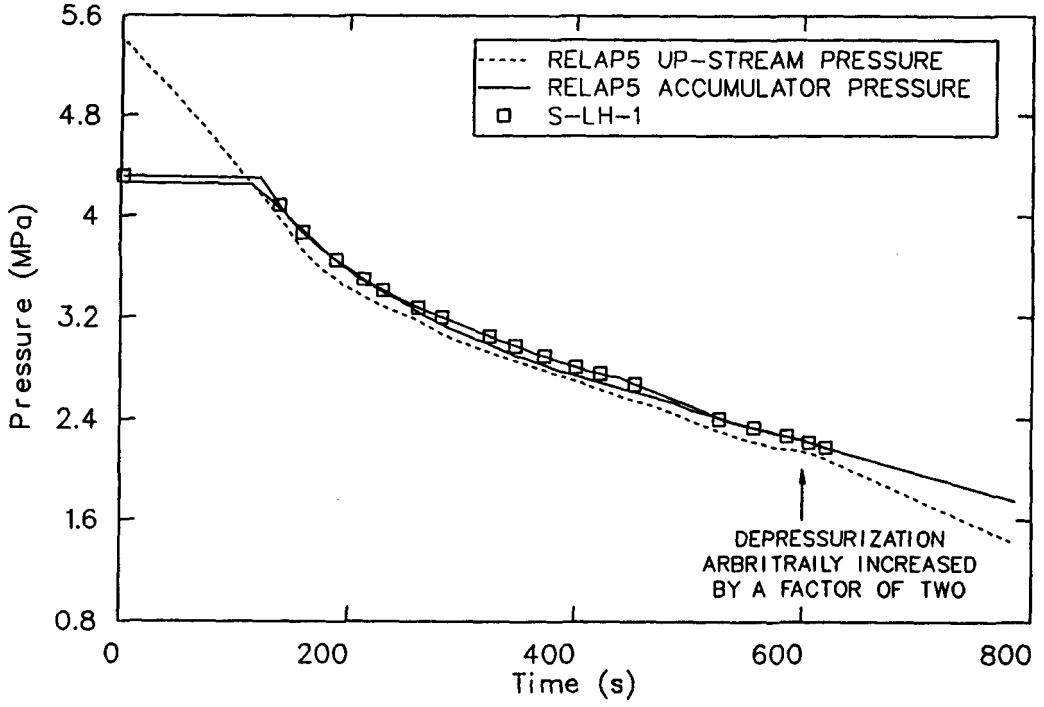

Figure 50. Comparison of calculated and measured intact loop accumulator pressure and calculated upstream pressure of Test S-NH-1.

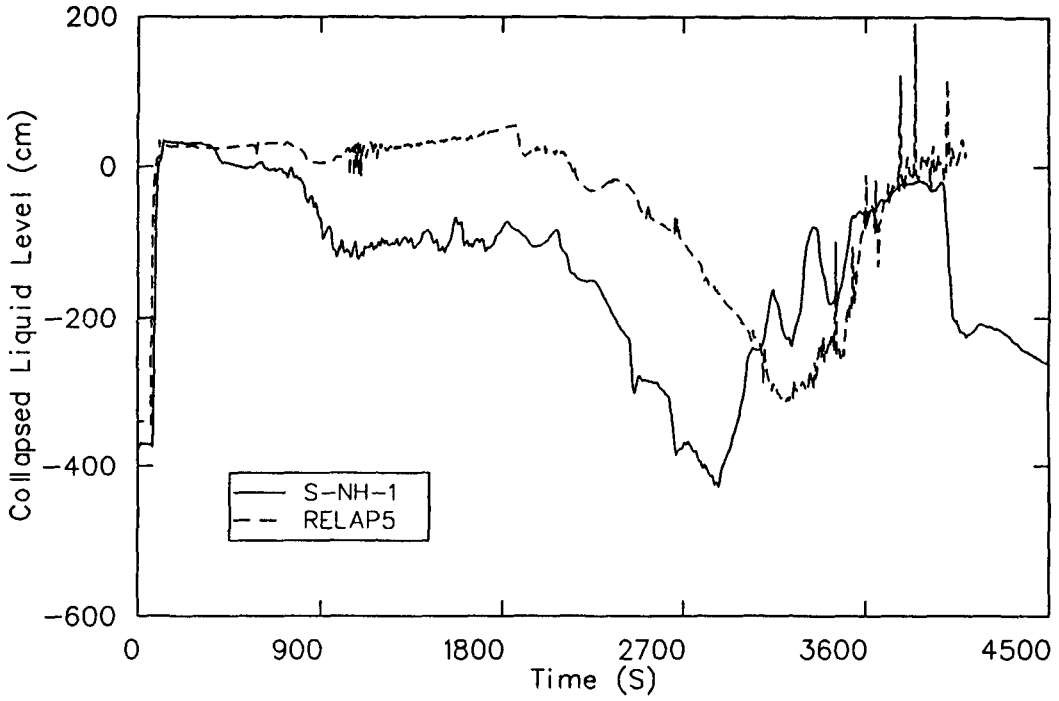

Figure 51. Comparison of calculated and measured downcomer liquid levels during the recovery phase of Test S-NH-1.

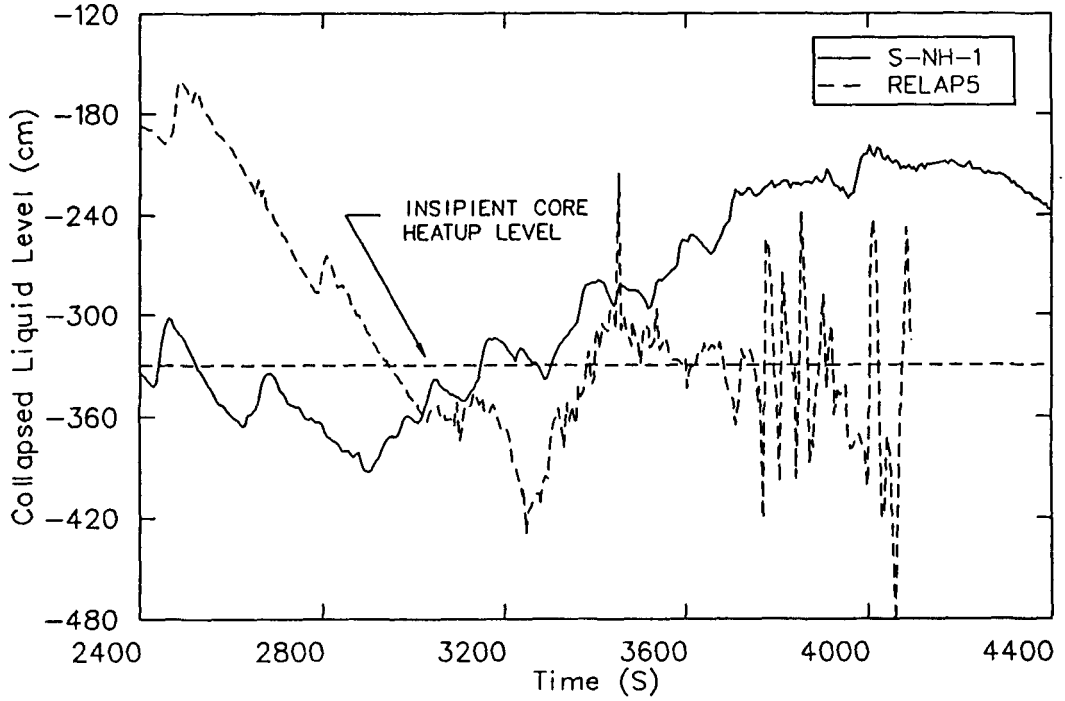

Figure 52. Comparison of calculated and measured vessel liquid levels during the recovery phase of Test S-NH-1.

Table 3. Comparison of measured and calculated sequence of events for Test S-NH-1

Event	Time (s) Measured	RELAP5
Break opened	0	0.0
Scram signal generated [pressurizer pressure = 13.1 MPa (1900 psia)]	61	57.5
Main steam valves began to close	62	58.5
Safety injection signal generated [pressurizer pressure = 12.51 MPa (1815.0 psia)]	67	62.5
Main feedwater stopped	68	63.5
Auxiliary feedwater actuated	68	63.5
Main coolant pumps began coastdown	70	65.5
Steam generator ADV valves latched open [PCT = 811°K (1000°F)]	2630	3072.0
Accumulator injection begun	2828	3232.0
Test termination [pressurizer pressure = 1.38 MPa (200 psia)]	5000	4092.0

early in the test and vessel upper plenum liquid level were correctly calculated. Primary system loop flow, including two-phase peaking in the downcomer, showed good agreement between the calculation and the test data. Overall, the system power response and temperature response were calculated to be in good agreement with the test data; however temperature discrepancies in the calculation and test data were noted between hot metal and fluid, primarily in the voided areas. A calculation involving the accumulator model that used the primary pressure data from Test S-NH-1 concluded that the accumulator model in RELAP5 worked well.

Test S-LH-2

The results of an assessment study using Semiscale Test S-LH-2 data are presented in this subsection. Test S-LH-2 was a 5% small break LOCA with nominal emergency core cooling. The adequacy of the Semiscale RELAP5 computer code for calculating the important small break LOCA thermal-hydraulic responses is discussed. Overall system responses related to primary system pressure, break flow, the system fluid mass distribution, and the core response are discussed. Also, the possibility of heatup following accumulator injection and prior to LPIS initiation is examined as a potential safety issue.[8]

A comparison of event sequences between RELAP5 and the experimental data is shown in Table 4. There are four distinct phases during the 5% small break LOCA: an early subcooled blowdown phase, involving draining of the pressurizer and vessel upper head and the attainment of saturation conditions in the system; a steam generator U-tube drainage phase, following pump coastdown and establishment of natural circulation; a manometric core level depression/reflux phase, caused by water plugs left in the pump suctions after steam generator drainage; and finally, the core boiloff and recovery phase, including accumulator injection and the final depressurization to LPIS setpoints. Only automatically occurring safety features were assumed for S-LH-2, and no operator intervention was allowed.

Upper Head/Pressurizer Drainage Phase. Test S-LH-2 was initiated when the blowdown valve in the cold leg was opened. The calculated and measured initial conditions are listed in Table 2.

RELAP5 correctly calculated the early primary system pressure response from 0 to 40 s (Figure 53), primarily because of a good calculation of break flow (Figure 54). As a result of a good calculation of the early depressurization rate, the reactor scram, feedwater termination, coolant pump coastdown initiation, MSIV full closure, and HPIS initiation were all calculated to occur at nearly the same time as the data, as shown in Table 4.

In general, the primary system pressure transient which occurs is an indication of the energy in the system and will be affected by:

- The mass balance between mass flow out of the system break and the HPIS flow[a] into the system, and
- An overall energy balance involving break flow, fluid-to-primary-piping heat transfer, primary-to-secondary heat transfer, HPIS flow into the system, and loop fluid flashing.

After reactor scram, core power was reduced to decay heat and the primary system depressurization rate was increased. At about 43 s, saturation conditions were achieved throughout the loops. The break flow then changed from single-phase subcooled flow to two-phase saturated flow. The energy of the fluid flashing throughout the system countered the energy lost in the break flow and greatly slowed the depressurization rate. The RELAP5 calculation and the data both show the retardation in pressure; however, RELAP5 has a lower depressurization rate.

RELAP5 correctly calculated that the pressurizer would drain first, followed by the vessel upper head. In both code calculations and data, the pressurizer drained quickly, after the break opened, followed by a slower drain of the vessel upper head, as shown on Figures 55 and 56. The sequential drainage between the pressurizer and upper head was due to the immediate flashing of fluid in the pressurizer because the fluid was initially saturated. After the break opened, liquid was pushed out of the pressurizer by the expanding steam bubble. The vessel upper head remained subcooled during the pressurizer drainage period.

Steam Generator U-Tube Drainage Phase. Following the drain of the vessel upper head, the steam

a. The HPIS flow rate is insignificant compared to break flow and therefore has little impact on primary depressurization phenomena.

Table 4. Comparison of calculated and measured sequence of events for Test S-LH-2

Event	Time (s) Measured	RELAP5
Break opened	0.3	0.0
Pressurizer low pressure [12.6 MPa (1827 psia)]	15.91	15.51
Core scram	19.57	20.11
Feedwater coast down to zero		
Intact loop	19.00	20.51
Broken loop	19.00	20.51
Coolant pump coastdown initiated		
Intact loop	20.65	20.52
Broken loop	20.65	21.24
MSIV full closure		
Intact loop	20.0	20.94
Broken loop	19.5	20.43
HPIS initiated		
Intact loop	41.6	41.43
Broken loop	41.6	41.43
Pressurizer emptied	34.8	39.03
Minimum core liquid level reached	591.7	500.0
Break uncovered	214.1	272.3
Intact loop pump suction cleared	205.4	255.0
Broken loop pump suction cleared	Did not clear	Did not clear
Accumulator flow initiated		
Intact loop	575.0	470.0
Broken loop	Not initiated	Not initiated

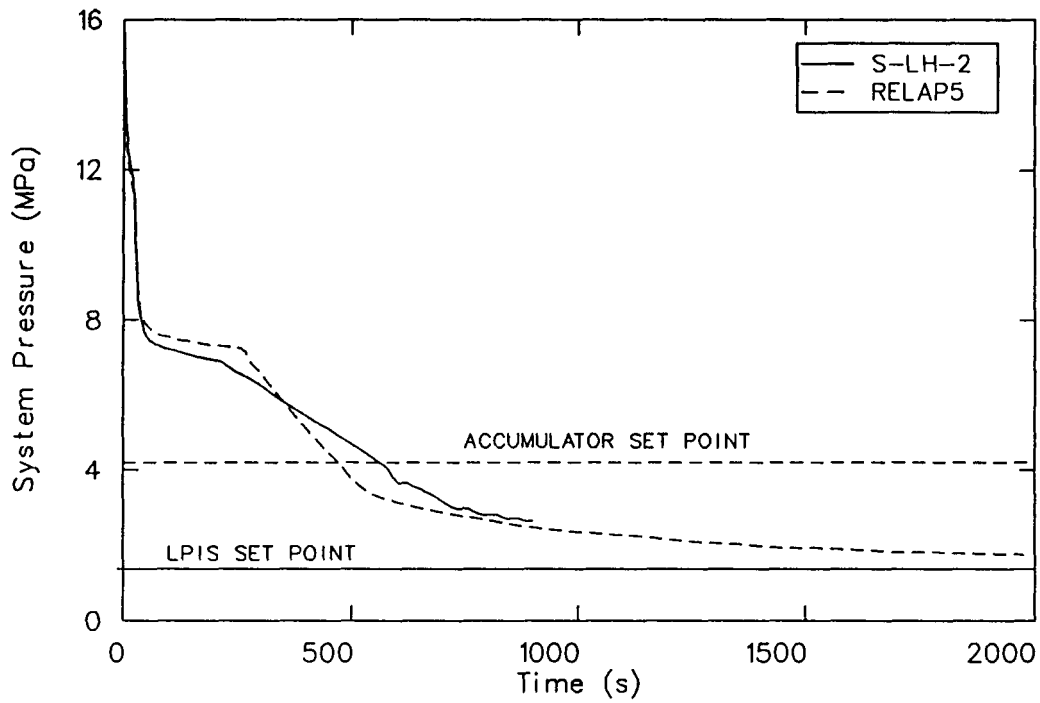

Figure 53. Comparison of calculated and measured primary system pressure of Test S-LH-2.

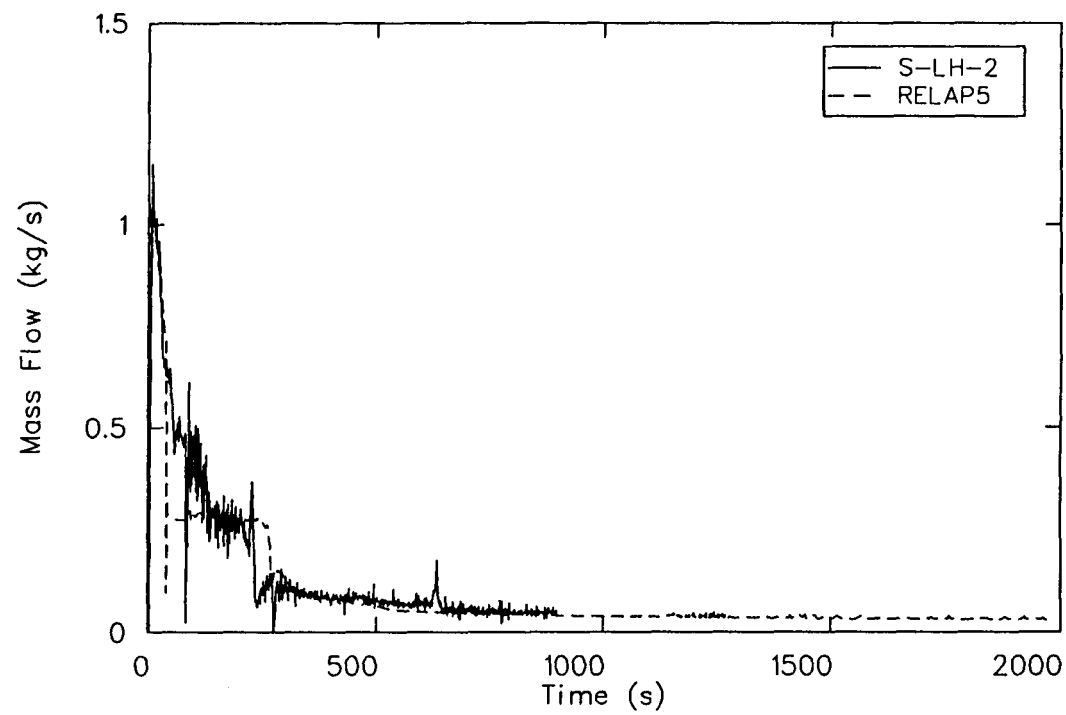

Figure 54. Comparison of calculated and measured break mass flow rate of Test S-LH-2.

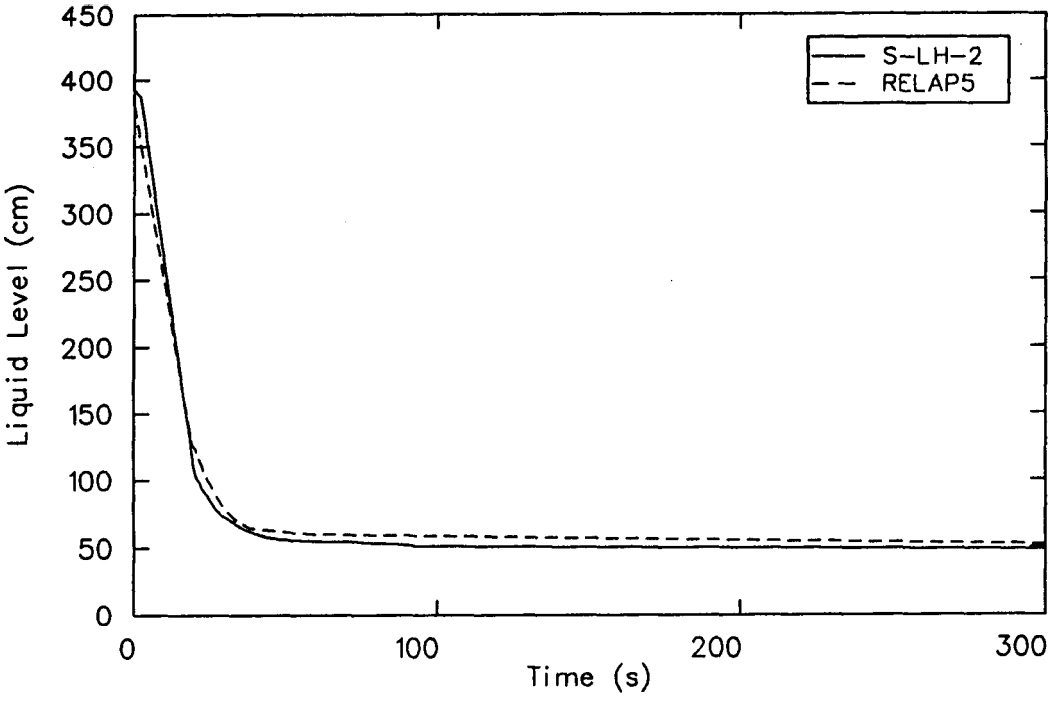

Figure 55. Comparison of calculated and measured pressurizer collapsed liquid level of Test S-LH-2.

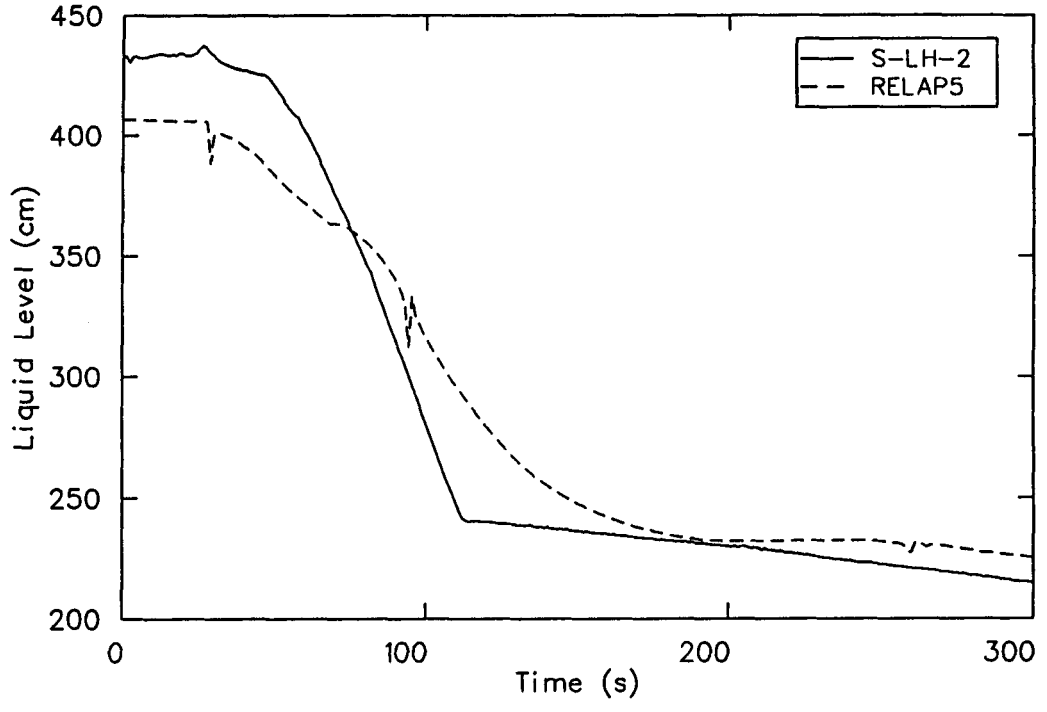

Figure 56. Comparison of calculated and measured upper head collapsed liquid level of Test S-LH-2.

generators drained in a differential manner. The broken loop drained first, followed by the intact loop.

When the pump coasted down to zero speed at 89 s, natural circulation in the intact loop was established in both the test and calculation. In the test, when the pump coasted down to zero speed, two-phase natural circulation was established in the intact loop and the decay heat was dissipated in the intact loop while allowing the broken loop steam generator U-tubes to drain (Figures 57 and 58). Figure 59 shows that following pump coastdown to zero speed at 89 s, there was actually an increase in intact loop hot leg volumetric flow which was associated with two-phase natural circulation peaking.[7] The intact loop steam generator plenum-to-plenum temperature difference (Figure 60) was very small (1 to 2 K), which also supported the two-phase natural circulation in the intact loop. The increase in intact loop hot leg flow (Figure 59, between 89 and 112 s) also caused a slight increase in the intact loop steam generator U-tube collapsed liquid level. At 125 s, reflux heat transfer was established in the broken loop, where steam created in the core traveled to the steam generator, condensed on the upflow side of the steam generator U-tubes, and drained back into the core. The broken loop then removed the decay heat in the reflux mode and the intact loop drained. A dramatic spike in the intact loop hot leg flow occurred as steam traveled to the intact loop U-tubes to replace the drained fluid. During this period, the break flow was a saturated two-phase mixture and the depressurization rate was slow, as shown on Figure 53. In the RELAP5 calculation, when the pump coasted down to zero speed, there was also an increase in intact loop hot leg flow (Figure 61) which was related to two-phase natural circulation flow peaking. Figure 62 shows that the intact and broken loop steam generator plenum-to-plenum temperature difference was in the range of 0 to 2 K, which implies two-phase natural circulation and reflux heat transfer.

The RELAP5 calculation of the steam generator drain period is similar to the data, as shown on Figures 61 through 64. Figures 63 and 64 compare the intact and broken steam generator U-tube drain and show that the broken loop drained first, followed by the intact loop.

Manometric Depression/Reflux Phase. In Test S-LH-2, following drainage of the steam generator U-tubes, liquid remained in the loop low points, including the pump suctions and the vessel. These loop seals were a block to the steam created in the core. A manometric balance of heads in the loop occurred as steam created in the core added to an expanding steam bubble bounded by the vessel liquid plug and plugs in the loop seals. As the bubble expanded, the intact loop seal cleared, which caused a free path for steam flow from the vessel to the break. Concurrent with this uncovery was an uncovery of the centerline break plane, which had a large effect on the break flow rate and primary depressurization. During this manometric balance period, reflux heat transfer occurred in both steam generators which is characterized by liquid heads in the upflow side of the tubes. These liquid heads influenced the overall head balance throughout the loop, most notably in the vessel. The vessel level was depressed during this period until the loop seals were cleared by the expanding steam bubble.

Following drainage of the primary U-tubes in the RELAP5 calculation, the reflux mode was established at 135 s in the broken loop and 143 s in the intact loop (Figures 65 and 66). The calculated liquid and vapor velocities behaved in a countercurrent manner after initiation of reflux. Both the test and calculation show that the fluid head on the upflow side of the U-tubes was higher than the down-flow side during the ongoing reflux period. The head on both the upflow side and down-flow side represents both frictional pressure drop and liquid gravity head contributions. The core liquid level was influenced by the hot head of fluid in the steam generator as well as other heads throughout the loop. As a net result of these heads, the core liquid level was depressed. This core level depression was correctly calculated by the RELAP5 code (Figure 67). RELAP5 correctly calculated the magnitude of the core liquid level depression seen on Figure 67 at about 200 s. Also, RELAP5 correctly showed no core heat up associated with the level depression, as shown on Figure 68. (Note that the heatup seen later in time was associated with a core boiloff and recovery phase discussed in the next section.)

The pump suction clearing was correctly calculated by RELAP5. Figures 69 and 70 show that the intact loop pump suction cleared at 205.4 s in the test and 250 s in the calculation, but the broken loop pump suction did not clear in either the test or the calculation (Figures 71 and 72).

RELAP5 calculated a larger depressurization rate when the pump suction seals cleared and the break uncovered (Figure 53). Because the pressure (Figure 53), upstream break density (Figure 73), break mass flow (Figure 54), and HPIS flow (Figures 74 and 75) were approximately the same as in the data

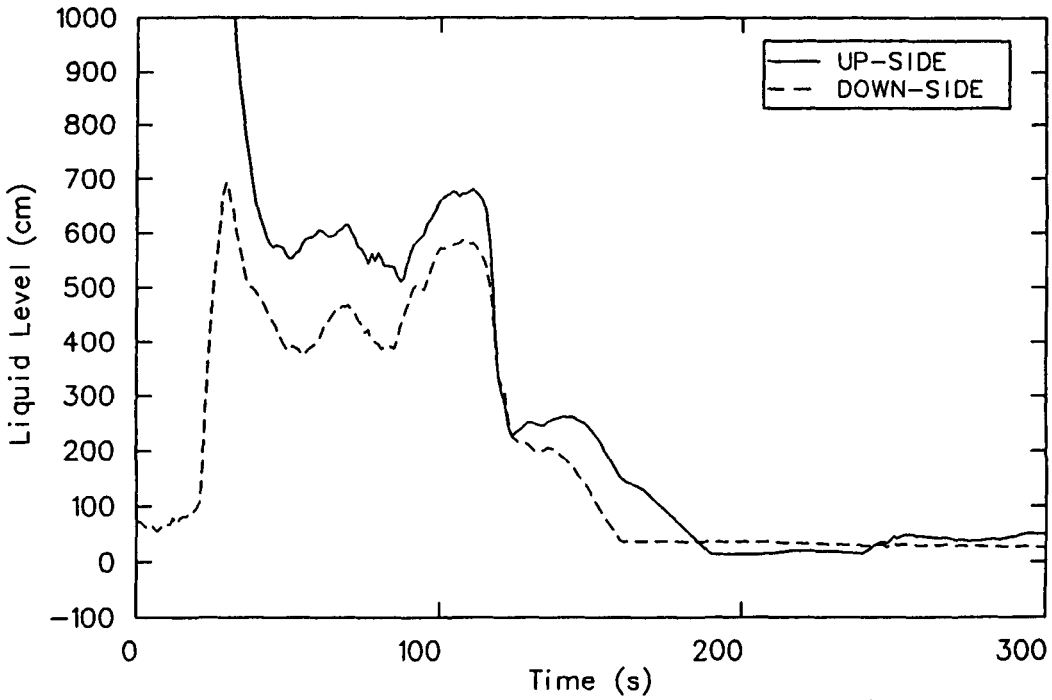

Figure 57. Measured intact loop U-tube collapsed liquid level of Test S-LH-2.

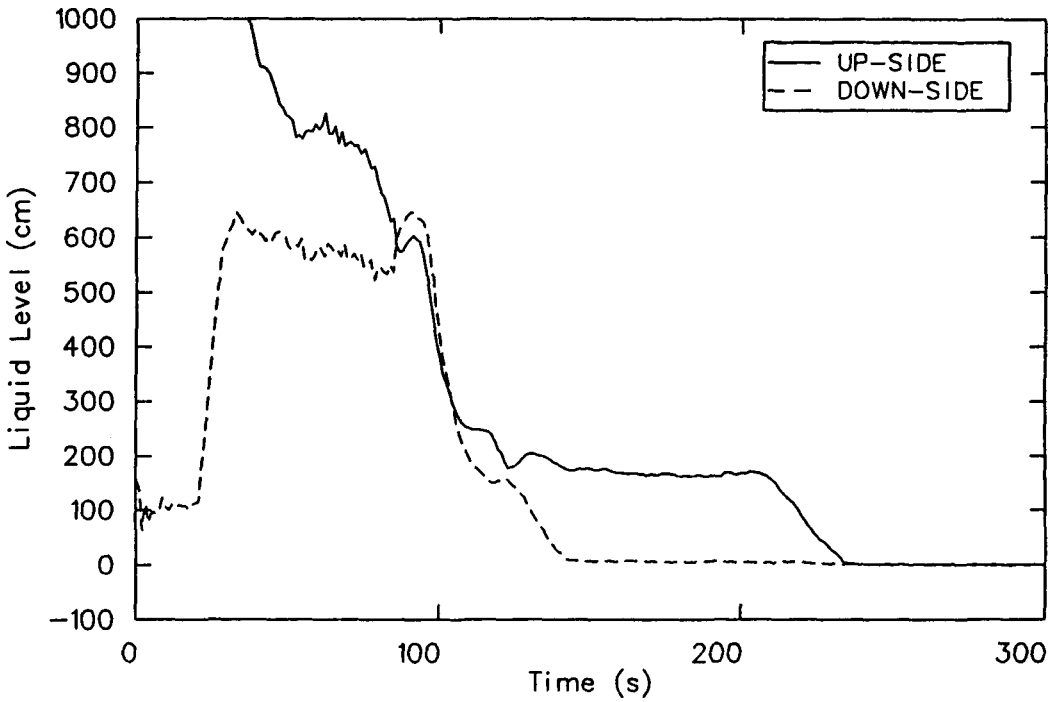

Figure 58. Measured broken loop U-tube collapsed liquid level of Test S-LH-2.

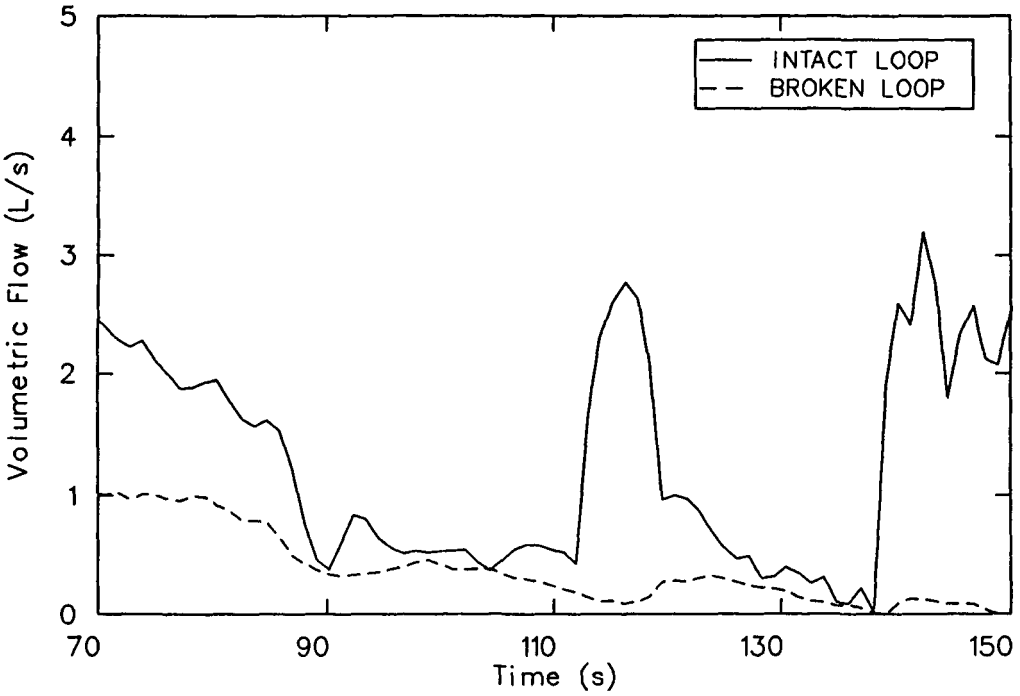

Figure 59. Measured volumetric flow in intact and broken loop hot legs of Test S-LH-2.

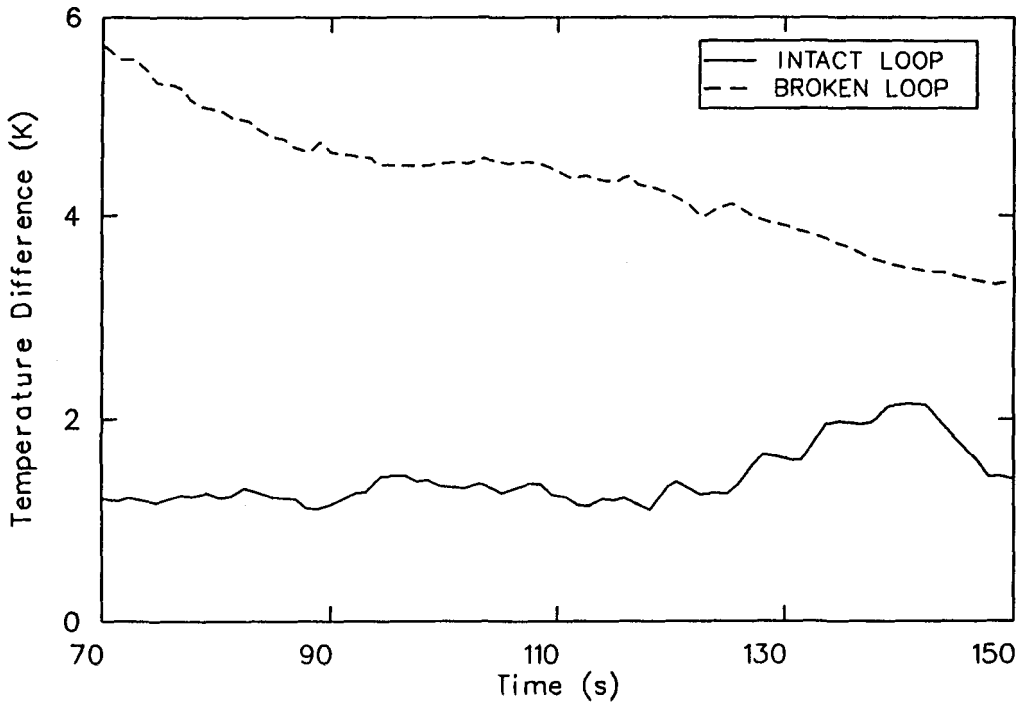

Figure 60. Measured steam generator primary plenum to plenum differential temperature for intact and broken loops of Test S-LH-2.

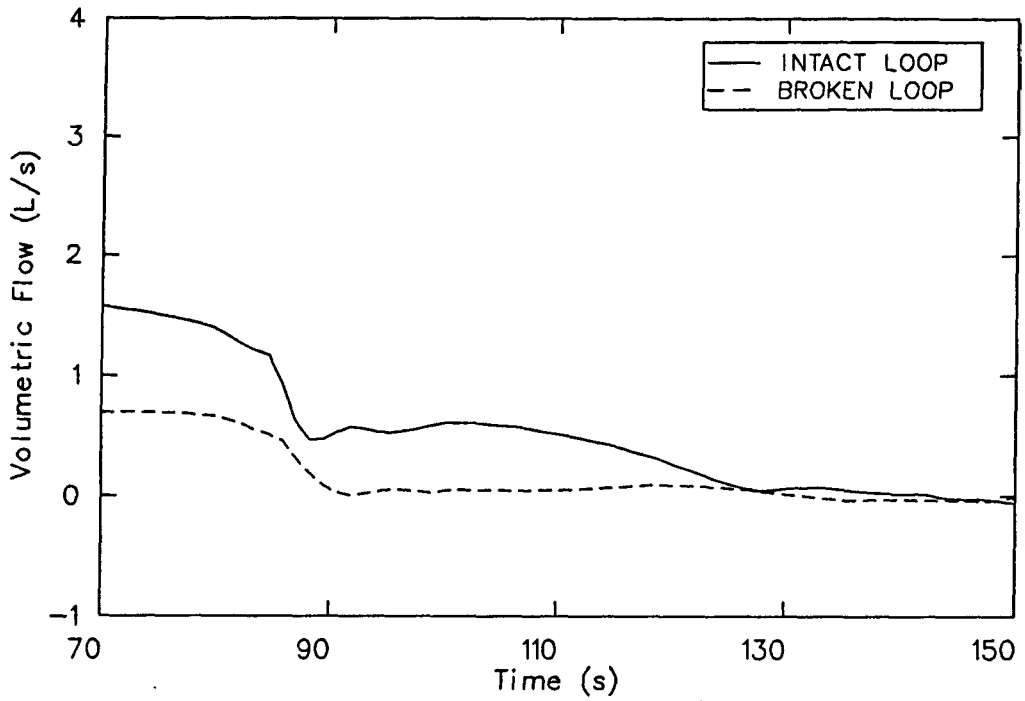

Figure 61. Calculated volumetric flow in intact and broken loop hot legs of Test S-LH-2.

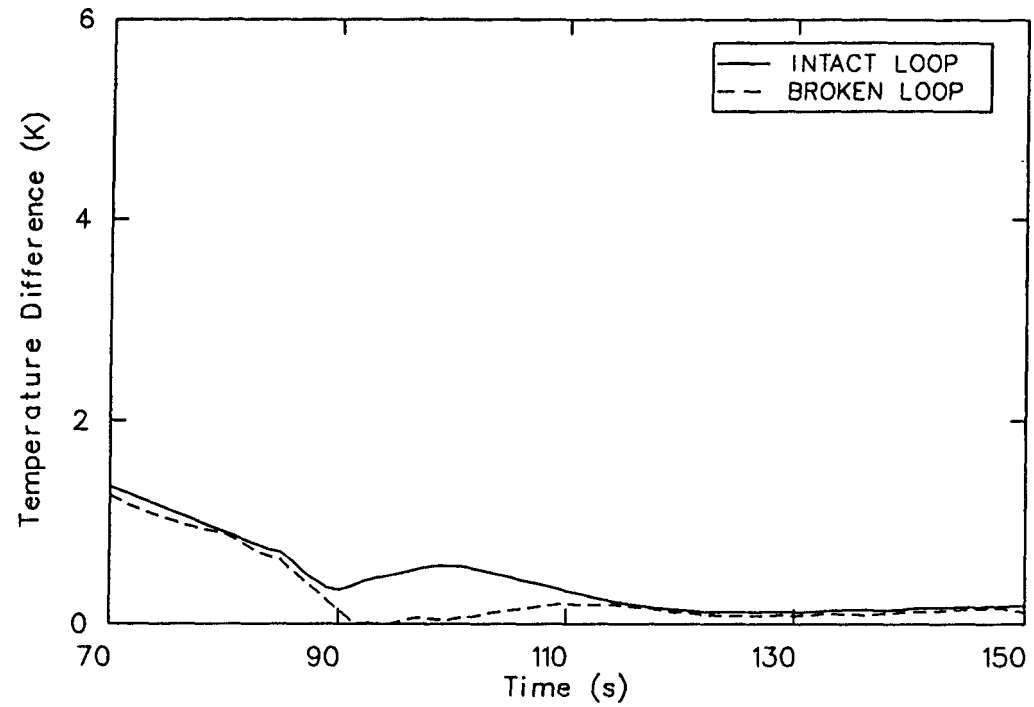

Figure 62. Calculated steam generator primary plenum to plenum differential temperature for intact and broken loops of Test S-LH-2.

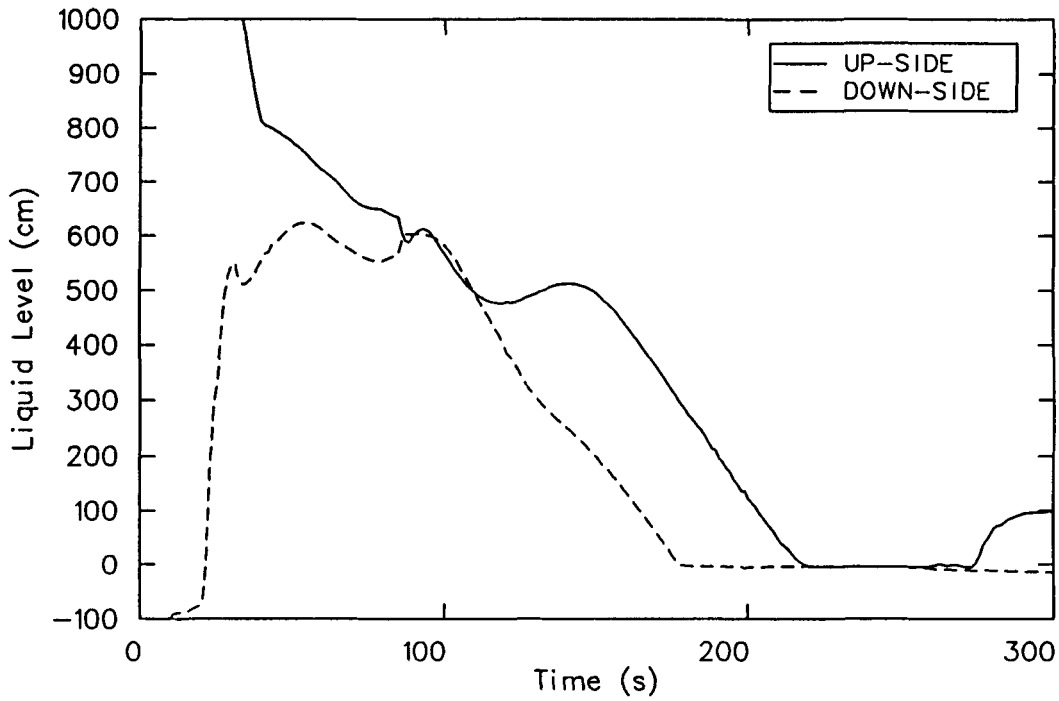

Figure 63. Calculated intact loop U-tube collapsed liquid level of Test S-LH-2.

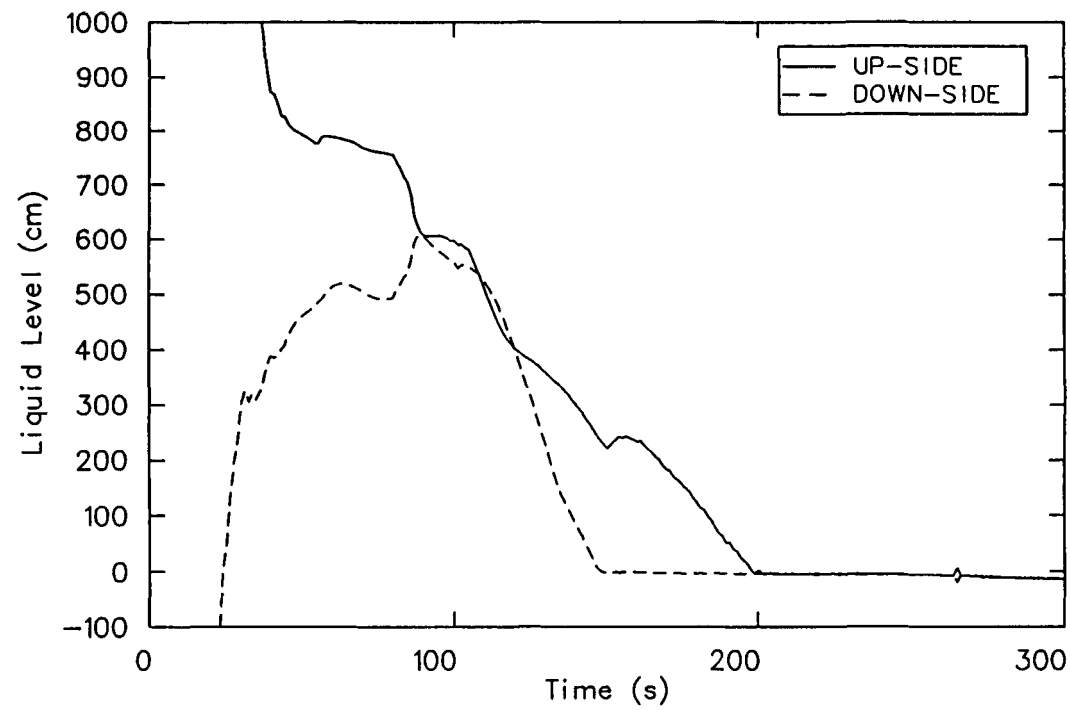

Figure 64. Calculated broken loop U-tube collapsed liquid level of Test S-LH-2.

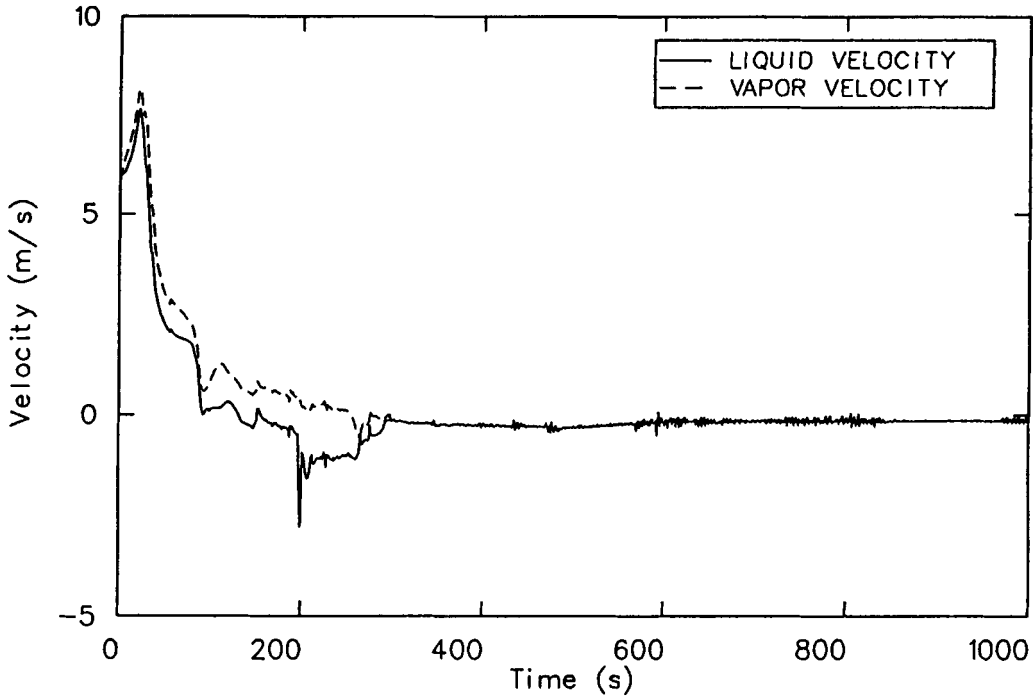

Figure 65. Calculated broken loop steam generator inlet velocities of Test S-LH-2.

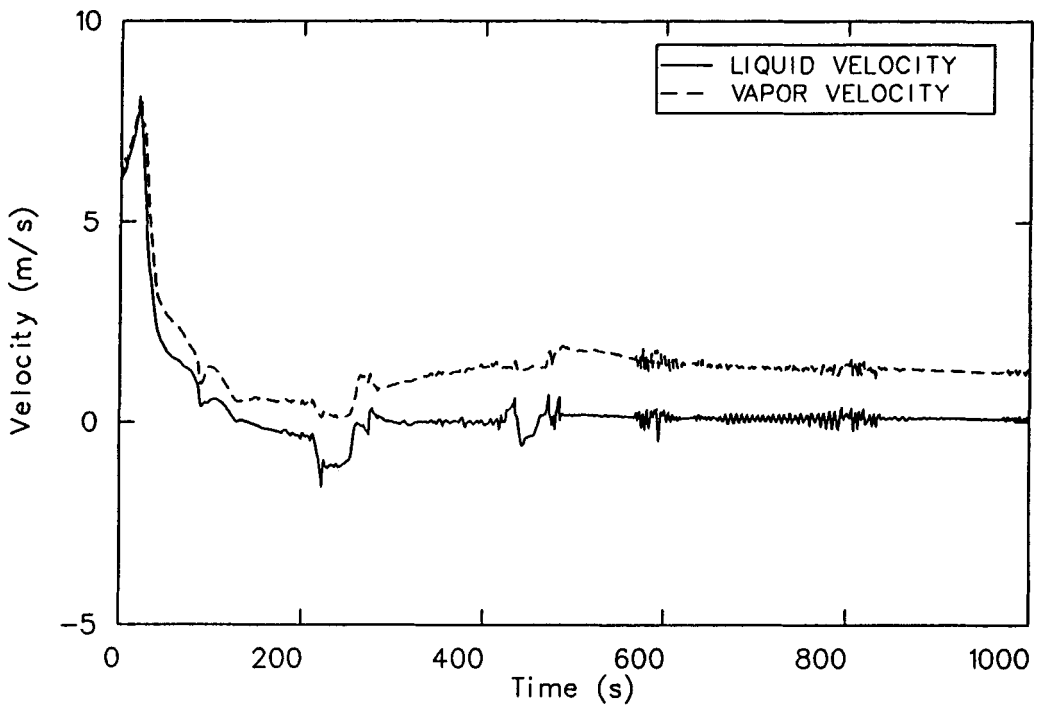

Figure 66. Calculated intact loop steam generator inlet velocities of Test S-LH-2.

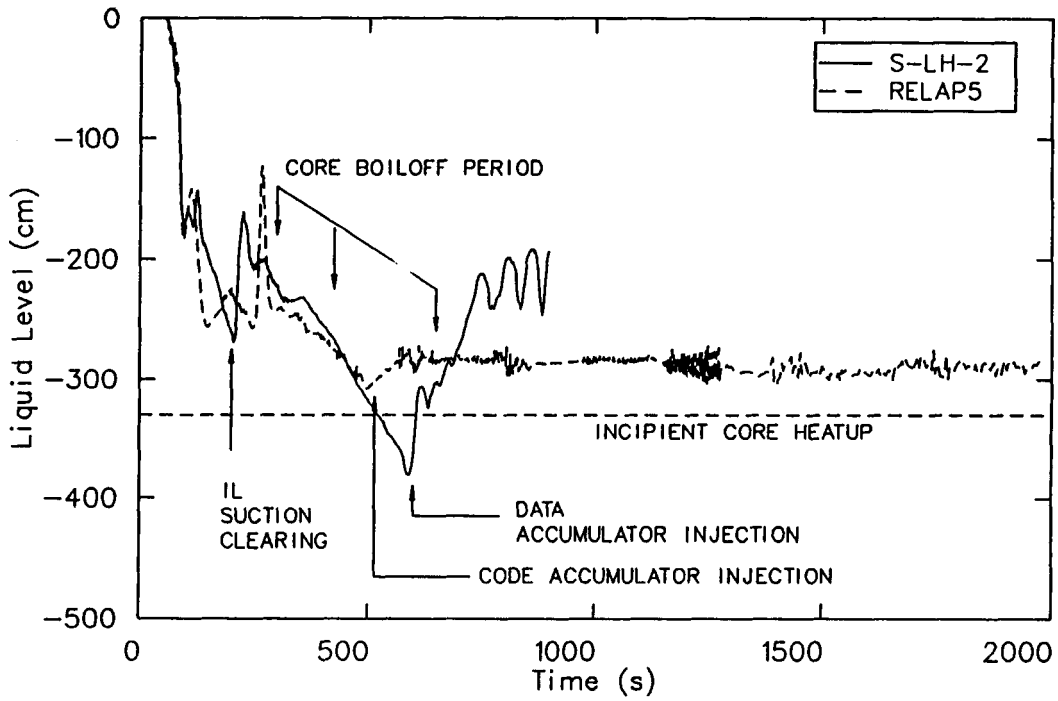

Figure 67. Comparison of the calculated and measured vessel collapsed liquid level of Test S-LH-2.

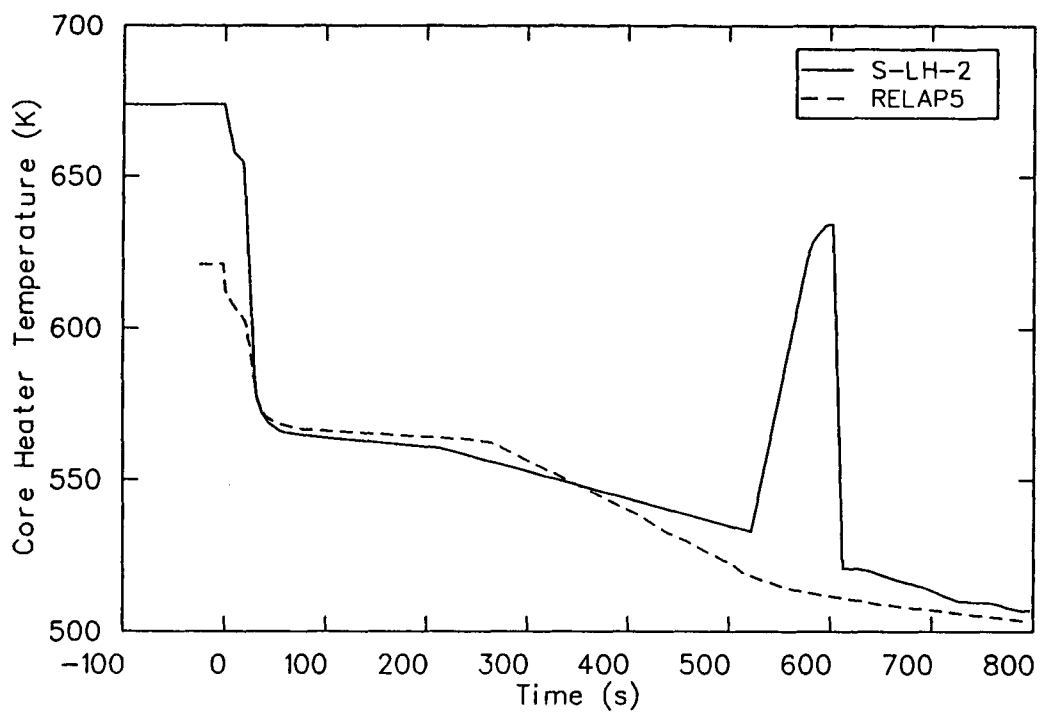

Figure 68. Comparison of the calculated and measured maximum heater rod temperature of Test S-LH-2.

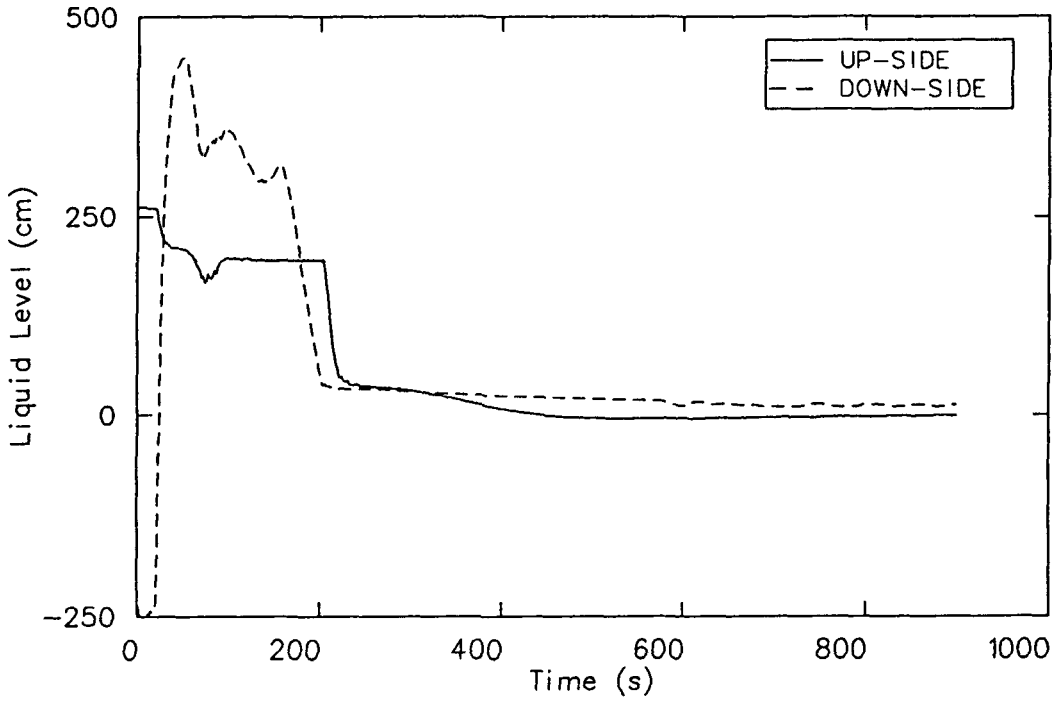

Figure 69. Measured intact loop pump suction collapsed liquid level of Test S-LH-2.

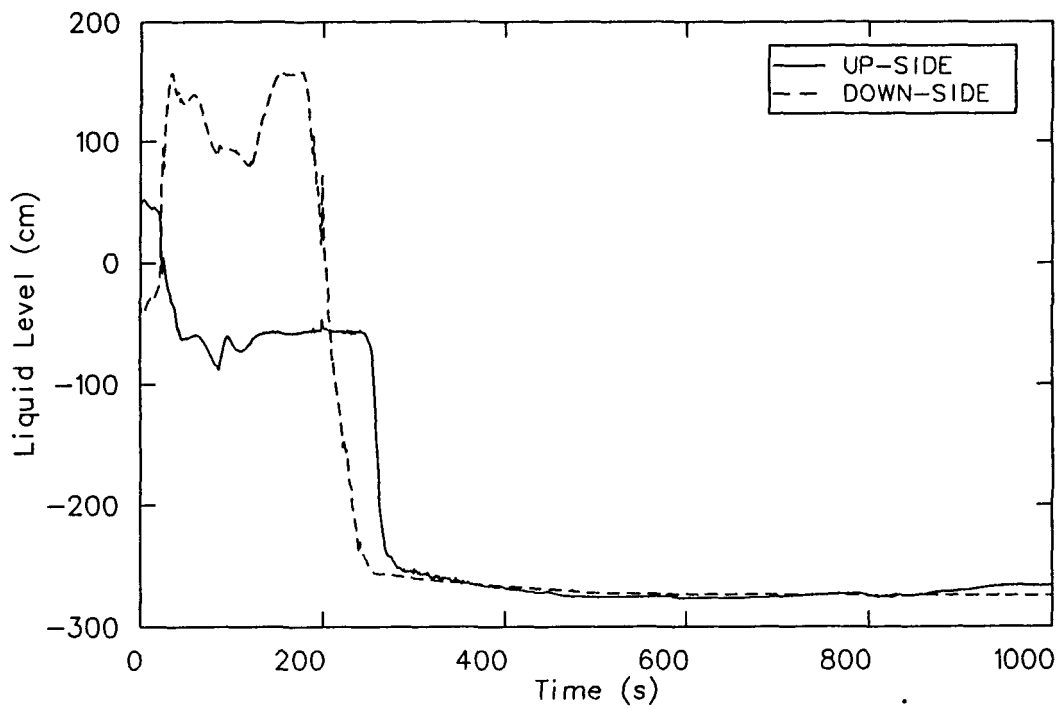

Figure 70. Calculated intact loop pump suction collapsed liquid level of Test S-LH-2.

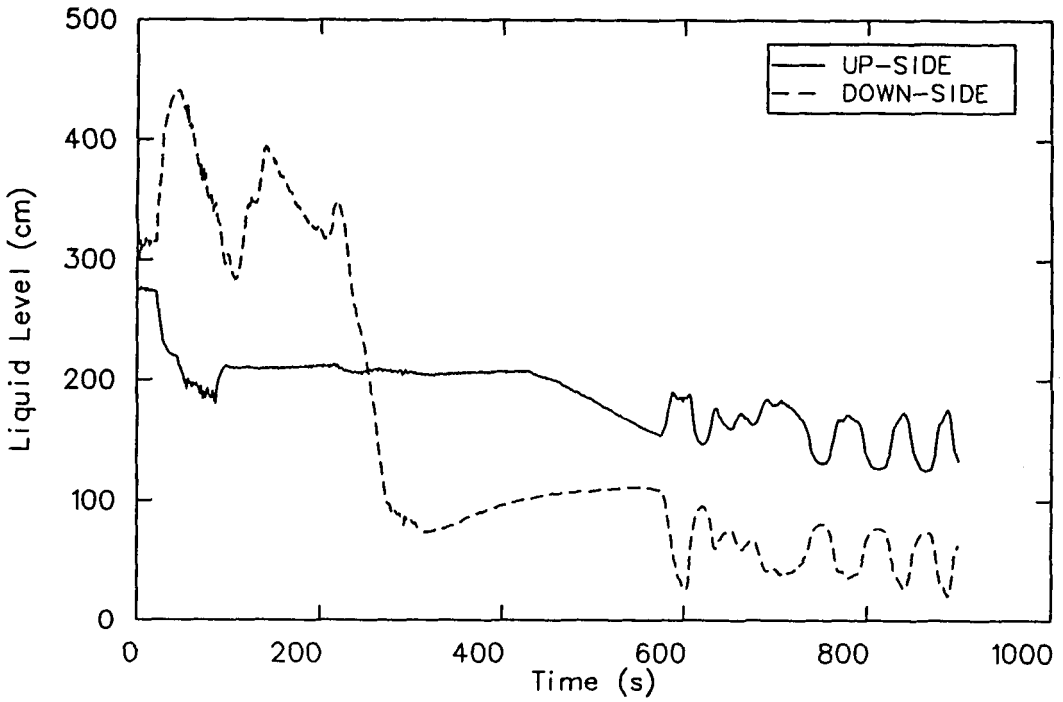

Figure 71. Measured broken loop pump suction collapsed liquid level of Test S-LH-2.

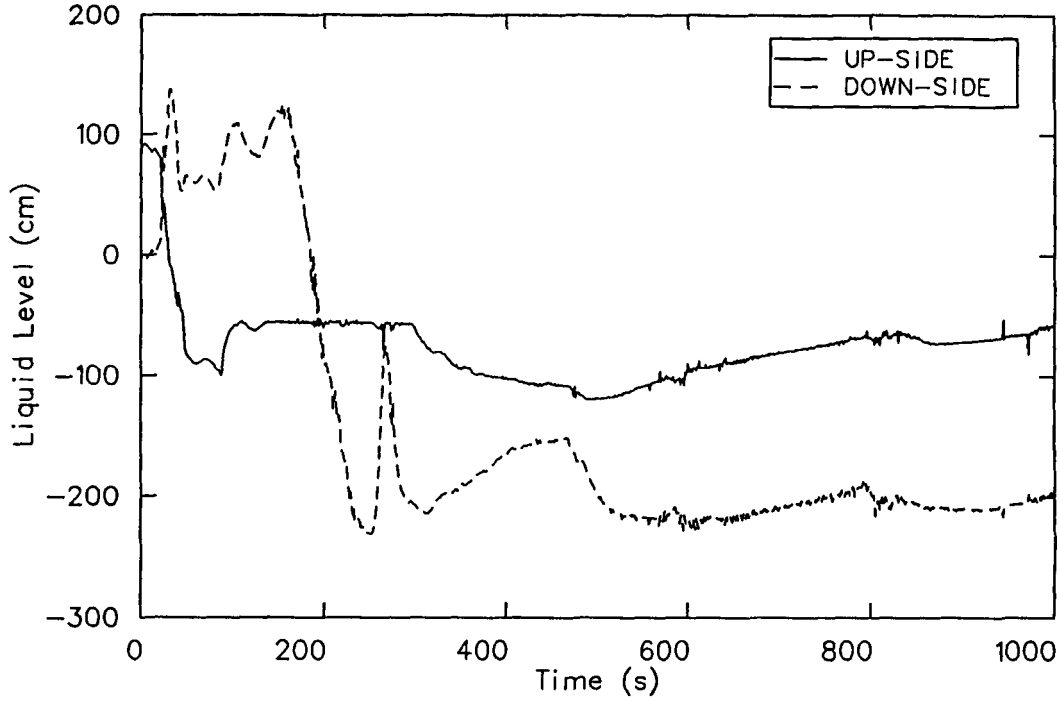

Figure 72. Calculated broken loop pump suction collapsed liquid level of Test S-LH-2.

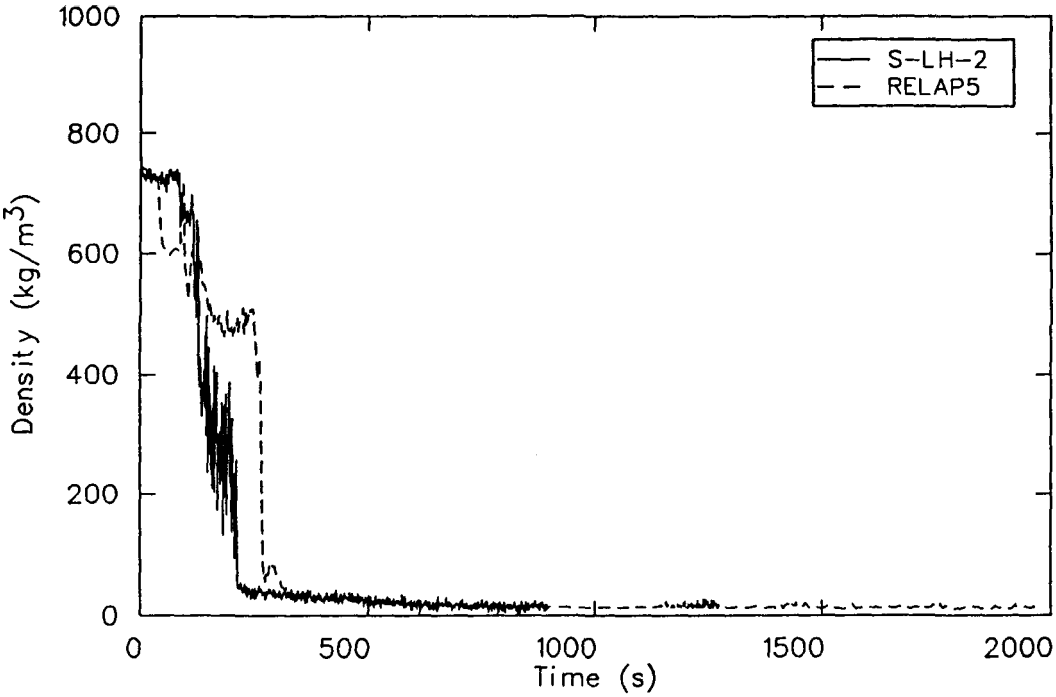

Figure 73. Comparison of calculated and measured upstream break density of Test S-LH-2.

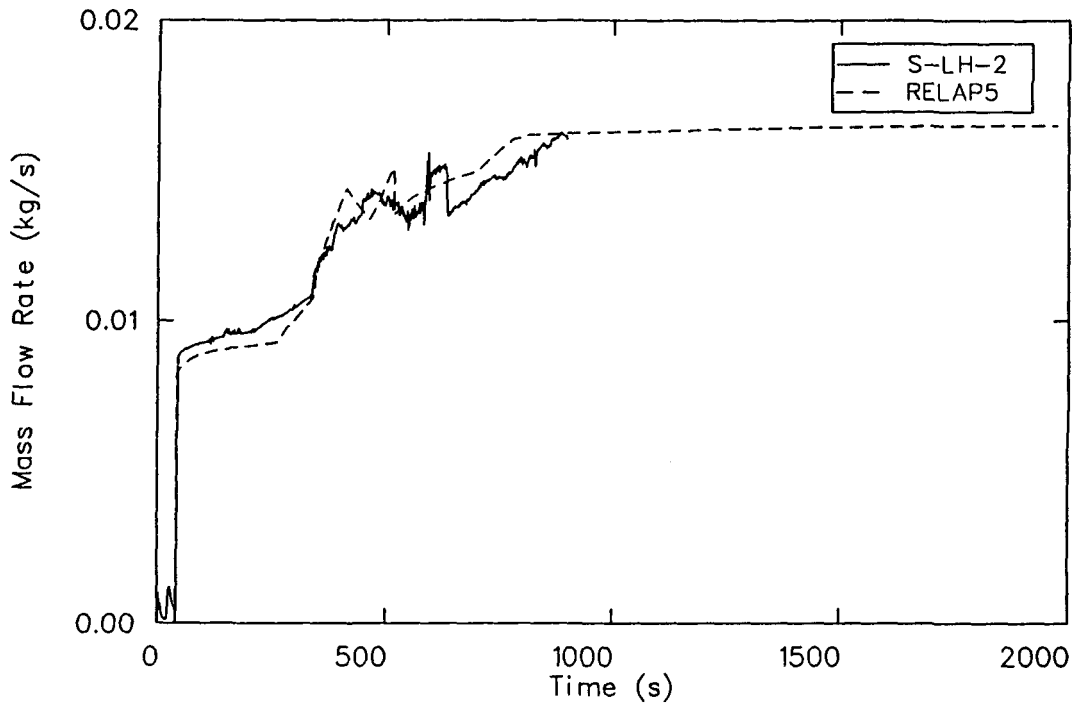

Figure 74. Comparison of calculated and measured intact loop HPIS flow of Test S-LH-2.

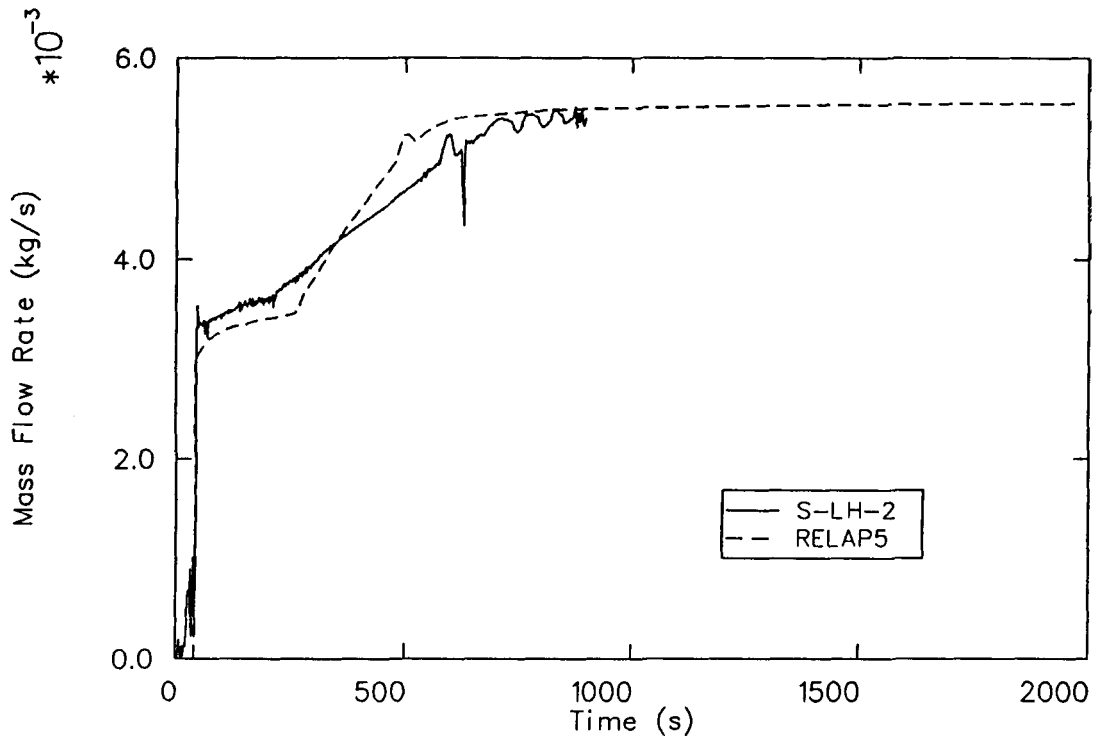

Figure 75. Comparison of calculated and measured broken loop HPIS mass flow of Test S-LH-2.

when the break uncovered, the calculated primary system depressurization rate should have been the same as in the test. However, the depressurization rate was about 2.45 psi/s in the calculation and about 1.21 psi/s in the test. This indicates that primary-to-secondary heat transfer, fluid-to-primary-piping heat transfer, or the energy associated with the break flow was improperly calculated by RELAP5. Another possibility for this increase in the calculated depressurization rate is that when the break uncovered the HPIS flow was injected into single-phase steam, which changed the condensation rate. An incorrect condensation rate would have contributed to the increased depressurization rate in the code. The larger the depressurization rate, the sooner the accumulator will be initiated, precluding the subsequent boiloff and heater rod temperatures. As a note, the results may then be nonconservative from the safety analysis viewpoint.

Core Boiloff and Recovery Phase. Following intact loop seal clearing and break uncovery, a relaxation of the manometric balance of pressure heads throughout the loops occurred and the core liquid level increased (Figure 67). Due to the higher depressurization rate following break uncovery (Figure 53), the accumulator was initiated earlier in the calculation (470 s) than in the test (575 s). The increased vessel level decrease seen on Figure 67 and the enhanced core heat up in the test but not in the calculation seen on Figure 68 can be accounted for by the time difference in accumulator injection.

The accumulator-injected mass was significantly lower in the calculation than in the test (Figure 76). The RELAP5 calculation used only intact loop accumulator injection, and the data had a communication line between the intact and broken loop accumulator which caused an enhanced injection into the intact loop only. This difference in accumulator injection resulted in a more rapid filling of the vessel in the test than in the code calculation, as shown on Figure 67.

From this study, a possible safety issue was examined by extending the RELAP5 calculation of Test S-LH-2. Figures 53 and 67 show that the experiment was terminated with the primary pressure well above the LPIS set point pressure of 1.38 MPa (200 psia), with a stable core level at about 2 m (79 in.) below the cold leg [0.7 m (28 in.) below the top of the core]. The following possible safety questions arose: can the primary pressure reach the LPIS set point before another core boiloff causes a second temperature excursion, and would the code accurately predict the response.

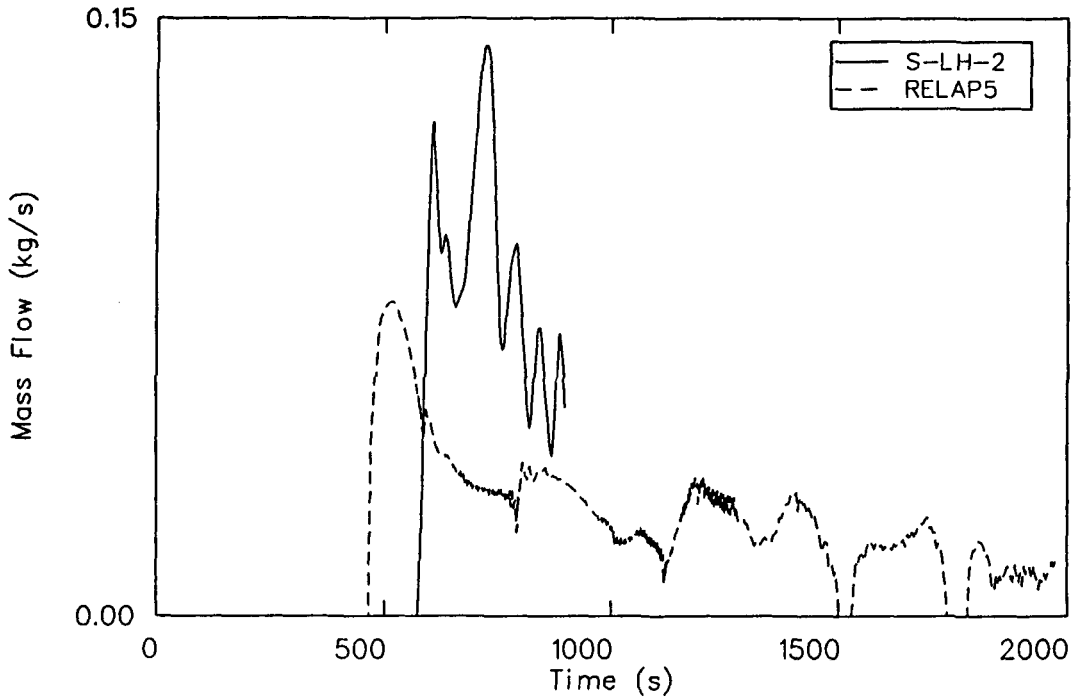

Figure 76. Comparison of calculated and measured intact loop accumulator mass flow rate of Test S-LH-2.

Parameters that influence this race between depressurization and core boiloff include core power, HPIS, break flow, primary-to-secondary heat transfer, primary-fluid-to-metal heat transfer, and leak rate. A RELAP5 restart was performed to investigate the depressurization to the LPIS setpoint. Figures 53 and 67 show the RELAP5 calculated response to 2000 s for the pressure and core liquid level, respectively. At 2000 s, the pressure was still above the LPIS set point; and the core liquid level calculated was just above the incipient core heatup point [3.2 m (126 in.) on Figure 67]. No conclusion can be inferred from this extended calculation because it represents only accumulator flow into the intact loop. However, it does point out a possible race between depressurization rate and liquid level depletion during and following accumulator injection. This potential safety issue should be addressed in future code calculations. Other Semiscale 5% small break LOCA's (UT-series) showed that the LPIS set point was reached without significant core uncovery; however, these experiments were designed for upper head injection which used a cold leg accumulator injection pressure of 2.8 MPa (406 psia) rather than the nominal 4.2 MPa (609 psia) injection pressure. RELAP5 calculations have shown that the primary depressurization rate during accumulator injection greatly influences the injection rate. The higher injection pressure of 4.2 MPa (609 psia) tends to cause a more rapid depletion of accumulator water during a period of higher break flow, which may lead to less water in the system later in time.

Summary. In conclusion, RELAP5 correctly calculated several of the important small break LOCA thermal-hydraulic responses for Test S-LH-2. The early primary system pressure response was correctly calculated because of a good calculation of break flow. However, RELAP5 calculated a larger depressurization rate when the pump suction seals cleared and the break uncovered. The system fluid mass distribution showed good agreement between the calculation and the test. Reflux seen in the test was also calculated by RELAP5. The magnitude of the core liquid level depression was correctly calculated, and no core heatup at the time of this level depression was calculated, as in the test. The vessel was filled more rapidly in the test than in the calculation because there was more accumulator injection mass in the test.

CONCLUSIONS AND RECOMMENDATIONS

Test S-NH-1

Generally, the RELAP5 calculation produced results qualitatively similar to the test. However, several important differences were observed, resulting in the following conclusions and recommendations:

1. The calculated break flow during single-phase saturation blowdown was generally lower than the measured value under a no-bias circumstance (C_D = 1.0). Thus, a slower core uncovery and a later heatup resulted in the calculation. To improve this underprediction, a larger single-phase discharge coefficient could be used, or the cross-flow option on the break junction could be eliminated. However, as revealed from the S-NH-1 pretest calculation,[2] the elimination of the cross-flow model on the break would overestimate the single-phase break flow. The use of a discharge coefficient greater than 1.0 is a non-physical condition and is therefore not recommended. Results from the assessment study using Semiscale Test S-LH-2 (the second test in this study) indicated that a discharge coefficient of 0.9 provided good agreement with the experimental data. Another assessment study[9] consisted of a small break Semiscale experiment (Test S-NH-3) in which a discharge coefficient of 0.95 was used. Still another study[10] concluded that the coefficient should be between 0.85 and 0.9. It is recommended that the code user select a discharge coefficient of 0.9 and check the obtained critical flow against the homogeneous equilibrium model or another accepted mode. Based on this comparison, the discharge coefficient can be adjusted accordingly.
2. Liquid hold-up observed in the broken loop steam generator in the experiment was not calculated, which also contributed to a later core uncovery. A possible reason for the liquid hold-up in the test but not the calculation was an increased heat sink caused by a small leak in the main steam line block valve. Leakage from the steam generator should be carefully modeled.
3. The observed drainage of the broken loop steam generator U-tubes in the test was not calculated to occur. As a result, the early but temporary core quench observed in the test was not calculated. In order to model such a phenomena, a sensitivity study of the U-tube nodalization should be performed. In addition, separate-effects test data should be generated to aid in assessing steam generator behavior.
4. After recovery actions were taken, faster system depressurization occurred in the calculation in both the secondary and primary systems. This caused an early activation of the accumulator and a less severe transient. One possible explanation for this faster-than-observed depressurization was the different stored energy relaxation of the metal in the steam generators. For a more precise prediction, it is suggested that separator efficiency in the calculation be carefully adjusted such that the moisture contained in the steam dome would be as close to the test amount as possible. Separate-effects testing relative to separator performance should be performed to provide a more complete data base for separator model improvement. Also, the heat transfer coefficients throughout the steam generator (U-tubes and walls) may contribute to the observed differences. Correction of the ratio of heat transfer area to volume of metal would also help this problem. The code user should ensure that geometric configurations are accurate so as not to bias the heat transfer calculation.
5. Because the one-velocity momentum equation predicted the two-phase break flow much better than the normal two-velocity option, it is possible that the interfacial drag used in RELAP5 for choked flow prediction is inaccurate. Also, comparing the calculated two-phase break flow to that from the pretest calculation[2] (which used the central-oriented horizontal stratification junction for break and measured data), it can be concluded that the liquid entrainment predicted by the horizontal stratification model was underestimated. Thus, the downward-oriented horizontal stratification junction for an actual central break produced results that agree quite well with the test data. The assessment study reported in Reference 9 also shows that the one-velocity momentum

equation produced best agreement with experimental data. These results and those cited in Reference 10 suggest that the interfacial hydraulic relationships should be the subject of further code development.

Test S-LH-2

The following conclusions are made based on Test S-LH-2 posttest analysis and comparison between test data and a RELAP5/MOD2 calculation.

1. RELAP5 correctly calculates the early blowdown behavior through the automatically occurring events, such as core scram, pump trip and MSIV closure; however, RELAP5 incorrectly calculates the primary pressure response once saturation conditions are obtained. Possible problem areas during this period include two-phase break flow (the horizontal stratification model is recommended for further investigation), primary-to-secondary heat transfer, and fluid-to-metal heat transfer.

   The results of this study and those presented in Reference 9 indicate that the critical flow calculation when two-phase conditions exist is best treated using the one-velocity momentum equation.
2. RELAP5 correctly calculated the core liquid level depression associated with pump suction seal formation and clearing; however, following break uncovery RELAP5 incorrectly calculated the primary depressurization rate. Parameters that affect this calculation that require further sensitivity studies include: primary-to-secondary heat transfer, interfacial heat transfer, break flow energy, and piping-to-fluid heat transfer. The difference between measured and calculated response is the combined result of these items. The specific breakdown of the effects are difficult to determine in integral tests. The implication is that separate-effects data are required to further develop individual models that can then be assessed against integral test data. The faster depressurization in the code caused an earlier attainment of the accumulator set point pressure of 4.2 MPa (609 psia) and thus reduced the time allowed for core boiloff and possible core rod temperature excursions. In short, the faster depressurization in the code leads to a nonconservative prediction of the core thermal response.

   Because the accurate prediction of core thermal response represents an important licensing concern, the mentioned code deficiencies take on relative importance in code development and improvement efforts.
3. The RELAP5 code correctly calculated the two-phase natural circulation and reflux phenomena during the draining of the steam generator U-tubes.

REFERENCES

1. V. Ransom et. al., *RELAP5/MOD2 Code Manual*, NUREG/CR-4312, EGG-2396, August 1985.

2. W. A. Owca, *Quick Look Report for Semiscale MOD-2C Experiment S-NH-1*, EGG-RTH-7147, February 1986.

3. W. A. Owca, *Appendix S-NH-1 and S-NH-2 of the Experiment Operating Specification for the Semiscale MOD-2C Small Break LOCA without HPI Experiment Series*, EGG-RTH-7050, October 1985.

4. G. G. Loomis, *Results of Semiscale Mod-2C Small Break (5%) Loss-of-Coolant Accident Experiments S-LH-1 and S-LH-2*, NUREG/CR-4438, EGG-2424, November 1985.

5. G. G. Loomis, *Summary of Semiscale Small Break Loss-of-Coolant Accident Experiments (1979 to 1985)*, NUREG/CR-4893, EGG-2419, September 1985.

6. E. Klingler, K. E. Suckett, *The Semiscale MOD-2C Small Break (0.5% and 2.1%) Configuration Report for Experiments S-NH-1, S-NH-2, S-NH-3, and S-NH-5*, EGG-RTH-7323, July 1986.

7. G. G. Loomis, K. Soda, *Results of Semiscale Mod-2A Natural Circulation Experiments*, NUREG/CR-2335, EGG-2200, September 1982.

8. G. G. Loomis, *Summary of the Semiscale Program (1965-1986)*, NUREG/CR-4045, EGG-2509, July 1987.

9. Mohamed M. Megahed, *RELAP5/MOD2 Assessment Simulation of Semiscale Mod-2C Test S-NH-3*, NUREG/CR-4799, EGG-2519, October 1987.

10. O. Rosdahl and D. Caraher, *ICAP Assessment of RELAP5/MOD2 Against Critical Flow Data from Marviken Tests JITII and CFT 21*, Studsvik/ND-6199, July 1986.